Synthesis and Characterization of Multiphase, Highly Branched Polymers

Ann R. Fornof

Dissertation submitted to the faculty of the
Virginia Polytechnic Institute and State University
in partial fulfillment of the requirements for the degree of

Doctor of Philosophy
In
Macromolecular Science and Engineering

Timothy E. Long, Chair
Don Leo, Member
James McGrath, Member
Judy Riffle, Member
Thomas Ward, Member
Garth Wilkes, Member

April 20, 2006
Blacksburg, Virginia

Keywords: Highly Branched, Polyurethane, Ionene, Ionic Conductivity, Rheology, Degree of Branching

Synthesis and Characterization of Multiphase, Highly Branched Polymers

Ann R. Fornof

ABSTRACT

Rheological modification is frequently cited as a key application for hyperbranched polymers. However, the high degree of branching in these polymers restricts entanglement and the resultant mechanical properties suffer. Longer distances between branch points may allow entanglements. Highly branched polymers, where linear units are incorporated between branch points, are synthesized with an *oligomeric* A_2 plus a monomeric B_3. Higly branched polymers differ from traditional hyperbranched polymers in that every monomeric repeating unit of a hyperbranched polymer is a potential branch point, which is not true for highly branched polymers.

The *oligomeric* A_2 plus B_3 synthetic methodology was used for the synthesis of highly branched ionenes and polyurethanes. Highly branched ionenes, which have a quaternary ammonium salt in the main chain, were synthesized with a modified Menshutkin reaction. The *oligomeric* A_2 was comprised of well-defined telechelic tertiary amine endcapped poly(tetramethylene oxide). Reduced mechanical properties were observed for highly branched polymers compared to linear counterparts.

Highly branched polyurethanes were synthesized with polyether soft segments including poly(ethylene glycol), poly(tetramethylene glycol), and poly(propylene glycol). Degree of branching was determined via a novel ^{13}C NMR spectroscopy approach, which

is described herein. The classical degree of branching was supplemented with an alternative degree of branching equation, which was tailored for highly branched architectures. The melt and solution viscosities of highly branched poly(ether urethane)s were orders of magnitude lower than the linear analogs. For the first time, the presence of entanglements was confirmed for highly branched polymers. Doping the highly branched polyurethane with lithium perchlorate, a metal salt, resulted in a significantly higher melt viscosity. The ionic conductivity of the highly branched polyurethane when doped with a metal salt was orders of magnitude higher than the linear analog.

Soybean oil was oxidized for synthesis of soy-based polyol monomers. Three regimes were determined, and for the first time, a correlation between hydroxyl number and a resonance from the double bonds of soybean oil in ^{1}H NMR spectroscopy was described. The relationship was used to accurately describe oxidation of soybean oil with time, temperature, and air flow rate. Soybean oil oxidation was catalyzed, and tack-free films were formed.

ACKNOWLEDGEMENTS

I would like to thank my advisor, Prof. Timothy E. Long, for his guidance and invaluable advice throughout my graduate career. He has truly helped me appreciate "pushing back the frontiers of polymer science". My committee members also significantly influenced the direction of my research. And I thank my committee members for their advice and help: Prof. Garth Wilkes, Prof. Tom Ward, Prof. Jim McGrath, Prof. Judy Riffle, and Prof. Don Leo. Thanks also to all of the staff, who have made my time in graduate school go more smoothly and enjoyably: Millie Ryan, Laurie Good, and Gary Scott. I also acknowledge the funding sources for my research: the Urethane Soy Systems Company, the MAP MURI, and the MS & IE IGERT. The opportunity to work with scientists from a variety of backgrounds was immeasurably helpful and interesting.

I would also like to thank all of my cohorts from Davidson 124a. Thanks to AJ Pasquale for having so much fun with me and for not letting me take myself too seriously. I would also like to thank Dr. Pasquale for his editing help, as well. I greatly appreciated Jeremy Lizotte's friendship and mentorship while we were in the lab together. I don't think that anyone has made me laugh quite so much while learning about science (and lifting weights), and I doubt I would have made it through my first year in graduate school without Jeremy's influence and care. Scott Trenor for his mischievous adventures kept things lively in the lab. I would like to thank the other half of the dynamic duo, Matt McKee, for his willingness to indulge my rants about science and life. I appreciate greatly Matt's patience and understanding in the lab. I would like to thank the more recent additions to Davidson 124a. Matthew Cashion was always willing to joke with (or

about) me. While it was difficult to hear myself think over John's heavy breathing and loud clock, John's wacky humor always made being in the lab an adventure. Rebecca Huyck was the first graduate woman to join me in Davidson 124a, and I greatly appreciate her friendship. The last few months would have been significantly more painful and less fun without her warmth in the lab. Thanks to Erika Borgerding for her help on these last few experiments. I am sure that she will carry on the tradition of great graduate students from Davidson. I also appreciate the help from the undergraduates, Matt and Allison, who worked with me in the lab over the years.

Thanks also to the other students and postdocs from the Long labs: Dave Williamson, Lars Kilian, Casey Elkins, Serkan Unal, Andy Duncan, Matt Hunley, Taigyoo Park, Sharlene Williams, Tomonori Saito, Amanda Willis, Gozde Ozturk, Qin Lin and Emily Anderson. Thanks to Brian Mather for his scientific advice and warm approach. The camaraderie of Afia Karikari and Kalpana Viswanathan has been a great bonus to graduating this year. I am glad that we were able to travel to conferences together and that we will experience graduation together. I greatly appreciate Dr. Cheryl Heisey's input on my writing. I would like to thank those people whose encouragement led me to pursue a doctorate degree: Dr. Jeff Hedrick, Prof. Chris Durning, Prof. Jeff Koberstein, and especially Dr. Christy Tyberg.

Thanks to all of my friends outside of the labs. The tailgating and happy hour crew provided some of the best times that I had in graduate school. Thanks to you all: DK, Doug, Josh, Som, Oak, Emmett, Lee, Sita, Chris, and Ben. Thanks especially to Mary for

all of the delicious food and your deliciously devilish sense of humor. I would like to thank the ultimate teams: Cleats and Cleavage and Jimmy Bang. Thanks for letting me join your ultimate family. Thanks especially to Lindsay and Corinne. Corinne, thank you for teaching me about ultimate, finally realizing how awesome I am, and letting me talk about my research. Lindsay has a fantastic perspective on life. She has the ability to make anyone around her feel special.

My family has been tremendously supportive during this sometimes tumultuous past few years. Thanks to my sister, Sarah Lewis, and my brother-in-law, Larry Lewis, for their love and support. I would like to express my deepest thanks to my parents, John and Judy Fornof. Their unconditional love and consideration during this process was tremendous. Thanks to my aunts and uncles, who despite their undying devotion to the Buckeyes, celebrated Hokie vicotories with me anyway.

I cannot imagine a better partner in life than my boyfriend, Mike Boylan-Kolchin. He has helped me to be a better person. On a number of levels, I would not be looking forward to getting our license plate “PhDz” without his love and encouragement.

Table of Contents

List of Figures

List of Tables

List of Schemes

Chapter 1: Introduction

1.1 Dissertation Overview

Polymer topology is a primary tool for adjusting the physical properties and functionality of polymers. Branching influences the processability and the applications of polymers. Hyperbranched polymers, where every monomer unit is a potential branch point, has received significant interest in the literature due to the globular structure, high functionality, and which lends itself to creative approaches to synthesis. The commercial availability and the symmetry of the monomers used in the A_2 plus B_3 synthetic approach to hyperbranched polymers are advantages when compared with the traditional polycondensation of AB_x-type monomers. Recently, the polymerization of oligomeric A_2 plus B_3 was proposed. The goal of this approach was to provide distances between branch points, which are long enough for entanglements.

The synergy between a high degree of branching and intermolecular interactions was investigated in this dissertation. Following this chapter, characterization techniques used for hyperbranched polymers were reviewed. The third chapter deals with systematic branching of ionenes. The effect of branching in the hard segment on the intermolecular interactions and mechanical properties was addressed. In the fourth chapter, highly branched PEG-based polyurethanes were synthesized. The degree of branching was determined with a novel ^{13}C NMR spectroscopy approach. An alternative degree of branching calculation was also proposed. The fifth chapter describes the reduced melt and solution viscosities of highly branched polymers compared to linear analogs. The ionic conductivity of highly branched polyurethanes was improved over linear analogs.

The sixth chapter focused on the synthesis of monomers from renewable resources for potential use in microphase separated polymers. The seventh chapter summarizes the accomplishments of this dissertation work.

Chapter 2: Review of the Literature

The determination of the fundamental effects of branching on a variety of applications ranging from rheological modification to electrospinning has received intense scrutiny.[1, 2] Long chain branching increases the melt viscosity compared to linear analogs due to an increase in entanglements. However, short-chain branched polymers have fewer entanglements causing a reduction in melt and solution viscosities and hydrodynamic radius. Long-chain branching also has a significant affect on the shear thinning of sparsely branched polymers. With the incorporation of a small number of long-chain branched polymers, the onset of shear-thinning occurs at lower frequencies than for linear counterparts.[1, 3] Numerous topologies were synthesized to probe the effects of branching from pom poms to star polymers. Dendrimers emerged as a novel, monodisperse, wholly branched topology. Dendritic polymers were interesting academically but the synthetic rigor required for dendrimers made them inaccessible for most industrial applications. Hyperbranched polymers emerged as an industrially viable, highly branched alternative to dendrimers. Unlike dendritic polymers, hyperbranched polymers have imperfections and are not wholly branched. Hyperbranched polymers are polydisperse with isomers and different geometries whereas dendrimers are monodisperse and have a single, well-defined architecture.

In the last fifteen years, a resurgence of interest in hyperbranched polymers has occurred. Flory's theoretical treatment of polymers synthesized with AB_x type monomers laid the groundwork for studies of hyperbranched polymers.[4, 5] The properties of hyperbranched polymers, which include increased solubility, low viscosity, large numbers of chain ends for functionalization, make this polymer class potentially useful

industrially and academically interesting. The lower viscosity of hyperbranched polymers compared to linear counterparts has received significant attention.[6-8] The globular shape of hyperbranched polymers and short distances between branch points prohibit entanglements.[9] However, the exclusion of entanglements created polymers without significant mechanical properties. This led to the frequent citation of rheological modification as an industrial application for hyperbranched polymers.[10-14] Recent work utilizing the synthetic strategy of an oligomeric A_2 plus B_3 monomer has introduced a high degree of branching with long linear segments for entanglements and improved mechanical properties compared with traditional hyperbranched polymers.[1, 7, 15, 16]

Spectroscopic and chromatographic methods are frequently used for the characterization of long- and short-chain branching. Determination of branch points with ^{13}C NMR spectroscopy is useful for branching concentrations greater than 10^{-4}.[17] Zimm and Stockmayer first proposed a contraction factor, g, for the description of long chain branching.[18] The contraction factor, g, is defined as the ratio of the radii of gyration for the branched and linear polymers, $\langle R_g^2 \rangle_{br}/\langle R_g^2 \rangle_{lin}$. Dilute solution measurements, typically size exclusion chromatography (SEC) with light scattering, are frequently used to find the radius of gyration for the calculation of g. Light scattering has limitations for the determination of the radius of gyration at small or moderate radii. The ratio of the intrinsic viscosities of branched and linear polymers, g', avoided the difficulties of light scattering and provided an avenue to determine an alternative contraction factor, where $g' = [\eta]_{br}/[\eta]_{lin}$.[19] The relationship between the two contraction factors, $g' = g^{\varepsilon}$, was based on the Fox-Flory equation, and it was suggested that $\varepsilon = 3/2$.[20] Zimm and Kilb reconsidered the value of ε about 10 years after the first publication and determined that

$\varepsilon = 1/2$.[21] Considerable debate continues about the relationship between the contraction factors. It was suggested that a power law relationship alone cannot describe the relationship between g and g'.[22-24] Spectroscopic and chromatographic methods including NMR, IR, and SEC lack the sensitivity to detect sparse long-chain branching, which has a substantial effect on rheological behavior.[25] Creative solutions to the problem of the characterization of long- and short-chain branched polymers have received sizeable effort. The sensitivity of dilute solution behavior that gives rise to the ratio g is insufficient to detect sparse long-chain branching that significantly affects melt rheological behavior.[26] Short-chain branching is frequently achieved through copolymerization. Therefore, the quantity of short-chain branching is typically identifiable through the amount of comonomer charged to the reaction. The distribution of short-chain branching, and its affect on mechanical properties has received considerable attention. The density and temperature rising elution fractionation are two techniques that indicate the amount and distribution of short-chain branching.[27]

The task of characterizing long- and short-chain branching has produced several techniques that are useful in the characterization of different topologies including hyperbranched polymers. However, the highly branched nature of hyperbranched polymers creates its own challenges for characterization. The greater branching density presents opportunities for the characterization of hyperbranched polymers. This review addresses the unique behavior and characterization of hyperbranched polymers. A brief treatment of synthetic strategies is warranted to understand the basis for the characterizaiton. However, most reviews on the subject of hyperbranched polymers are devoted primarily to the synthetic considerations.[28-33]

2.1 Introduction to Common Synthetic Routes

The approaches to step-growth polymerization of hyperbranched polymers can be broken down into two primary synthetic strategies: 1.) those that use AB_x monomers and 2.) polymerizations based on A_2 and B_3 monomers. Synthesis of hyperbranched polymers via step growth polymerization is traditionally performed with AB_x monomers, where $x \geq 2$. The polycondensation of AB_x monomers is a one-pot synthesis, and it was theoretically determined that no gelation will ensue from this type of reaction.[11, 34-39] One distinct disadvantage of AB_x-type polymerizations is the synthetic effort required for the synthesis of the AB_x monomers, which are frequently not commercially available. A variety of synthetic techniques and monomer chemistries were employed for the synthesis of hyperbranched polymers with AB_x monomers. The most common polymers synthesized from AB_x monomers include polyesters[40-42], polyphenylenes[11, 43, 44], and polyamides[45, 46]. Several hyperbranched polyesters are commercially available, which is becoming more frequent but is still a distinction for hyperbranched polymers.[47, 48]

Another common step-growth approach for the synthesis of hyperbranched polymers is the addition of A_2 plus B_3 monomers. The commercial availability of A_2 and B_3 monomers is a primary advantage of this synthetic route. Careful synthetic techniques are necessary to avoid gelation. Slow monomer addition, dilution, and exact stoichiometry are all techniques employed to avoid gelation. An illustration of the differences between AB_x and A_2 plus B_3 polymerizations is shown in Figure 2.1.

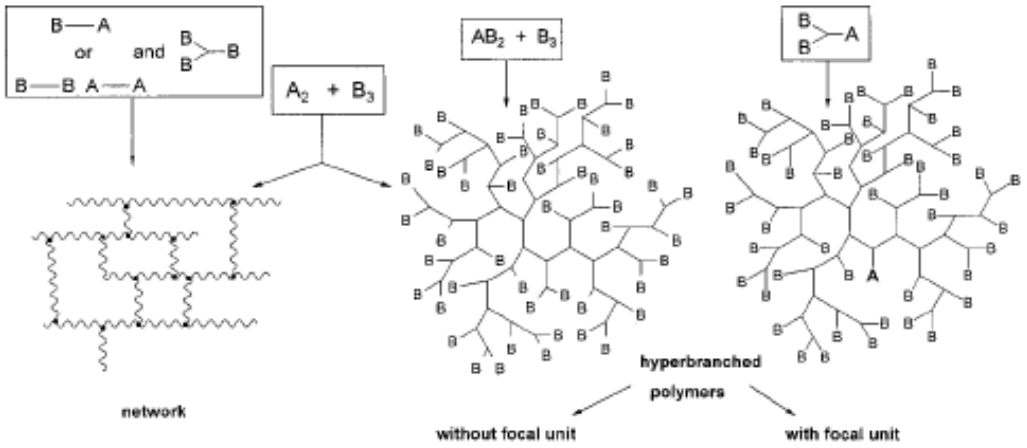

Figure 2.1: Depiction of differences between A_2 plus B_3 polymerization and hyperbranched polymers from AB_2 monomers [29]

Self-condensing vinyl polymerization (SCVP) occurs with monomers containing one vinyl group, A, and one initiating group, B*, (AB* monomers). Hyperbranched polymers synthesized from SCVP typically rarely crosslink when living/controlled conditions are used. The polydispersity of SCVP hyperbranched polymers is theoretically much greater than that of hyperbranched polymers from AB_2 monomers.[49] Synthetic techniques for lower polydispersity hyperbranched polymers are frequently used.[50, 51] Cations, radicals, and carbanions are all possibilities for the active center in SCVP.[15, 52, 53] An example of an SCVP monomer and the first few steps are shown in Figure 2.2.

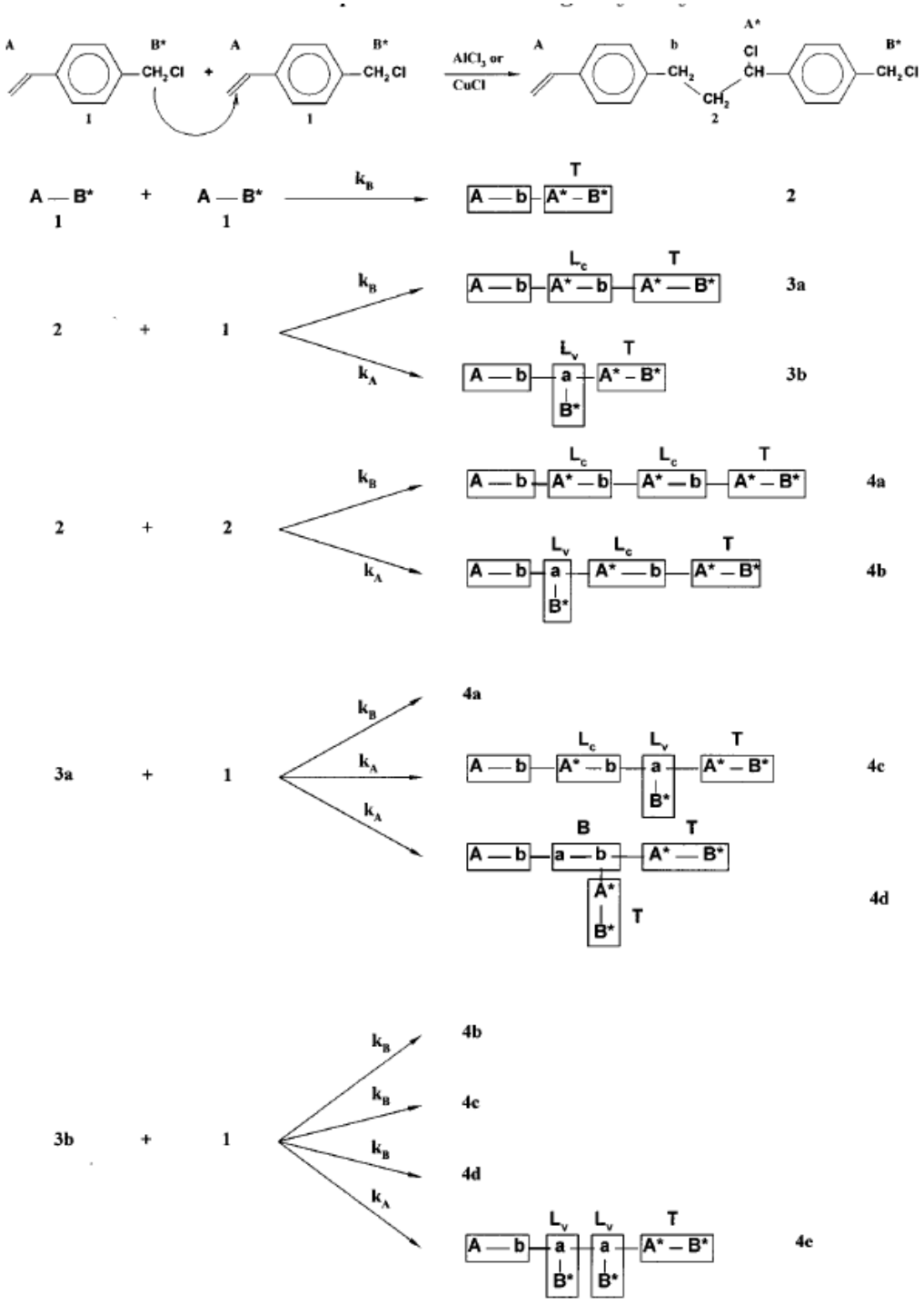

Figure 2.2: First steps of SCVP polymerization[54]

2.2 Degree of Branching Characterization

While dendrimers are monodisperse and have a regular structure, hyperbranched polymers are polydisperse and have irregular dendritic structures, which include isomers and different geometrical shapes. The degree of perfection of the hyperbranched polymer was described with the degree of branching calculation. The degree of branching is one of the most important characterizations of a hyperbranched polymer in that it describes the branching efficiency.[32]

2.2.1 Degree of Branching Calculations

Hawker et al. described a degree of branching equation to describe the irregular structures of hyperbranched polymers.[36] In this equation, three units are described: dendritic, D; linear, L; and terminal, T. The units that contribute to a wholly branched polymer are divided by all of the units in the hyperbranched polymer.

$$DB = (D + T)/(D + L + T) \quad (1)$$

A greater incorporation of linear units results in a decrease in the degree of branching. This equation is frequently utilized for the description of the degree of branching for hyperbranched polymers synthesized with AB_2 monomers.[55-57] Kim et al. described a branching factor, f_{br}, which is similar to the degree of branching equation that Hawker et al. proposed, to replace the conventional degree of branching (α)[58] for hyperbranched polymers from AB_2 monomers.

$$f_{br} = (T+B)/N_0 \quad (2)$$

In this equation, the branching factor is equal to the sum of the mole fraction of terminal units to the mole fraction of the branched units, which was described as dendritic in the

previous equation, divided by N_0. N_0 is the sum of the terminal, branched, and linear units of the hyperbranched polymer.[32, 59]

Several years after the original degree of branching equations were proposed Hölter et al. sought to describe a DB equation for hyperbranched polymers that was accurate for low molecular weight hyperbranched polymers from AB_2 monomers. The following equation was proposed:

$$DB = 2D/(2D + L) \quad (3)$$

The results from the equation described by Hölter et al. are approximately the same as those from Eqn (1) for high molecular weight polymers. Frequently, DB is calculated from Eqns (1) and (3), and a comparison of the results is reported.[60-62] Hölter et al. also addressed DB for the general case of hyperbranched polymers from AB_m monomers, where $m \geq 2$. The DB for the random reaction, where the reactivity of A and B groups remains the same throughout the reaction, was described as:

$$DB = [(m-1)/m]*\exp(m-1) \quad (4)$$

It was found that at high values of m the DB approaches a value of 0.368.

A degree of branching was proposed to describe hyperbranched polymers from self-condensing vinyl polymerization (SCVP).[54] A schematic of the first steps of an SCVP polymerization is shown in Figure 2.2.

The incorporation of two linear units, L_c and L_v, made a new definition of a degree of branching for SCVP hyperbranched polymers useful. Prior to the introduction of the degree of branching calculation for hyperbranched polymers synthesized with SCVP, the

authors modified the degree of branching from eqn (1). Yan et al. proposed the following equation for the degree of branching calculation:

$$DB = 2B/(1-M-2A') \quad (5)$$

where B is the number of branched units; M is the residual amount of monomer; and A' is the fraction of vinyl groups attached to the polymer (i.e. A' = A-M). The authors note that 1-M-A' is the fraction of all units in the polymer. The DB for hyperbranched polymers from the SCVP approach was higher for conversions less than 90% than the DB for hyperbranched polymers synthesized from condensation of AB_2 monomers (Figure 2.3). The lower DB at high conversion for hyperbranched polymers from SCVP was attributed to a nonequal distribution of A* and B*, which are the propagating radicals.

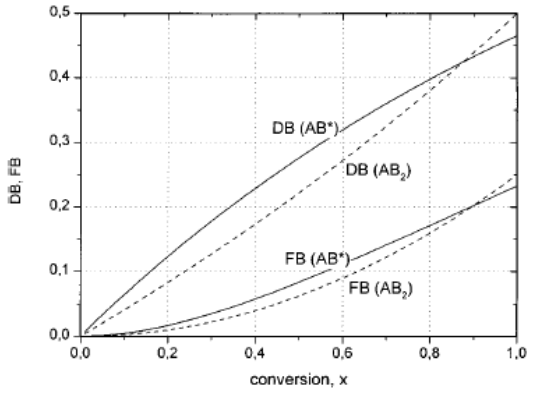

Figure 2.3: DB and fraction of branch points with conversion for SCVP hyperbranched polymers and AB_2 hyperbranched polymers[54]

2.2.2 Degradation of Hyperbranched Polymers for Degree of Branching Determination

The degree of branching, or the percent of monomeric units that contributed to branching is one of the most useful ways of describing hyperbranched polymers. Eqn (1) is traditionally used for the description of the DB.[36] Degree of branching is also useful in

examining steric or electronic effects on branching efficiency.[63, 64] Branching and degree of branching was shown to have a significant effect on the physical properties.

The primary approach for determining the ratios of the dendritic, linear, and terminal groups is with ^{1}H or ^{13}C NMR spectroscopy.[65, 66] However, there are numerous instances where the resonances of the dendritic, linear, and terminal units are not well-resolved. Hölter et al. proposed an alternative calculation of degree of branching, which requires the resolution of only two of the three types of units[67]:

$$DB = 2D/(2D + L) \approx 2T/(2T + L) \quad (5)$$

However, there still are hyperbranched polymers that do not have well-resolved resonances from either dendritic and linear units or terminal and linear units.

Kambouris et al. proposed an alternative to NMR spectroscopy for the determination of the ratio of dendritic, linear, and terminal units of hyperbranched polymers.[68] The new route to determining these ratios involved the degradation of the hyperbranched polymer bonds. The dendritic, linear, and terminal groups could be differentiated because the endgroups were modified prior to degradation. There are two conditions that are required for this process to accurately describe the ratio of the dendritic, linear, and terminal groups. First, the process for degrading the polymeric bonds must not adversely affect the modified endgroups. Second, the only products of the degradation must be the elementary subunits and complete degradation to these elementary subunits must occur. The subunits remaining after degradation of the polymer are then analyzed typically with a chromatographic technique such as HPLC or RP-HPLC.

The first use of the degradative process for degree of branching determination involved hyperbranched polyesters synthesized from the AB_2 monomer methyl 4,4-bis(4'-hydroxyphenyl)pentanoate. The hyperbranched polyester had hydroxyl endgroups, which were modified with methyl iodide and silver oxide to produce methoxy endgroups. The methoxy endgroups were hydrolytically stable while the ester linkages between subunits were not (Figure 2.4). After hydrolysis in a basic solution, the three subunits were detected with HPLC and the degree of branching was determined. The degree of branching (49%) was close to the theoretically predicted degree of branching for a statistical reaction (50%).[68]

Another study that utilized the reductive degradation method for the determination of the degree of branching confirmed the results with ^{1}H NMR spectroscopy. Bolton et al. synthesized hyperbranched aryl polycarbonates with A_2B and AB_2 monomers, where the A_2B-based hyperbranched polymers had fluoroformate endgroups and the AB_2-based hyperbranched polymers had *tert*-butyldimethylsilyl ether endgroups.[69] Both aryl polycarbonates were treated with lithium aluminum hydride and the carbonate linkages were reduced to the subunits. The ratio of the subunits was determined with HPLC, and a degree of branching of approximately 50% was found for both hyperbranched polycarbonates. The ^{1}H NMR spectroscopy characterization of the degree of branching correlated well with the degree of branching determined through the reductive degradation process.[69]

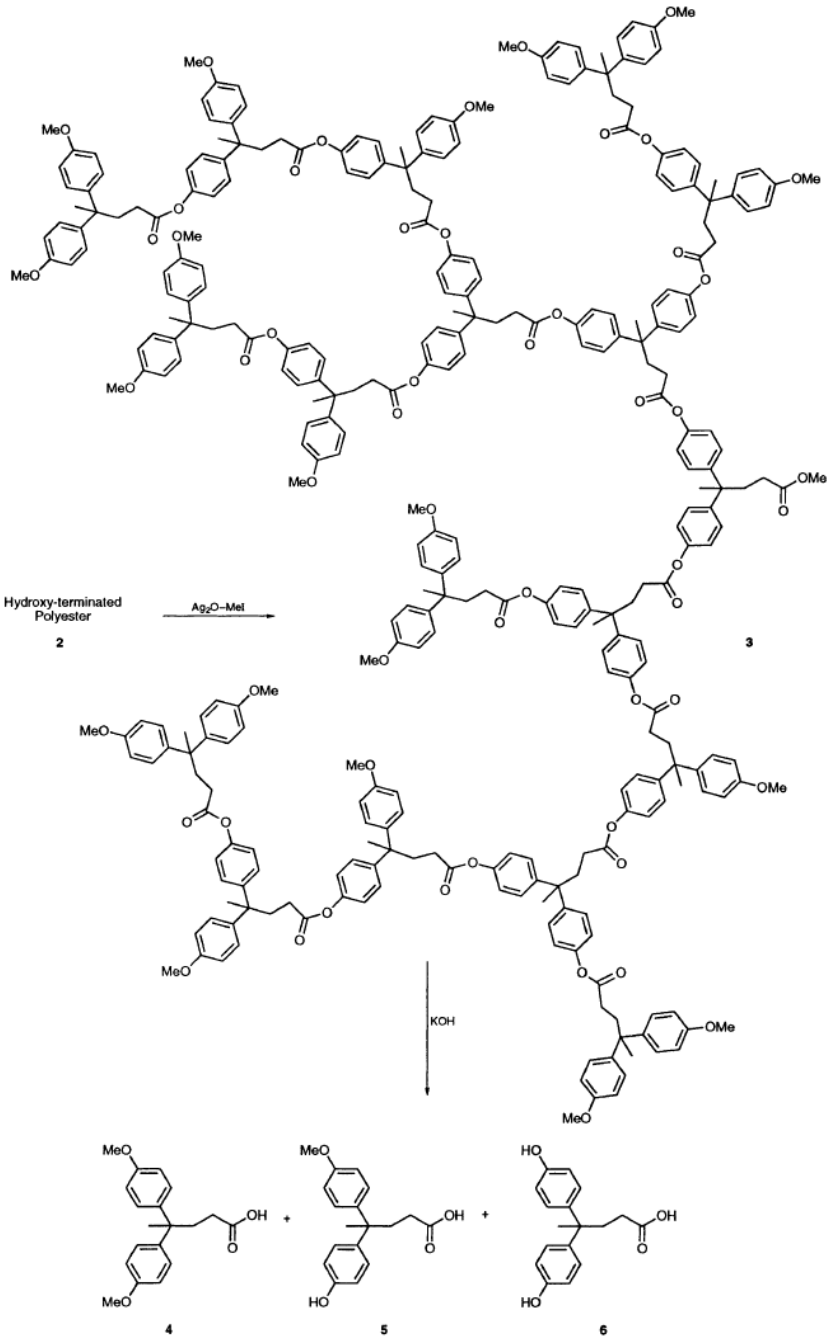

Figure 2.4: Endcapping and degradation of an aryl polyester for degree of branching analysis [69]

The characterization of the degree of branching for hyperbranched lysine was performed with the reductive degradation technique. The hyperbranched lysine was

reduced to its subunits through hydrolysis. A combination of amino acid analysis and RP-HPLC was used to determine the ratios of dendritic, linear, and terminal subunits.[70]

2.2.3 Indirect Methods for the Determination of the Degree of Branching

Another way to determine the degree of branching for hyperbranched polymers that do not have well-resolved NMR resonances or are degradable to distinct monomer units is the kinetic approach.[71] Ishizu et al. used model compounds to determine the rate of initiation and propagation of the photopolymerization of 2-(N,N-diethyldithiocarbamyl)methylstyrene in benzene.[72] The degree of branching was calculated from an equation proposed by Yan et al. for SCVP hyperbranched polymers.[54]

Markoski et al. similarly tracked the development of the structure of hyperbranched polymers with model compounds. While the rate constants were not calculated in this study, a similar approach to Ishizu et al. was taken. An AB/AB_2 polymerization, where $0.25 > x_{AB} > 1.0$, was modeled with small molecules that could not polymerize but included A, B, and B_2 functionalities. The model compounds were reacted under similar conditions and stoichiometric ratios as for the polymerization. The products were analyzed with ^{1}H NMR spectroscopy and HPLC. The ratios of dendritic, linear, and terminal units were determined from the model compounds and reactions. The degree of branching was indirectly calculated from these ratios. For several compositions, the indirect method of degree of branching determination was verified with direct determination with ^{1}H NMR spectroscopy. These approaches provide useful alternatives to conventional analysis with NMR spectroscopy for the determination of the relative ratios of dendritic, linear, and terminal units in hyperbranched polymers.

2.2.4 Enhancement of the Degree of Branching

Hölter et al. found that the maximum DB for a hyperbranched polymer from an AB_2 monomer is 0.5, where the A and B groups have equal reactivity and a random reaction occurred.[67] The DB for a dendrimer is 1. To improve the DB of hyperbranched polymers, Hölter et al. proposed three approaches: a) higher reactivity of linear units compared to terminal units, b) polymerization of dendritic monomers, and c) slow addition of monomers.[73] Slow addition of monomers results in sequential addition of single monomer units, which leads to an improved degree of branching. The higher reactivity of linear units compared to terminal units greatly improved the degree of branching in the theoretical treatment of the system. For example, a DB of 0.8 was attainable when the linear unit was five times more reactive than the terminal.

Synthesis of hyperbranched polymers from prefabricated dendron monomers also enhanced the degree of branching. However, to achieve high DB, a high generation (> 8) of the dendron monomer was required. This tactic would theoretically result in high degrees of branching. However, there would be a high cost associated with the synthesis of dendritic monomers.

The final method for degree of branching enhancement was the slow addition of monomers. The ideal case, where AB_2 monomers are added slowly, was addressed. It was assumed that sterics did not influence the polymerizaiotn and that the coupling reaction was quantitative. The slow monomer addition led to an increase in the DB to 0.67.

Slow addition of monomers has a profound effect on the DB from A_2 plus B_3 polymerizations. Schmaljohann et al. evaluated the kinetics of hyperbranched A_2 plus B_3

polycondensations through calculation of differential equations using an iterative process.[74] It was determined that the most influential variable for the enhancement of DB was the slow addition of either both monomers or just the B_3 monomer to the A_2 (Figure 2.5). The reactivity of the B_3 units was important to the degree of branching, as well.

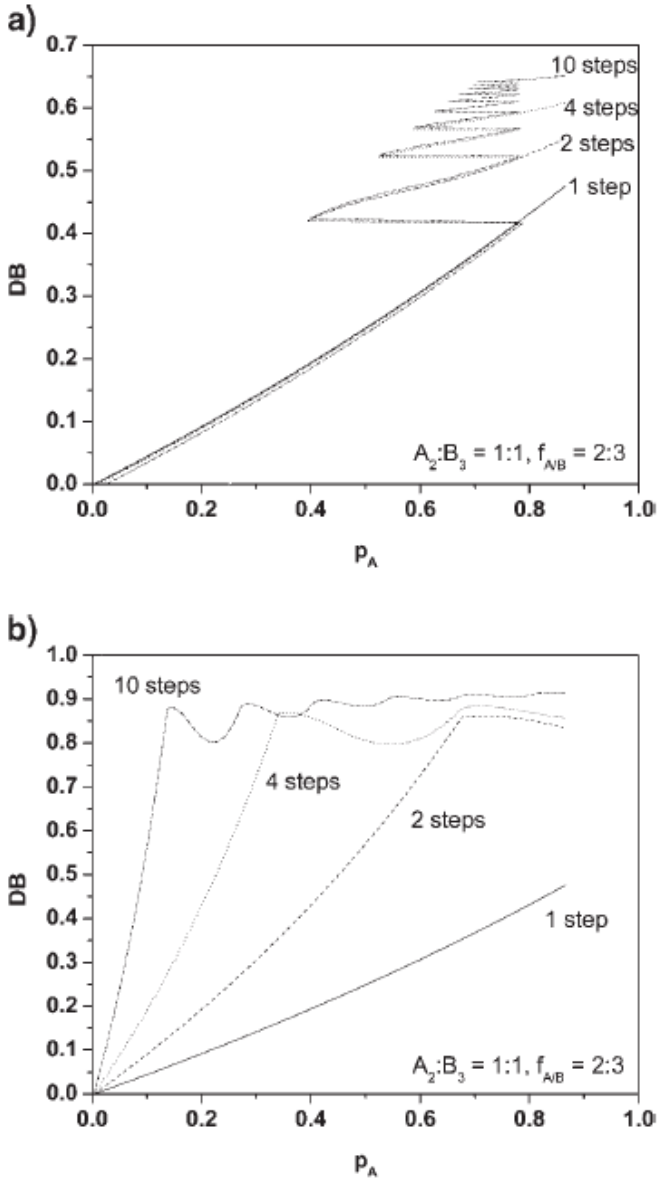

Figure 2.5: DB versus conversion for different steps of monomer addition a) simultaneous addition of A_2 and B_3, b) addition of B_3 to a solution of A_2[74]

2.3 Molecular Weight Characterization of Hyperbranched Polymers

2.3.1 Characterization of Hyperbranched Polymers with Size Exclusion Chromatography

Size exclusion chromatography (SEC) is useful for the characterization of molecular weight and molecular weight distribution of linear polymers. This information is important for hyperbranched polymers, as well. A triple detector system with concentration, light scattering, and viscosity detectors provides the most detailed information about hyperbranched polymers.

The relationship between molecular weight and intrinsic viscosity is well-described with the Mark-Houwink equation for linear polymers.

$$[\eta] = k*M_v^a \quad (1)$$

The constant, k, and exponent, a, have implications for the structure of the polymer. The Mark-Houwink exponent is typically in the range of 0.6 to 0.8 for flexible, linear polymers in a good solvent. Branched polymers frequently have Mark-Houwink exponents of less than 0.6 due to the more compact nature of branched polymers.[75] However, dendrimers do not follow this relationship. There is a maximum in the molecular weight versus intrinsic viscosity curve for dendritic polymers. Hyperbranched polymers are similar to dendritic polymers in that these polymers are globular and highly branched. However, hyperbranched polymers follow the Mark-Houwink relationship of molecular weight and intrinsic viscosity (Figure 2.6). The exponent, a, is smaller for hyperbranched polymers than linear analogs due to the more compact structure of

hyperbranched polymers.[40, 41, 76, 77] Behera et al. synthesized a series of hyperbranched polyethers with different lengths of spacer segments between branch points. The hyperbranched polyether had a Mark-Houwink exponent of 0.37, which indicated a highly branched structure. As the spacer length increased from 0 to 10 carbons, the Mark-Houwink exponent increased from 0.37 to 0.54. With the introduction of longer distances between branch points, the polyethers were less branched, which was reflected in the much higher Mark-Houwink exponent for the polyethers.[78]

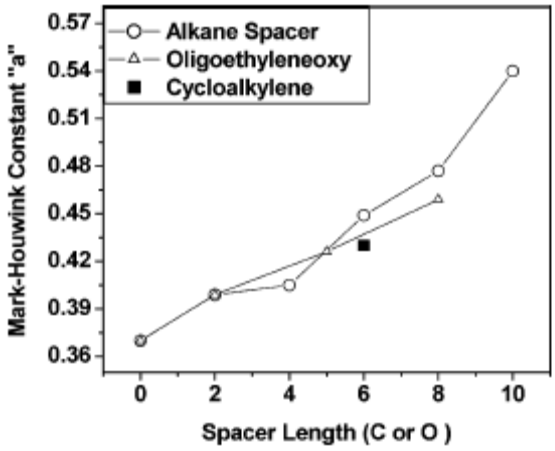

Figure 2.6: Variation of Mark-Houwink exponent with increasing spacer segment length in hyperbranched polyethers[78]

Hyperbranched polymers from the step-growth polymerization of AB_x or A_2 and B_3 monomers have broad polydispersities (Figure 2.7).[40, 79] Few studies have addressed the molecular weight distributions of hyperbranched polymers.

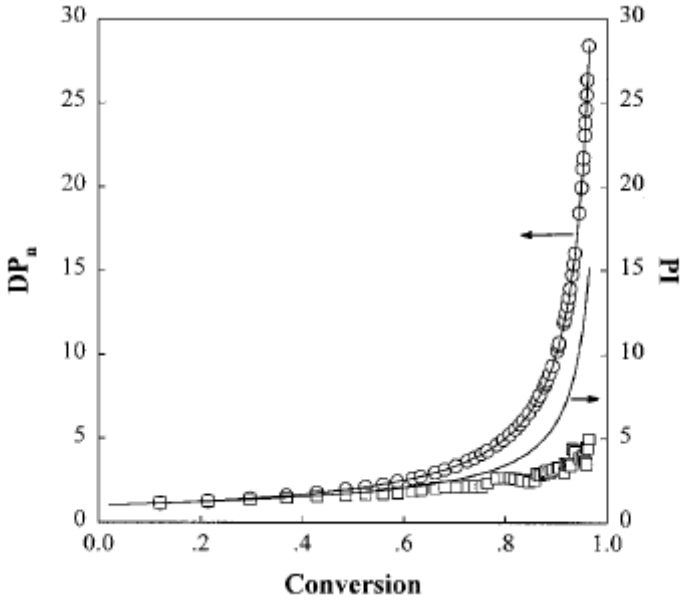

Figure 2.7: Number average degree of polymerization and polydispersity vs. conversion, where the solid lines are theoretical predictions[79]

Kunamaneni et al. used an AB/AB_2 hyperbranched polymer system over a range of molecular weights (3,000 to 250,000 g/mol) to characterize the molecular weight distribution over a wide molecular weight range.[80] The hyperbranched polyesters showed a power law relationship between number density and molecular weight with an exponential cut-off at a characterizstic upper cut-off mass, M_{char}, $n(M) \sim M^{-\tau}$ x exp ($-M/M_{char}$). Rescaling of the data with M_w led to a universal curve for all of the hyperbranched polymers. This indicated that the hyperbranched polymers followed static scaling with τ and the ratio M_{char}/M_w, regardless of the molecular weight of the polymer. The value of τ was found to agree with mean-field scaling, which was surprising as percolation scaling was expected. Percolation scaling typically describes networks well. The disagreement with percolation scaling was attributed to a lower concentration of

loops for hyperbranched polymers when compared to networks.[80] The results agreed well with the recent scaling hypothesis proposed by Buzza for the molecular weight distribution of hyperbranched polymers, which follows a mean field theory.[81] The fractal dimensions were also determined within this theoretical work.

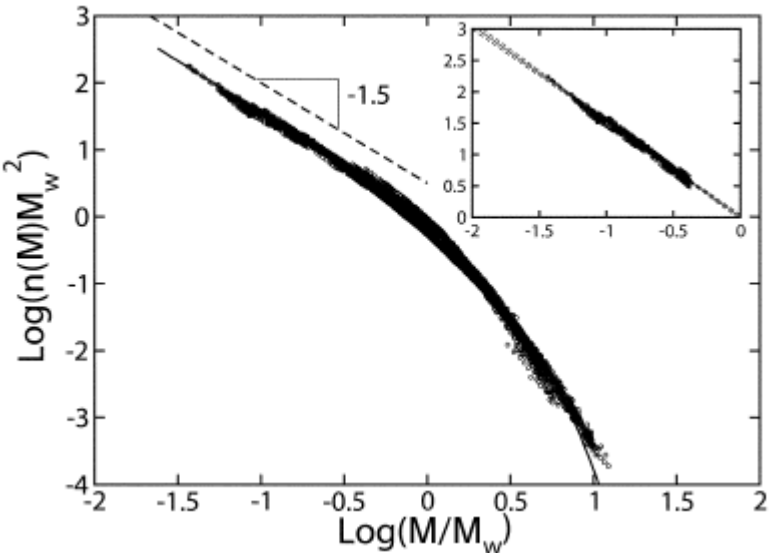

Reproduced by permission of The Royal Society of Chemistry

Figure 2.8: Universal scaling plot, where τ is approximately 1.53[82]

2.3.2 Characterization of Hyperbranched Polymers with Matrix Assisted Laser Desorption/Ionization-Time of Flight Mass Spectrometry (MALDI-TOF/MS)

Molecular weight characterization is traditionally performed with SEC. However, a useful technique for the molecular weight characterization of hyperbranched polymers is MALDI-TOF/MS. Several researchers have utilized MALDI-TOF/MS to confirm the molecular weights determined with SEC.[83] Muthukrishnan et al. synthesized

hyperbranched glycopolymers with a sugar-carrying acrylate. The molecular weights of the hyperbranched polymers ranged from 3,200 to 29,200 g/mol, which is within the range that MALDI-TOF/MS can reasonably be used for molecular weight determination. The polymers were first characterized with SEC/viscometry, and the molecular weights and dispersities were confirmed with MALDI-TOF/MS. [84]

Cyclics form during the polymerization of hyperbranched polymers.[15] The contribution of cyclics to the molecular weight distribution is difficult to determine with traditional techniques. While cyclics are a small contributor to the distribution of most hyperbranched polymers, even small amounts of cyclics can have a significant affect on physical properties of hyperbranched polymers. Kricheldorf et al. described in detail the contribution of cyclics to a wide variety of step-growth chemistries.[85] The authors made the distinction between thermodynamically and kinetically controlled polymerizations. Cyclization is more prevalent in kinetically controlled polymerizations. The authors advocate a modification of the classical theory from Flory[4], which describes the polymerization of AB_x monomers, to account for cyclics in the distribution of hyperbranched polymers.

2.4 Rheological Behavior of Hyperbranched Polymers

Janzen and Colby[17] aptly described the difficulty characterizing long-chain branching, which is defined as branches that are long enough to entangle. Determination of the presence and exact topologies of long-chain branched polymers, most notably polyethylene, is particularly difficult due to the sparse distribution of branch points.[86] Rheological characterization was one of the few characterization techniques to elucidate the structural differences among long-chain branched polymers.[17] Hyperbranched

polymers have very high branching densities because each monomer presents an opportunity for branching. This topology differs significantly from long-chain branched polymers. The melt and solution rheological behavior of hyperbranched polymers received interest due to the unique architecture. Many techniques are useful for the elucidation of the molecular structures of hyperbranched polymers, and the flow behavior of hyperbranched polymers has proven useful as a complimentary technique for the determination of the molecular structure and intermolecular interactions.

2.4.1 Melt Rheology of Hyperbranched Polymers

Studies of the melt rheology of hyperbranched polymers have brought to light several trends for this topology. The first and most interesting point was that hyperbranched polymers are not entangled. The primary manifestation of the lack of entanglement with a power law of approximately 1.0 was the linear relationship between zero shear rate viscosity, η_0, and weight-average molecular weight, M_w. The well-known η_0-M_w relationship for linear polymers follows a power law relationship of approximately 1.0 for unentangled polymers and 3.4 for entangled polymers. Branching was shown to have a significant effect on this relationship.[87] Long-chain branching tends to create a greater dependence of η_0 on M_w when the molecular weight of the branch is sufficiently high to promote entanglements. Hyperbranched polymers are short-chain branched polymers and the preponderance of short chains impeded entanglements. This caused a weaker dependence of η_0 on M_w than expected for polymers of high molecular weight ($>10^6$ g/mol).[9]

Kharchenko et al.[88] synthesized linear, star, and hyperbranched polystyrenes for the investigation of the role of architecture on rheological behavior as well as the

conformation and orientation. The hyperbranched polystyrenes were synthesized through a controlled polymerization of styrene and divinylbenzene. The η_0-M_w relationship was investigated for both linear and hyperbranched polymers of similar composition. The linear polystyrene followed the classical scaling of $M_w^{3.4}$ with η_0. However, for comparable molecular weights, the hyperbranched polymers followed a weaker scaling of $M_w^{1.1}$ with η_0 (Figure 2.9). The weaker dependence was attributed to the high branching functionality and the disruption of entanglements by short branches. The hyperbranched polystyrene with a M_w of greater than 10^6 g/mol had distances between branch points greater than the critical molecular weight for entanglement, M_c, and agreed with the weak scaling of M_w with η_0.[88]

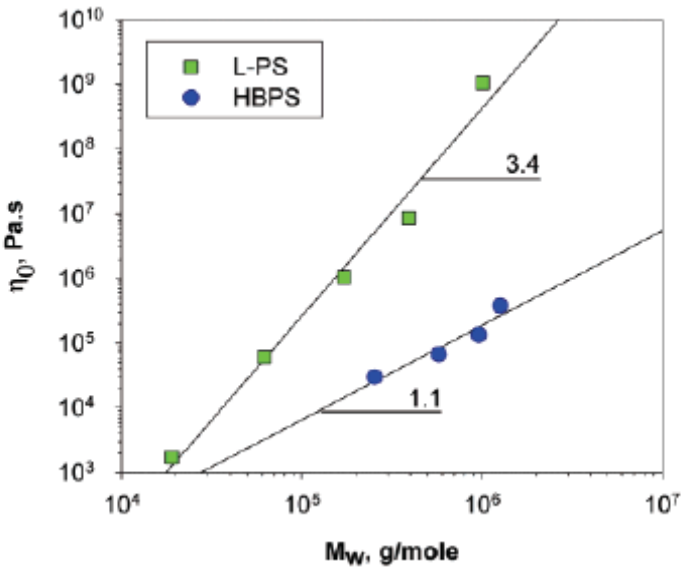

Figure 2.9: Weaker scaling of η_0 with M_w of hyperbranched polystyrene compared to linear polystyrene[88]

Luciani et al. utilized commercially available aliphatic hyperbranched polyesters based on a tetrafunctional ethoxylated pentaeryrthritol core with 2,2-*bis*-

(hydroxymethyl)propionic acid repeating units to determine the effect of increasing molecular weight on η_0.[89] Regardless of the experimental, the η_0 asymptotically approached scaling behavior of $M_w^{1.0}$ (Figure 2.10).

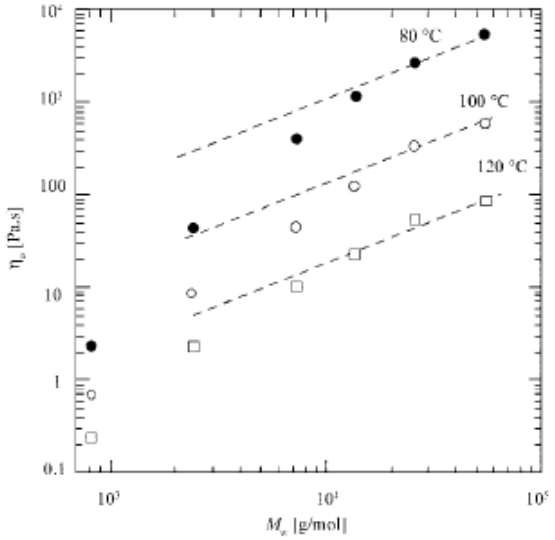

Figure 2.10: Relationship between η_0 and M_w for hyperbranched polyesters[89]

The weak scaling of η_0 with M_w was attributed to Rouse-like behavior and a lack of entanglements in these polymers. The molecular weights of the hyperbranched polyesters were in the range of 2,400 to 55,510 g/mol.

While several studies attributed the weaker scaling of η_0 with M_w to Rouse-like behavior, modeling of the experimental data was not used to substantiate this observation.[89] Suneel et al. confirmed that hyperbranched polymers followed dynamic scaling based on Rouse-like behavior through an evaluation of experimental data with a

Rouse model.[9] The hyperbranched polymers studied were synthesized with the AB_2 monomer 5-(hydroxyalkoxy)isophthalate. A hyperscaling relationship ($d_f = 3$) was consistent with the fractal dimension in the melt. The scaling was similar to that of near-critical gels.[90] While slow relaxation modes were observed in the terminal behavior of the hyperbranched polyesters, the slow relaxations were attributed to the ultrahigh molecular weight fraction of the distribution and not entanglements. The good fit of the dynamic scaling model based on the Rouse model to the experimental dynamic modulus data indicated that the hyperbranched polymers were unentangled polymeric fractals (Figure 2.11).[9] The hyperbranched polyesters were fractionated and the rheological behavior was compared to the unfractionated hyperbranched polymer.[82] The fractionated hyperbranched polyesters fit a dynamical scaling model based on the Rouse model, which incorporated the Schulz-Zimm parameterization of the molecular weight distribution. The authors concluded that the hyperbranched polymers regardless of molecular weight distribution were unentangled based on the good fit of the experimental data to the Rouse-based dynamic scaling model.[82]

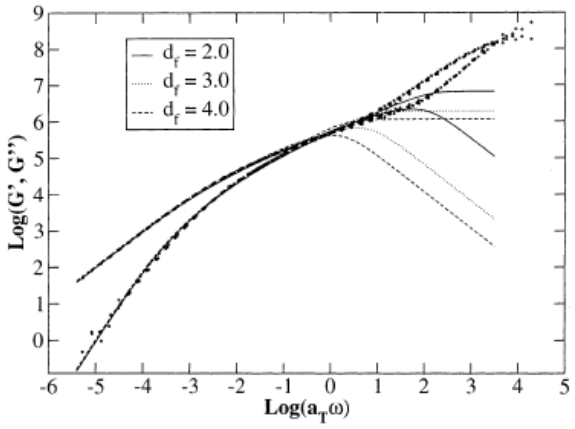

Figure 2.11: Good fit of Rouse-based dynamic scaling model to loss and storage modulus from hyperbranched polyesters indicating that the polyesters were unentangled[9]

Linear polymers frequently have η_0's with Arrhenius temperature dependence, and the flow activation energy can be calculated from this relationship (1).

$$\eta_0(T) \alpha \exp(E_a/RT) \quad (1)$$

Graessley observed that randomly long-chain branched polymers have higher flow activation energies than linear analogs.[91] The higher activation energy corresponded to a slower cooperative diffusion of polymers in the melt.[92] There are conflicting reports about the flow activation energy of hyperbranched polymers compared to linear analogs. The majority of studies dealing with the activation energy for flow in the melt indicated that hyperbranched polymers had higher activation energies than the comparable linear polymers.[89, 93-95] However, Kwak et al.[96] and Choi et al.[97] found that for hyperbranched poly(ε-caprolactone), the activation energy decreased for branched polymers when compared to linear analogs (Figure 2.12). While those studies that indicated the activation energy increased for hyperbranched polymers were performed on different

chemistries (i.e. polyethylene and aliphatic polyester), the studies that showed that the activation energy for flow decreased from linear to branched polymers were both on the same poly(ε-caprolactone)s.[89, 93-97] The authors attributed the higher flow activation energy to the high degree of branching in the hyperbranched polymers increasing the rigidity of the polymers.[89] The greater molecular mobility of hyperbranched poly(ε-caprolactone)s than linear poly(ε-caprolactone)s was speculated to be the cause of the lower flow activation energies for hyperbranched poly(ε-caprolactone)s.[96] Discrepancies in activation energy trends was also observed for branched polyesters.[1] This was attributed to differences in the temperature coefficients of linear and branched melts.[98]

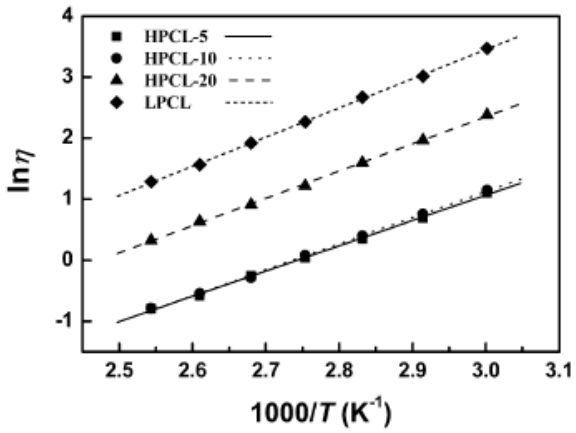

Figure 2.12: Temperature dependence of viscosity for hyperbranched poly(ε-caprolactone)s[97]

Figure from (http://www.sciencedirect.com/science/journal/00323861)

Hyperbranched polymers have a periphery of functionality due to the high degree of branching, which creates a large number of endgroups (Figure 2.12).[33]

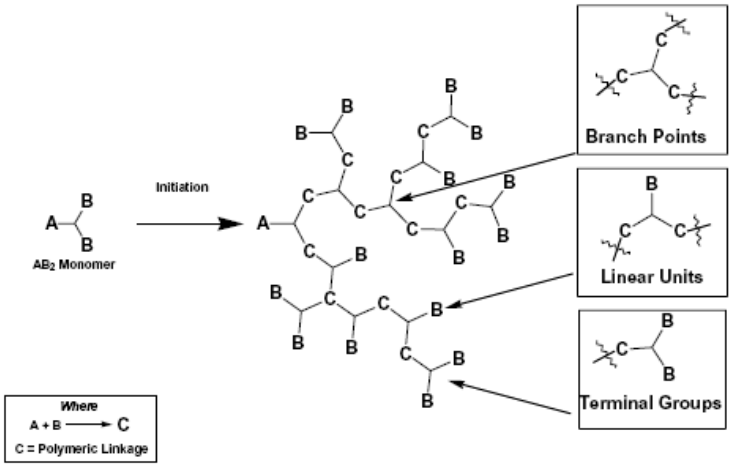

Figure 2.13: Illustration of hyperbranched polymer with a large number of terminal, B, groups[33]

(Figure from http://www.sciencedirect.com/science/journal/00143057)

However, the influence of endgroups on the rheological properties of hyperbranched polymers has received sparse attention.[99] Dendritic poly(propylene imine)s were studied with methyl and benzyl acrylate endgroups.[100, 101] After accounting for the changes in T_g with different endgroups, it was found that there was a maximum in the η_0 versus M_w curve for increasing bulk of the endgroup. One study on the influence of endgroups on the rheology of hyperbranched polymers focused on aliphatic hyperbranched polyesters with hydrogen-bonding endgroups. The endgroups of the aliphatic hyperbranched polyester were hydroxyl groups. The molecular weight and consequently the concentration of endgroups were changed. The lower molecular weight hyperbranched polyesters, which were those with the highest concentration of hydrogen bonding endgroups, had higher flow activation energy (Figure 2.14). The higher activation energy for flow in the melt was ascribed to the increased interaction of the hydrogen bonding

polyester endgroups when the concentration of these endgroups was greater as in the lower molecular weight polyesters.[93]

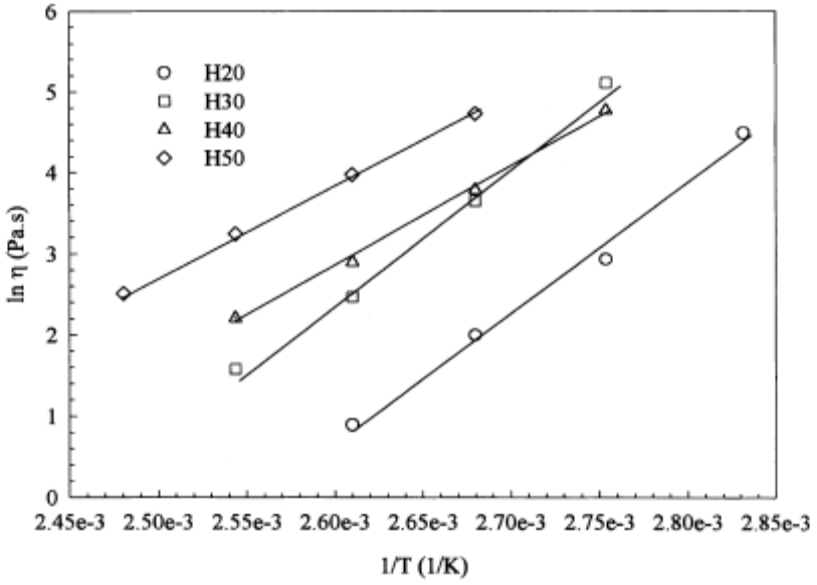

Figure 2.14: Influence of temperature on viscosity of hyperbranched polyesters with increasing molecular weight from sample H20 (2,100 g/mol) to H50 (7,500 g/mol)[93]
Figure from (http://www.sciencedirect.com/science/journal/00323861)

The scaling of the loss, G", and storage, G', moduli in the terminal zone has received significant attention in hyperbranched polymers. The terminal zone occurs at low frequency and is related to the relaxation mechanism of chain dynamics. For linear polymers, G" scales directly with frequency, ω, and G' scales with ω^2. Several studies have shown that hyperbranched polymers follow non-terminal scaling at low frequencies.[95] Kunamaneni et al. found for hyperbranched polyesters that the exponents for G" scaling with frequency were in the range of 0.92 to 0.96 and 1.22 to 1.42 for G'.[82] While exact dependencies varied for hyperbranched polymers, most researchers found

that G' and G" for hyperbranched polymers were less dependent on frequency than linear counterparts (Figure 2.15).[9, 96, 102, 103] Robertson et al. determined that hyperbranched polyisobutylene synthesized through the copolymerization of isobutylene and an inimer, 4-(2-methoxy-isopropyl) styrene (p-methoxycumyl styrene) reached terminal scaling only at very low frequencies.[104] However, the non-terminal scaling observed for most hyperbranched polymers has been observed for other non-linear topologies including dendritically branched polystrenes[105], long-chain branched polyethylene[106], side chain dendritic poly(ether urethane)s[107], and multiarm polybutadiene and polyisoprene stars[108]. The non-terminal scaling for the moduli was typically attributed to long relaxation times occurring in these topologies during the low frequencies. The source of these long relaxations seems to remain undetermined. It is generally agreed, however, that the source of these relaxations was not due to a physical structure. Generally, the behavior was attributed to a modification of relaxation behavior.

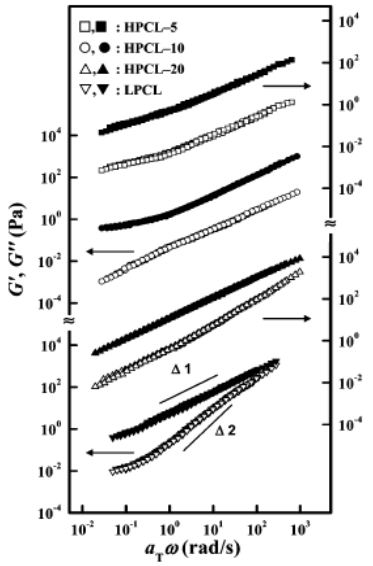

Figure 2.15: Non-terminal scaling of hyperbranched poly(ε-caprolactone)s[96]

Many researchers also noted that no intersection of G' and G" was observed in the terminal region for hyperbranched polymers. The longest relaxation time is calculated from this intersection.[109] The absence of an intersection was interpreted as an indication of a lack of entanglements in hyperbranched polymers.[9, 96]

The lack of entanglements in hyperbranched polymers results in lower melt viscosity compared to linear analogs.[88, 110] The significant reduction in melt viscosity of hyperbranched polymers compared to linear analogs has made hyperbranched polymers interesting for several applications. Blends with linear polymers, not necessarily of similar chemistry, as an aid for polymer processing has been explored.[13, 111, 112]

The rheological behavior of hyperbranched polymers has given insight into the intermolecular interactions. Most evidence from melt rheology of hyperbranched polymers pointed to a lack of entanglements for this topology. The relationship between η_0 and M_w was much weaker than for linear, entangled analogs, which indicated that the hyperbranched polymers remained unentangled even at molecular weights above 1,000,000 g/mol. The flow behavior of hyperbranched polymers exhibited Rouse-like behavior. No crossover between G' and G" in the terminal region was observed, which indicated that no entanglements were present in the hyperbranched polymers. Non-terminal behavior was observed for G' and G" at low frequencies. However, the cause of the non-terminal behavior has yet to be determined.

2.4.2 Solution Rheological Behavior of Hyperbranched Polymers

Several studies focused on the solution rheological behavior of hyperbranched polymers. Nunez et al. used hyperbranched aliphatic polyesters dissolved in 1-methyl-2-pyrrolidinone for the determination of solution rheological behavior.[113] The

hyperbranched polyesters exhibited Newtonian behavior over the shear rates examined and at all concentrations, which ranged from 10 to 50 wt%. The solution viscosity increased slightly with higher generation of the hyperbranched polyester. Star-shaped polymers have exhibited relative independence of solution rheological behavior with molecular weight, also.[114] The authors also blended the hyperbranched polyesters with linear poly(2-hydroxyethyl methacrylate), and significant decreases in the solution viscosity of the blends was observed compared to the linear polymer solution. However, it is important to note that the molecular weight of the linear polymer was much higher, approximately 300,000 g/mol, than the hyperbranched additives, which ranged in molecular weight from 1,750 to 14,600 g/mol. Therefore, the authors of this review believe it is difficult to discern the impact of the globular structure of the hyperbranched polymer on the solution behavior of the blends.

Thompson et al. observed that a decrease in the degree of branching of hyperbranched poly(ether imide)s resulted in an earlier onset of shear thinning for 40 wt% solutions. The onset of normal stresses also increased with a decrease in the degree of branching. The rheo-optics indicated that the hyperbranched poly(ether imide) with the lowest degree of branching had the greatest birefringence, and the hyperbranched poly(ether imide) with the highest degree of branching exhibited the lowest birefringence. Birefringence is a result of the optical anisoptropy of sheared polymers and is proportional to the degree of entanglement. The trend of decreasing birefringence with increasing branching is consistent with the hyperbranched polymers with a higher degree of branching having a globular, unentangled structure.[115]

2.5 Thermal Properties of Hyperbranched Polymers

A number of factors contribute to the different thermal properties of hyperbranched polymers compared to linear or even long-chain branched polymers. The increase in the number of endgroups can affect the degradation rate, if the endgroups play a role in degradation of the polymer, and the increased movement and free volume from a higher concentration of endgroups compared to linear or long-chain branched analogs can affect the thermal properties of the hyperbranched polymers.

2.5.1 Influence of Endgroups on Glass Transition of Hyperbranched Polymers

While endgroups influence the thermal properties of linear polymers, especially low molecular weight linear polymers, the effect of endgroups on thermal properties for hyperbranched polymers is more pronounced due to the periphery of endgroups. For a hyperbranched polymer of the same chemical structure, degree of branching, and similar molecular weight, bulky endgroups hinder chain motion and increase the T_g. Elrehim et al. synthesized hyperbranched poly(urethane urea)s through an AA* plus B*B_2 and endcapped the hydroxyl endgroup with either an aromatic or aliphatic isocyancate.[116] The T_g increased by approximately 30 ^oC when the bulky phenyl group was replaced with an aliphatic group. The ability to adjust the T_g significantly through slight modifications of the endgroup provides versatility for applications of hyperbranched polymers.

While the structure of endgroups was found to have an affect on the thermal transitions of hyperbranched polymers, differences in polarity and hydrogen bonding capability of endgroups has even greater influence on thermal transitions.[11, 117, 118] The

large changes in thermal transitions observed for changes in the polarity or hydrogen bonding cabability of hyperbranched polymers has led to significant interest. The size of flexible endgroups, which reduce the effectiveness of hydrogen boding, also influences the T_g of hyperbranched polymers. Schmaljohann et al. found that increasing the length of the alkyl endcapper of aromatic hyperbranched polyesters originally endcapped with hydroxyl groups dramatically decreased the T_g of the hyperbranched polymers (Figure 2.16). The decrease in T_g with increasing alkyl length was attributed to a reduction in hydrogen bonding capability. The crystallization of the long alkyl ($>C_{12}$) endgroups led to intramolecular phase separation. The T_g was found to increase once the length of the alkyl endcapper had exceeded C_{12}, which was associated with the crystallization of the long alkyl chains. An increase in the number of hydroxyl endgroups endcapped with long alkyl chains also caused a significant decrease in the T_g of the hyperbranched polyester. The reduction in intermolecular interactions caused greater mobility at lower temperatures and a lower T_g (Figure 2.16).

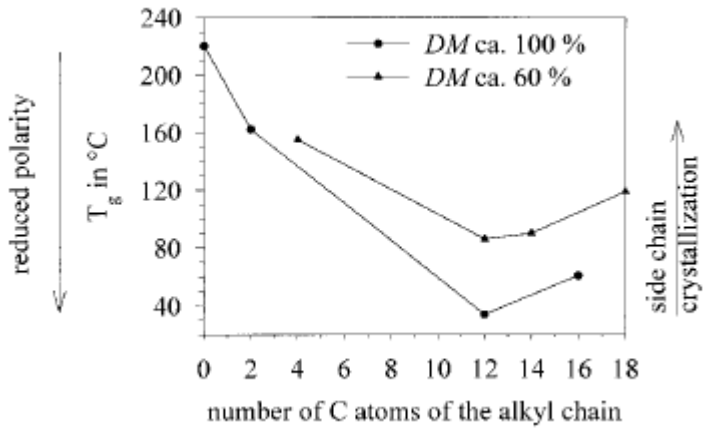

Reproduced by permission of The Royal Society of Chemistry

Figure 2.16: Influence of the increasing length of alkyl endcapper, which reduced the hydrogen bonding capability, on Tg of an aromatic hyperbranched polyester[68]

Baek et al. made a direct comparison of hyperbranched poly(phenylquinoxaline)s with different endgroups having different polarity.[119] The poly(phenylquinoxaline)s were terminated with either hydroxyl groups, which had hydrogen bonding capability, or with fluorine, a non-polar functionality. The effect of these endgroups on the thermal properties was investigated. Linear analogs of the hydroxyl- and fluorine-terminated poly(phenylquinoxaline)s were synthesized for comparison, as well. Little difference was observed between the T_g's of fluorine-terminated linear and hyperbranched poly(phenylquinoxaline)s (220 and 225 ^oC, respectively). However, the T_g of the hydroxyl-terminated hyperbranched poly(phenylquinoxaline)s was approximately 50 ^oC higher than the linear analog. Among the hyperbranched poly(phenylquinoxaline)s the hydroxyl-terminated polymer had a T_g that was approximately 75 ^oC higher than the fluorine-terminated hyperbranched

poly(phenylquinoxaline). The large number of endgroups provided a useful route to the modification of the thermal behavior of the polymers without changing the backbone chemistry. The glass transition temperature could also be used as a tool to detect differences in endgroups of hyperbranched polymers.

The incorporation of linear units into the hyperbranched polymer was carried out through changing the ratio of AB:AB_2 monomers from 0:100 to 100:0. As the topology of the polymer shifted from hyperbranched to linear, the T_g of the hydroxyl-terminated polymers gradually decreased with the reduction in hydrogen bonding endgroups. The gradual change in topology from hyperbranched to linear resulted in little difference in terms of T_g for the fluorine-terminated polymers. The degradation temperature for 5 % weight loss for the fluorine-terminated polymers over the range of topologies were all quite similar. The hydroxyl-terminated poly(phenylquinoxaline)s was dependent on the number of endgroups, where those with more hydroxyl endgroups were less thermally stable.[119]

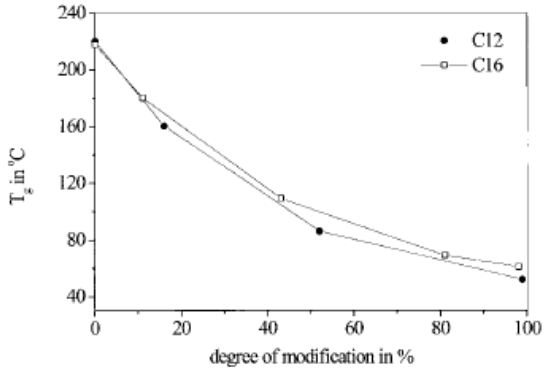

Figure 2.17: Reduction in Tg with replacement of hydroxyl, hydrogen bonding, endgroups with alkyl, non-polar, endgroups118

2.5.2 Thermal Stability of Hyperbranched Polymers

Hyperbranched polymers, where the chemical structure of the polymer is typically thermally stable, remained thermally stable despite the increase in the number of endgroups and branching (e.g. polyarylenes) (Figure 2.18).[120-122] However, changes in endgroup chemistry affects the thermal stability of hyperbranched polymers. Terminal groups with hydrogen bonding capability produced different trends in thermal stability based on the backbone chemistry of the polymers. While hyperbranched poly(amino esters) increased the temperature at which 5 % weight loss occurred with a decrease in hydrogen bonding capability, the opposite trend was observed for poly(phenylquinoxaline)s.[119, 123] Fossum and Tan synthesized linear poly(arylene ether ketone)-*co*-hyperbranched poly(arylene ether oxide) copolymers. The thermal stability of the copolymers was improved significantly with the incorporation of the hyperbranched poly(arylene ether oxide). This effect was attributed to the greater thermal stability of triarylphosphine oxide than the linear homopolymer.[124] The thermal stability of hyperbranched polymers depends significantly on the chemical structure of the polymer and endgroups. However, the impact of the endgroup's thermal stability is magnified for hyperbranched polymers when compared to linear counterparts.

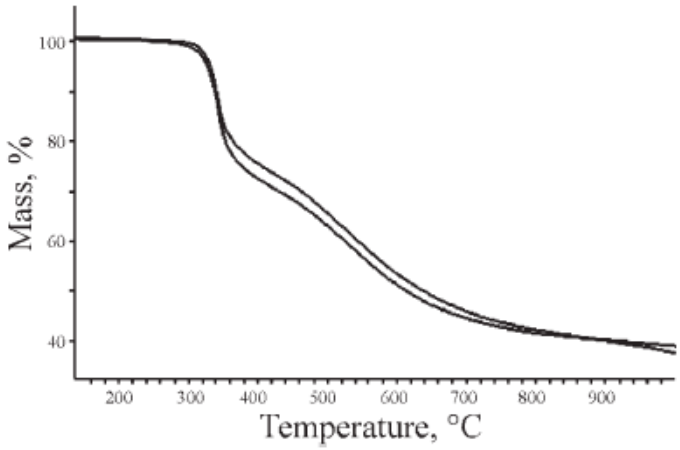

Reproduced by permission of The Royal Society of Chemistry

Figure 2.18: Good thermal stability of two hyperbranched fluoropolymers[121]

2.5.3 Impact of Hyperbranched Topology on Crystallization

Structural symmetry is a requirement for crystallization in polymers. Disruption of symmetry, whether from a kink in the structure due to the chemistry or a branch point, will disrupt crystallinity in a polymeric system.[125] While branching in polymers at low levels is known to reduce the degree of crystallinity, the much greater degree of branching in hyperbranched polymers contrbituted to a greater influence on the crystallinity than traditional long-chain branched polymers.[126] Hyperbranched polymers are frequently weakly crystalline or amorphous when the linear analogs are semi-crystalline with a high degree of crystallinity.[30, 127, 128]

Mai et al. demonstrated that a systematic change in the degree of branching while the molecular weight remained constant of hyperbranched polymers greatly affects polymer crystallization.[129] A series of hyperbranched poly[3-ethyl-3-(hydroxymethyl)oxetane] (PEHO) with degrees of branching ranging from 5.6 to 45%

were characterized with ^{13}C NMR spectroscopy, SEC, XRD, and DSC. Others have shown that with higher degrees of branching, a reduction in crystallinity is observed for hyperbranched polymers.[130, 131] However, these studies did not control the molecular weight while changing the degree of branching. Therefore, molecular weight effects could not be disregarded for the previous studies. A decrease in the relative degree of crystallinity with increasing degree of branching was observed (Figure 2.19). Also, an increase in linear units led to an increase in the degree of crystallinity while an increase in dendritic and terminal units had the opposite effect.[129]

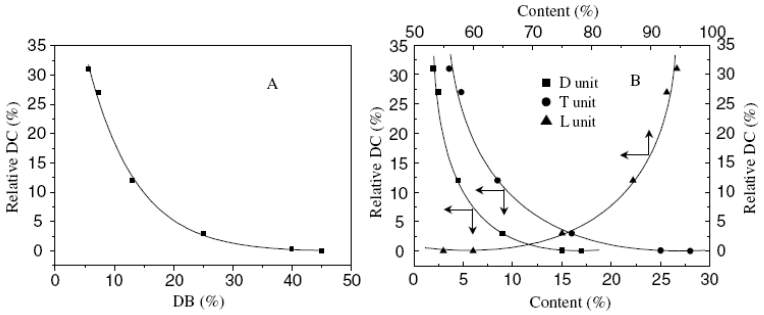

Figure 2.19: Influence of the degree of branching on the relative degree of crystallinity and the influence of dendritic, linear, and terminal units on the relative degree of crystallinity[129]

Large degrees of branching were shown to disrupt cyrstallinity. However, the endgroup of hyperbranched polymers can have an effect on crystallization in the system, as well. It was shown that crystallinity was disrupted by branching in the bulk of the hyperbranched polymers. However, endcapping the hyperbranched polymer with long alkyl groups (> 12 carbons) can lead to crystallization of the endgroups.[116, 132]

2.6 References

1. McKee, M. G.; Wilkes, G. L.; Colby, R. H.; Long, T. E. *Macromolecules* **2004** 37, 1760-1767.

2. McLeish, T. C. B.; Milner, S. *Adv. Polym. Sci.* **1999** 143, 195-256.

3. Flory, P. J. *J. Am. Chem. Soc.* **1941** 63, 3083-3090.

4. Flory, P. J. *J. Am. Chem. Soc.* **1952** 74, 2718-2723.

5. Scherrenberg, R.; Coussens, B.; van Vilet, P.; Edouard, G.; Brackman, J.; de Brabander, E. *Macromolecules* **1998** 31, 456-461.

6. Mourey, T. H.; Turner, S. R.; Rubenstein, M.; Frechét, J. M. J.; Hawker, C. J.; Wooley, K. L. *Macromolecules* **1992** 25, 2401-2406.

7. Uppuluri, S.; Keinath, S. E.; Tomalia, D. A.; Dvornic, P. R. *Macromolecules* **1998** 31.

8. Suneel; Buzza, D. M. A.; Groves, D. J.; McLeish, T. C. B.; Parker, D.; Keeney, A. J.; Feast, W. J. *Macromolecules* **2002** 35, 9605-9612.

9. Hawker, C. J.; Farrington, P. J.; Mackay, M. E.; Wooley, K. L.; Fréchet, J. M. J. *J. Am. Chem. Soc.* **1995** 117, 4409-4410.

10. Kim, Y. H.; Webster, O. W. *Macromolecules* **1992** 25, 5561-5572.

11. Hsieh, T.-T.; Tiu, C.; Simon, G. P. *Polymer* **2001** 42, 7635-7638.

12. Hong, Y.; Cooper-White, J. J.; Mackay, M. E.; Hawker, C. J.; Malmstrom, E.; Rehnberg, N. *J. Rheol.* **1999** 43, 781-793.

13. Mulkern, T. J.; Beck Tan, N. C. *Polymer* **2000** 41, 3193-3203.

14. Unal, S.; Lin, Q.; Mourey, T. H.; Long, T. E. *Macromolecules* **2005** 38, 3246-3254.

15. McKee, M. G.; Park, T.; Unal, S.; Yilgor, I.; Long, T. E. *Polymer* **2005** 46, 2011-2015.

16. Unal, S.; Oguz, C.; Yilgor, E.; Gallivan, M.; Long, T. E.; Yilgor, I. *Polymer* **2005** 46, 695-696.

17. Unal, S.; Yilgor, I.; Yilgor, E.; Sheth, J. P.; Wilkes, G. L.; Long, T. E. *Macromolecules* **2004** 37, 7081-7084.

18. Janzen, J.; Colby, R. H. *J. Mol. Struct.* **1999** 485-486, 569-584.

19. Zimm, B. H.; Stockmayer, W. H. *J. Chem. Phys.* **1949** 17, 1301-1314.

20. Radke, W.; Müller, A. H. E. *Macromolecules* **2005** 38, 3949-3960.

21. Flory, P. J., In *Principles of Polymer Chemistry*. 16th ed.; Cornell University Press: Ithaca, NY, 1986.

22. Zimm, B. H.; Kilb, R. W. *J. Polym. Sci.* **1959** 37, 19-42.

23. Berry, G. C. *J. Polym. Sci., Polym. Phys. Ed.* **1968** 6, 1551-1554.

24. Berry, G. C. *J. Polym. Sci.: Part B: Polym. Phys.* **1988** 35, 1377-1397.

25. Radke, W.; Gerber, J.; Wittmann, G. *Polymer* **2003** 44, 519-525.

26. Tackx, P.; Tackx, J. C. J. F. *Polymer* **1998** 39, 3109-3113.

27. Kraus, G.; Stacy, C. J. *J. Polym. Sci., Polym. Phys. Ed.* **1972** 10, 657-672.

28. Gupta, P.; Wilkes, G. L.; Sukhadia, A. M.; Krishnaswamy, R. K.; Lamborn, M. J.; Wharry, S. M.; Tso, C. C.; DesLauriers, P. J.; Mansfield, T.; Beyer, F. L. *Polymer* **2005** 46, 8819-8837.

29. Voit, B. *J. Polym. Sci.: Part A: Polym. Chem.* **2005** 43, 2679-2699.

30. Voit, B. *J. Polym. Sci.: Part A: Polym. Chem.* **2000** 38, 2505-2525.

31. Jikei, M.; Kakimoto, M. *Prog. Polym. Sci.* **2001** 26, 1233-1285.

32. Gao, C.; Yan, D. *Prog. Polym. Sci.* **2004** 29, 183-275.

33. Kim, Y. H. *J. Polym. Sci.: Part A: Polym. Chem.* **1998** 36, 1685-1698.

34. Yates, C. R.; Hayes, W. *Eur. Polym. J.* **2004** 40, 1257-1281.

35. Flory, P. J. *J. Am. Chem. Soc.* **1952** 74, 2718-2723.

36. Uhrich, K. E.; Hawker, C.; Fréchet, J. M. J.; Turner, S. R. *Macromolecules* **1992** 25, 4583-4587.

37. Hawker, C. J.; Lee, R.; Fréchet, J. M. J. *J. Am. Chem. Soc.* **1991** 113, 4583-4588.

38. Malmstrom, E.; Johansson, M.; Hult, A. *Macromolecules* **1995** 28, 1698-1703.

39. Yang, G.; Jikei, M.; Kakimoto, M. *Macromolecules* **1999** 32, 2215-2220.

40. Kumar, A.; Ramakrishnan, S. *J. Chem. Soc., Chem. Commun.* **1993**, 1453-1454.

41. Turner, S. R.; Voit, B. I.; Mourey, T. H. *Macromolecules* **1993** 26, 4617-4623.

42. Turner, S. R.; Walter, F.; Voit, B. I.; Mourey, T. H. *Macromolecules* **1994** 27, 1611-1616.

43. Massa, D. J.; Shriner, K. A.; Turner, S. R.; Voit, B. I. *Macromolecules* **1995** 28, 3214-20.

44. Morgenroth, F.; Müllen, K. *Tetrahedron* **1997** 45, 15349-15366.

45. Fukuzaki, E.; Nishide, H. *J. Am. Chem. Soc.* **2005** 128, 996-1001.

46. Hobson, L. J.; Kenwright, A. M.; Feast, W. J. *Chem. Comm.* **1997** 1877-1879.

47. Chikh, L.; Arnaud, X.; Guillermain, C.; Tessier, M.; Fradet, A. *Macromol. Symp.* **2003** 199, 209-221.

48. Zagar, E.; Zigon, M.; Podzimek, S. *Polymer* **2006** 47, 166-175.

49. Burgath, A.; Sunder, A.; Frey, H. *Macromol. Chem. Phys.* **2000** 201, 782-791.

50. Müller, A. H. E.; Yan, D.; Wulkow, M. *Macromolecules* **1997** 30, 7015-7023.

51. Cheng, K.-C. *Polymer* **2003** 44, 877-882.

52. Simon, P. F. W.; Müller, A. H. E. *Macromol. Theory Simul.* **2000** 9, 621-627.

53. Mori, H.; Walther, A.; Andre, X.; Lanzendoerfer, M. G.; Müller, A. H. E. *Macromolecules* **2004** 37, 2054-2066.

54. Ivan, B.; Erd-di, G.; Kali, G.; Hollo-Szabo, G.; Zsebi, Z.; Szesztay, M. In *New functional hyperbranche and star polymers*, 228th ACS National Meeting, Philadelphia, PA, August 22-26, 2004; PMSE: Philadelphia, PA, 2004.

55. Jin, M.; Lu, R.; Bao, C.; Xu, T.; Zhao, Y. *Polymer* **2004** 45, 1125-1131.

56. In, I.; Kim, S. Y. *Macromol. Chem. Phys.* **2005** 206, 1862-1869.

57. Chang, Y.-T.; Shu, C.-F.; Leu, C.-M.; Wei, K.-H. *J. Polym. Sci.: Part A: Polym. Chem.* **2003** 41, 3726-3735.

58. Wu, F.-I.; Shu, C.-F. *J. Polym. Sci.: Part A: Polym. Chem.* **2001** 39, 3851-3860.

59. Flory, P. J., In *Principles of Polymer Chemistry*. Cornell University Press: Ithaca, NY, 1953.

60. Kim, Y. H.; Webster, O. W. *J. Am. Chem. Soc.* **1990** 112, 4592-4593.

61. Hao, J.; Jikei, M.; Kakimoto, M. *Macromolecules* **2003** 36, 3519-3528.

62. Cheng, K.-C. *Polymer* **2003** 44, 1259-1266.

63. Li, X.; Yuesheng, L.; Tong, Y.; Shi, L.; Liu, X. *Macromolecules* **2003** 36, 5537-5544.

64. Yan, D.; Müller, A. H. E.; Matyjaszewski, K. *Macromolecules* **1997** 30, 7024-7033.

65. Hanselmann, R.; Hoelter, D.; Frey, H. *Macromolecules* **1998** 31, 3790-3801.

66. Hawker, C. J.; Chu, F. *Macromolecules* **1996** 29, 4370-4380.

67. Zhang, J.; Wang, H.; Li, X. *Polymer* **2006** 47, 1511-1518.

68. Blencowe, A.; Davidson, L.; Hayes, W. *Eur. Polym. J.* **2003** 39, 1955-1963.

69. Hölter, D.; Burgath, A.; Frey, H. *Acta Polymer.* **1997** 48, 30-35.

70. Kambouris, P.; Hawker, C. J. *J. Chem. Soc. Perkin Trans. 1* **1993**, 2717-2721.

71. Bolton, D. H.; Wooley, K. L. *J. Polym. Sci.: Part A: Polym. Chem.* **2002** 40, 823-835.

72. Menz, T. L.; Chapman, T. *Polym. Prep.* **2003** 44, 842-843.

73. Ishizu, K.; Ohta, Y.; Kawauchi, S. *Macromolecules* **2002** 35, 3781-3784.

74. Ishizu, K.; Ohta, Y.; Kawauchi, S. *J. Appl. Polym. Sci.* **2005** 96, 1810-1815.

75. Höelter, D.; Frey, H. *Acta Polymer.* **1997** 48, 298-309.

76. Schmaljohann, D.; Voit, B. *Macromol. Theory Simul.* **2003** 12, 679-689.

77. Garamszegi, L.; Nguyen, T.; Plummer, C. J. G.; Månson, J.-A. E. *J. Liq. Chrom. Related Tech.* **2003** 26, 207-230.

78. Li, J.; Gauthier, M. *Macromolecules* **2001** 34, 8918-8924.

79. Pavlov, G. M.; Errington, N.; Harding, S. E.; Korneeva, E. V.; Roy, R. *Polymer* **2001** 42, 3671-3678.

80. De Luca, E.; Richards, R. W. *J. Polym. Sci.: Part B: Polym. Phys.* **2003** 41, 1339-1351.

81. Yamaguchi, N.; Wang, J.-S.; Hewitt, J. M.; Lenhart, W. C.; Mourey, T. H. *J. Polym. Sci.: Part A: Polym. Chem.* **2002** 40, 2855-2867.

82. Behera, G. C.; Ramakrishnan, S. *Macromolecules* **2004** 37, 9814-9820.

83. Lee, Y. U.; Jang, S. S.; Jo, W. H. *Macromol. Theory Simul.* **2000** 9, 188-195.

84. Kunamaneni, S.; Buzza, D. M. A.; Parker, D.; Feast, W. J. *J. Mater. Chem.* **2003** 13, 2749-2755.

85. Buzza, D. M. A. *Eur. Phys. J. E* **2004** 13, 79-86.

86. Jayakannan, M.; Van Dongen, J. L. J.; Behera, G. C.; Ramakrishnan, S. *J. Polym. Sci.: Part A: Polym. Chem.* **2002** 40, 4463-4476.

87. Muthukrishnan, S.; Jutz, G.; André, X.; Mori, H.; Müller, A. H. E. *Macromolecules* **2005** 38, 9-18.

88. Sun, X.; Moreira, R. G. *J. Food Proc. Pres.* **1996** 20, 157-167.

89. Muenstedt, H.; Dietmar, A. *J. Non-Newtonian Fluid Mech.* **2005** 128, 62-69.

90. Kharchenko, S. B.; Kannan, R. M.; Cernohous, J. J.; Venkataramani, S. *Macromolecules* **2003** 36, 399-406.

91. Luciani, A.; Plummer, C. J. G.; Nguyen, T.; Garamszegi, L.; Månson, J.-A. E. *J. Polym. Sci.: Part B: Polym. Phys.* **2004** 42, 1218-1225.

92. Colby, R. H.; Gillmor, J. R.; Rubenstein, M. *Phys. Rev. E: Stat. Phys., Plasmas, Fluids, Relat. Interdiscip. Top.* **1993** 48, 3712-3716.

93. Kunamaneni, S.; Buzza, D. M. A.; De Luca, E.; Richards, R. W. *Macromolecules* **2004** 37, 9295-9297.

94. Graessley, W. W. *Macromolecules* **1982** 15, 1164-1167.

95. Bailey, R. T.; North, A. M.; Pethrick, R. A., In *Molecular Motion in High Polymers*. Oxford University Press: New York, 1981.

96. Hsieh, T.-T.; Tiu, C.; Simon, G. P. *Polymer* **2001** 42, 1931-1939.

97. Ye, Z.; Zhu, S. *Macromolecules* **2003** 36, 2194-2197.

98. Ye, Z.; AlObaidi, F.; Zhu, S. *Macromol. Chem. Phys.* **2004** 205, 897-906.

99. Kwak, S.-Y.; Choi, J.; Song, H. J. *Chem. Mater.* **2005** 17, 1148-1156.

100. Choi, J.; Kwak, S.-Y. *Polymer* **2004** 45, 7173-7183.

101. Böhme, F.; Clausnitzer, C.; Gruber, F.; Grutke, S.; Huber, T.; Pötschke, P.; Voit, B. *High Perform. Polym.* **2001** 13, 21-31.

102. Tande, B. M.; Wagner, N. J.; Kim, Y. H. *Macromolecules* **2003** 36, 4619-4623.

103. Sendijarevic, I.; McHugh, A. J. *Macromolecules* **2000** 33, 590-596.

104. Kharchenko, S. B.; Kannan, R. M.; Cernohous, J. J.; Venkataramani, S.; Babu, G. N. *J. Polym. Sci.: Part B: Polym. Phys.* **2001** 39, 2562-2571.

105. Simon, P. F. W.; Müller, A. H. E.; Pakula, T. *Macromolecules* **2001** 34, 1677-1684.

106. Robertson, C. G.; Roland, C. M.; Puskas, J. E. *J. Rheol.* **2002** 46, 307-320.

107. Dorgan, J. R.; Knauss, D. M.; Al-Muallem, H. A.; Huang, T.; Vlassopoulos *Macromolecules* **2003** 36, 380-388.

108. García-Franco, C. A.; Srinivas, S.; Lohse, D. J.; Brant, P. *Macromolecules* **2001** 34, 3115-3117.

109. Jahromi, S.; Palman, J. H. M.; Steeman, P. A. M. *Macromolecules* **2000** 33, 577-581.

110. Pakula, T.; Vlassopoulos, D.; Fytas, G.; Roovers, J. *Macromolecules* **1998** 31, 8931-8940.

111. Rubenstein, M.; Colby, R. H., In *Polymer Physics*. Oxford University Press: New York, 2003.

112. Gretton-Watson, S. P.; Alpay, E.; Steinke, J. H. G.; Higgins, J. S. *Ind. Eng. Chem. Res.* **2005** 44, 8682-8693.

113. Plummer, C. J. G.; Rodlert, M.; Bucaille, J.-L.; Grünbauer, H. J. M.; Månson, J.-A. E. *Polymer* **2005** 46, 6543-6553.

114. Hong, Y.; Coombs, S. J.; Cooper-White, J. J.; Mackay, M. E.; Hawker, C. J.; Malmström, E.; Rehnberg, N. *Polymer* **2000** 41, 7705-7713.

115. Nunez, C. M.; Chiou, B.-S.; Andrady, A. L.; Khan, S. A. *Macromolecules* **2000** 33, 1720-1726.

116. Marsalko, T. M.; Majoros, I.; Kennedy, J. P. *J. Macromol. Sci., Pure Appl. Chem.* **1997** A34, 775-792.

117. Thompson, D. S.; Markoski, L. J.; Moore, J. S.; Sendijarevic, I.; Lee, A.; McHugh, A. J. *Macromolecules* **2000** 33, 6412-6415.

118. Elrehim, M. A.; Voit, B.; Bruchmann, B.; Eichorn, K.-J.; Grundke, K.; Bellman, C. *J. Polym. Sci.: Part A: Polym. Chem.* **2005** 43, 3376-3393.

119. Ishida, Y.; Sun, A. C. F.; Jikei, M.; Kakimoto, M. *Macromolecules* **2000** 33, 2832-2838.

120. Chen, H.; Yin, J. *J. Polym. Sci.: Part A: Polym. Chem.* **2002** 40, 3804-3814.

121. Baek, J.-B.; Harris, F. W. *Macromolecules* **2005** 2005, 1131-1140.

122. Peng, H.; Lam, J. W. Y.; Tang, B. Z. *Polymer* **2005** 46, 5746-5751.

123. Powell, K. T.; Cheng, C.; Gudipati, C. S.; Wooley, K. L. *J. Mater. Chem.* **2005** 15, 5128-5135.

124. Abdelrehim, M.; Komber, H.; Langenwalter, J.; Voit, B.; Bruchmann, B. *J. Polym. Sci.: Part A: Polym. Chem.* **2004** 42, 3062-3081.

125. Wu, D.; Liu, Y.; Chen, L.; He, C.; Chung, T. S.; Goh, S. H. *Macromolecules* **2005** 38, 5519-5525.

126. Fossum, E.; Tan, L.-S. *Polymer* **2005** 46, 9686-9693.

127. Ungar, G.; Zeng, X.-B. *Chem. Rev.* **2001** 101, 4157-4188.

128. Sato, Y. *J. Appl. Polym. Sci.* **1981** 26, 27-39.

129. Jayakannan, M.; Ramakrishnan, S. *J. Polym. Sci.: Part A: Polym. Chem.* **2000** 38, 261-268.

130. DeSimone, J. M. *Science* **1995** 269, 1060-1061.

131. Mai, Y.; Zhou, Y.; Yan, D.; Hou, J. *New J. Phys.* **2005** 7, 1-9.

132. Magnusson, H.; Malmström, E.; Hult, A.; Johansson, M. *Polymer* **2002** 43, 301-306.

133. Trollsås, M.; Atthoff, B.; Claesson, H.; Hedrick, J. L. *Macromolecules* **1998** 31.

134. Schmaljohann, D.; Häuβler, L.; Pötschke, P.; Voit, B. I.; Loontjens, T. J. A. *Macromol. Chem. Phys.* **2000** 201, 49-57.

135. Seo, Y.; Kim, J.; Kim, K. U.; Kim, Y. C. *Polymer* **2000** 41, 2639-2646.

136. Weng, W.; Chen, G.; Dajun, W. *Polymer* **2003** 44, 8119-8132.

Chapter 3: Synthesis and Characterization of Highly Branched Ionenes Containing Poly(tetramethylene oxide)

(Fornof, A.R.; Mallakpour, S.; Park, T.; Long, T.E. *Polymer* **2006**, *to be submitted*)

3.1 Abstract

Linear and highly branched ionenes, which are defined as polyelectrolytes with quaternary amines in the main chain, were synthesized. A modified Menschutkin reaction enabled the synthesis of highly branched ionenes, where the soft segment consisted of well-defined poly(tetramethylene oxide) (PTMO) and the ionic sites were incorporated at the branch points. The highly branched ionenes comprised well-defined linear segments between branch points. The influence of branched ionic segments was investigated, and the influence of the distance between branch points was examined. Two PTMO precursors were prepared, 2,000 and 7,000 g/mol, which are below and above the critical molecular weight for entanglement (PTMO M_c = 2,500 g/mol). The thermal stability and transitions of the linear and highly branched ionenes were determined using TGA, DMA, and DSC. The TGA and DSC of the ionenes were similar regardless of macromolecular topology. However, the DMA indicated a significant difference in the temperature dependence of the storage modulus for the linear and highly branched ionenes, where branching significantly reduced the storage modulus after crystalline melting of the PTMO soft segment. While molecular weight was not

determined for these systems, the influence of branching on the tensile properties was determined and implied that branching in the ionic hard segment influenced symmetry and impeded ionic aggregation resulting in different mechanical performance.

Keywords: ionenes, branching, mechanical behavior, ionic aggregation

3.2 Introduction

Ionenes, which are macromolecules that contain quaternary ammonium salts in the main chain, are considered a subset of cationic polyelectrolytes. Our primary interest in ionenes stems from the numerous applications for microphase separated, elastomeric polycations. Applications for these elastomeric polycations range from gene transfection agents to ionically conductive elastomers.[133-135] Ionenes serve as ideal models for polyelectrolytes due to various structural parameters, including counterion selection, diverse functional precursors, block, alternating, and random copolymerization. [136, 137] The Menschutkin reaction[138], which involves quantitative reactions of primary alkyl dihalides and tertiary diamines, is the conventional approach for the synthesis of polymeric ionenes.[139-141] The ease of adjusting the distance between ionic sites through changing the molecular weight of the diamine and/or dihalide enables this subclass of ionomers as excellent models for fundamental investigations of charge density and counterion binding in biological applications and model polyelectrolytes.[142-144] Most work on ionenes has focused on the synthesis and characterization of ionenes with linear topology.[145-147] However, a few studies have focused on the synthesis and solution properties of star-shaped (3- and 4-arm), hyperbranched, and comb ionenes with wholly aliphatic soft segments. [148, 149] For example, studies based on rotaxanes focused on structure-property relationships for this unique architecture.[150]

Linear ionenes with well-defined distances between ionic sites display microphase separation.[151] The well-defined, segmented, structure of ionenes, which leads to the microphase separated morphologies, differed from conventional random placement of ionic groups as pendant groups in ionomers.[152, 153] Microphase separated ionenes are

attractive elastomeric materials due to high tensile strength (>30 MPa) and elongation (>1000%). However, ammonium based ionenes have interesting mechanical properties and ionic conductivity are also thermally unstable.[154-156] Ionenes undergo depolymerization through dequaternization of the ammonium cation, also known as the Hofmann elimination.[141] Ionenes can undergo a re-quaternization of the ammonium cation at elevated temperatures; however, the process is slow and frequently does not regenerate the original higher molecular weights prior to degradation.[141] The proclivity for degradation through the Hoffmann reaction depends on the basicity of the counterion, but the lack of thermal stability precludes some ionenes from melt processing.[150] One earlier approach in order to improve the melt processibility included the incorporation of a plasticizer.[152]

Branching significantly influences melt viscosity, which leads to improvements in melt processibility, in the absence of additives. Dendritic and hyperbranched polymers[28] are frequently described as rheological modifiers.[10, 32] However, the high degree of branching in these polymers restricts entanglement and resulting mechanical properties are often inferior relative to linear analogs.[37] Our research group has described highly branched polymers, where linear units are incorporated between branch points, using an *oligomeric* A_2 plus a monomeric B_3.[1, 7, 15, 16] The greater distance between branch points produces polymers with a high degree of branching, and acceptable mechanical properties.[16] Also, these highly branched polymers offer reduced viscosities compared to linear analogs, which may improve both melt and solution processibility.[157]

In this work, highly branched ionenes were synthesized via the *oligomeric* A_2 plus B_3 methodology. The effect of branching on the mechanical properties, rheological

behavior, and aggregation of ionic sites was explored. The incorporation of branching is proposed to influence the processibility of ionenes as well as elucidate the influence of branch points in the ionic segment on microphase separation through indirect techniques and mechanical performance.

3.3 Experimental

3.3.1 Materials

Chromatographic grade tetrahydrofuran (THF) was purchased from EMD Chemicals and distilled over sodium immediately prior to use. Irganox 1076 was obtained from Ciba Specialty Chemical Co. Trifluoromethanesulfonic anhydride (TFMSA), methyl 3-(dimethylamino) propionate, and 2,4,6-tris(bromomethyl)mesitylene (TBMM) were purchased from Aldrich and used without further purification. Dichloromethane (DCM), toluene, and hexanes were purchased from EMD Chemicals and used without further purification.

3.3.2 Synthesis of telechelic bis(dimethylamino) poly(tetramethylene oxide)

Synthesis of a 2,000 g/mol telechelic bis(dimethylamino) poly(tetramethylene oxide) (BAPTMO) oligomer involved the addition of TFMSA (3.38 mL, 0.02 mol) with a syringe to a solution of dry THF (10.00 g, 0.1389 mol) and DCM (10.00 g, 0.1177 mol) in a three-necked, round-bottomed, 250-mL flask in an ice bath. After 15 min, dry THF (30.00 g, 0.4167 mol) was added dropwise to the solution. Once the dry THF was completely added (approximately 15 min), the reaction was mechanically stirred for 90 min at 0 ^{o}C. Toluene (100 mL) was added to the reaction with excess methyl 3-

(dimethylamino) propionate (11.4 mL, 0.08 mol). The reaction was removed from the ice bath and continued for 30 min at room temperature with mechanical stirring. The solution was precipitated into hexanes to remove residual methyl 3-(dimethylamino) propionate, and hexanes were decanted. The reaction was poured into a 500-mL, round-bottomed flask with approximately 50 mL toluene and 100 mL 25 wt% aqueous NaOH solution. The reaction was refluxed for 30 min to remove residual acid and to convert the quaternary amine end groups to tertiary amines via a reverse Michael addition. The aqueous layer was discarded, and the toluene solution was dried over $MgSO_4$ and filtered. The solution was precipitated into hexanes to remove residual 2-ethyl acrylate, which is the byproduct of the reverse Michael addition. The BAPTMO product was dried under reduced pressure at 60 ^oC overnight to remove residual solvent. The BAPTMO in a solution of THF and isopropanol (3:1 vol:vol mixture) was titrated with 0.1 N HCl in isopropanol in order to determine the number average molecular weight.

3.3.3 Synthesis of highly branched ionenes

2,000 g/mol BAPTMO (4.7680 g, 2.384 mmol) was dissolved in dry THF at 15 wt%. TBMM (0.9516 g, 2.384 mmol) was dissolved in a two-necked, round-bottomed, 500-mL flask with dry THF to 3 wt%. The BAPTMO solution was slowly added dropwise to the TBMM solution under reflux conditions. The reaction proceeded for 1 h with magnetic stirring. At the end of the reaction, 0.02 g Irganox 1076 was added, and the solution was cast on a glass plate. The cast film was dried for 16 h at 25 ^oC and ambient pressure, and residual THF was removed under reduced pressure at 60 ^oC for 24 h.

3.3.4 Synthesis of linear ionenes

Linear ionenes were synthesized using 1,4-dibromo-*p*-xylene. For example, the 2,000 g/mol BAPTMO (4.3700 g, 2.2185 mmol) was added to a solution of dry THF and 2.5% excess 1,4-dibromo-*p*-xylene (0.5915 g, 2.241 mmol). The reaction proceeded under reflux until the magnetic stir bar was not able to rotate due to the high viscosity of the solution (approximately 1 h). The films were cast on glass slides, dried at 25 ^{o}C and ambient pressure for 16 h, and finally dried under reduced pressure at 60 ^{o}C for 24 h to ensure the removal of THF.

3.3.5 Characterization

The stress–strain behavior of the films was determined with mini dog-bone films (2.91 x 10 mm), where 10 mm is the guage length, which were cut using a bench-top die. An Instron Model 4400 Universal Testing System and Series IX software were used for stress-strain experiments. A crosshead speed of 50 mm/min was used until failure, and load versus displacement was recorded. Three to five samples were measured and their results were averaged to determine modulus, yield strength, and strain-at-break for each composition. Hysteresis experiments were performed after the films were stretched to either 100 or 200% strain at a crosshead speed of 50 mm/min and then immediately returned to the initial position (0% strain) at the same rate. Dynamic mechanical analysis (DMA) was performed on a TA Instruments DMA Q800 in tension mode at 5 °C/min and 1 Hz. A Perkin-Elmer Pyris 1 cryogenic instrument was used for differential scanning calorimetry (DSC) at a heating rate of 10 ^{o}C/min under nitrogen. A Varian Unity 400 MHz NMR spectrometer was employed at 25 ^{o}C using *d*-chloroform.

3.3 Results and Discussion

The highly branched topology provided an opportunity for fundamentally probing the effect of branching on the structure and mechanical performance of ionenes. Highly branched ionenes were synthesized via a modified Menschutkin reaction, and dihalides were replaced with trifunctional reactive halides. Tris(bromomethyl)mesitylene (TBMM) and bis(dimethylamino) poly(tetramethylene oxide) (BAPTMO) were used in a 1:1 molar stoichometry. BAPTMO was synthesized from the living cationic polymerization of tetrahydrofuran (THF) (Scheme 3.1). Trifluoromethanesulfonic anhydride was used as the initiator to achieve a difunctional PTMO. The molecular weight of PTMO was controlled through adjustment of the monomer to initiator ratio, which is a typical strategy for control of molecular weight for living polymerizations. The living cationic PTMO was endcapped with methyl 3-(dimethylamino) propionate instead of dimethyl amine, which was used previously,[141] to avoid further alkylation of the amine during the endcapping process. Upon completion of the reaction of living PTMO with methyl 3-(dimethylamino) propionate, the quaternary amine was converted to a tertiary amine through a reverse Michael addition. The products of the reverse Michael addition were the BAPTMO and methyl acrylate. The methyl acrylate was efficiently removed during precipitation and BAPTMO was subsequently used as the *oligomeric* A_2 in the synthesis of highly branched ionenes. Two molecular weights of BAPTMO were synthesized (approximately 2,000 and 7,000 g/mol), and the molecular weights calculated from integration of ^{1}H NMR spectra agreed well with titration of the amine endgroups (Table 3.1). BAPTMO (A_2) was added dropwise to a dilute solution of

TBMM (B_3) in dry THF over a period of an hour to reduce the potential for crosslinking (Scheme 3.2).

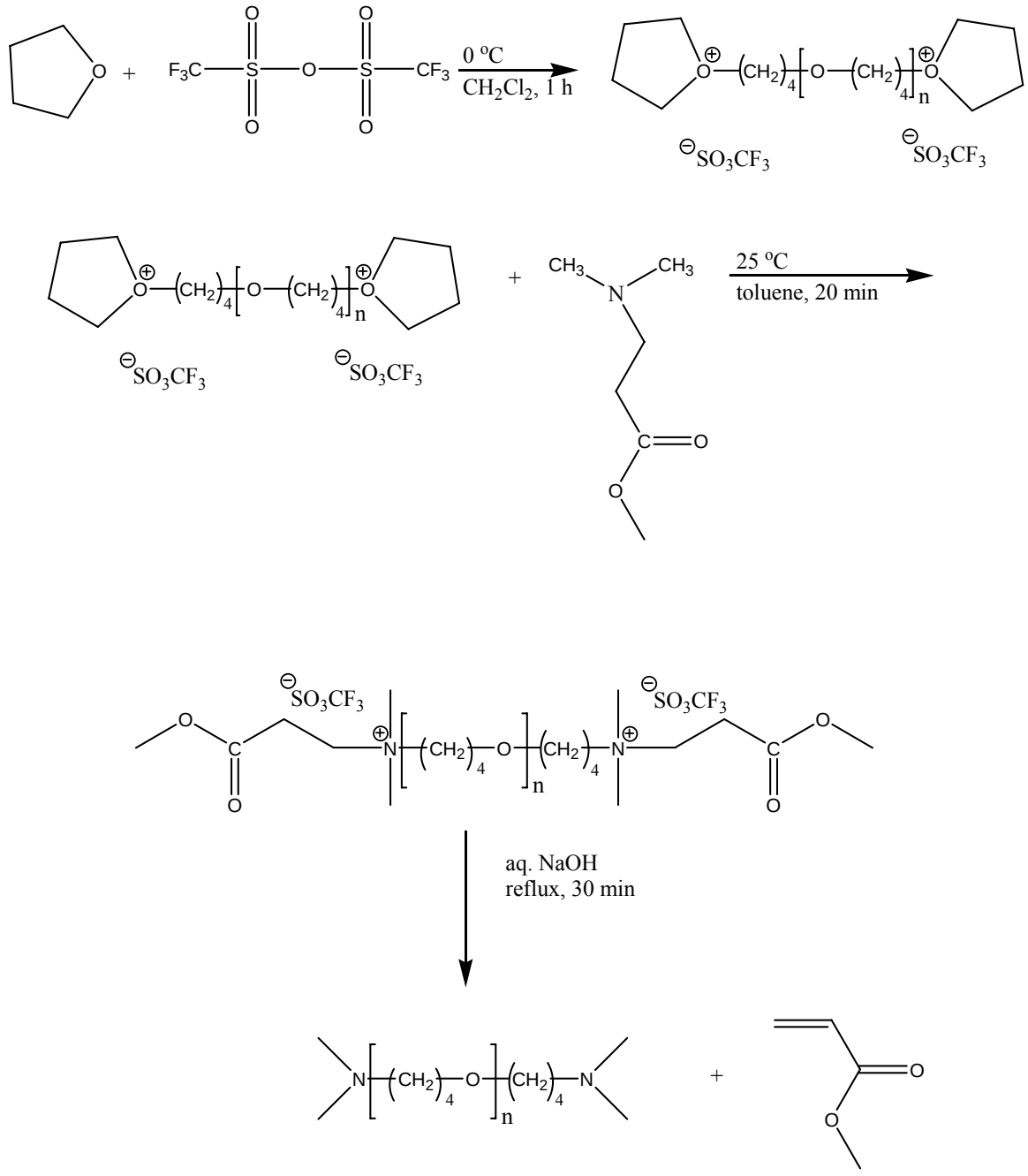

Scheme 3.1: Synthesis of BAPTMO, *oligomeric* A_2

Slow addition and dilute solutions are frequently used for A_2 plus B_3 polymerizations to avoid gelation.[158] The reaction was prone to crosslinking at higher concentrations but remained soluble at a final concentration of 6 wt% or below. The ionenes were cast on a glass plate and dried. The resulting films were translucent, pale-ivory, and ductile.

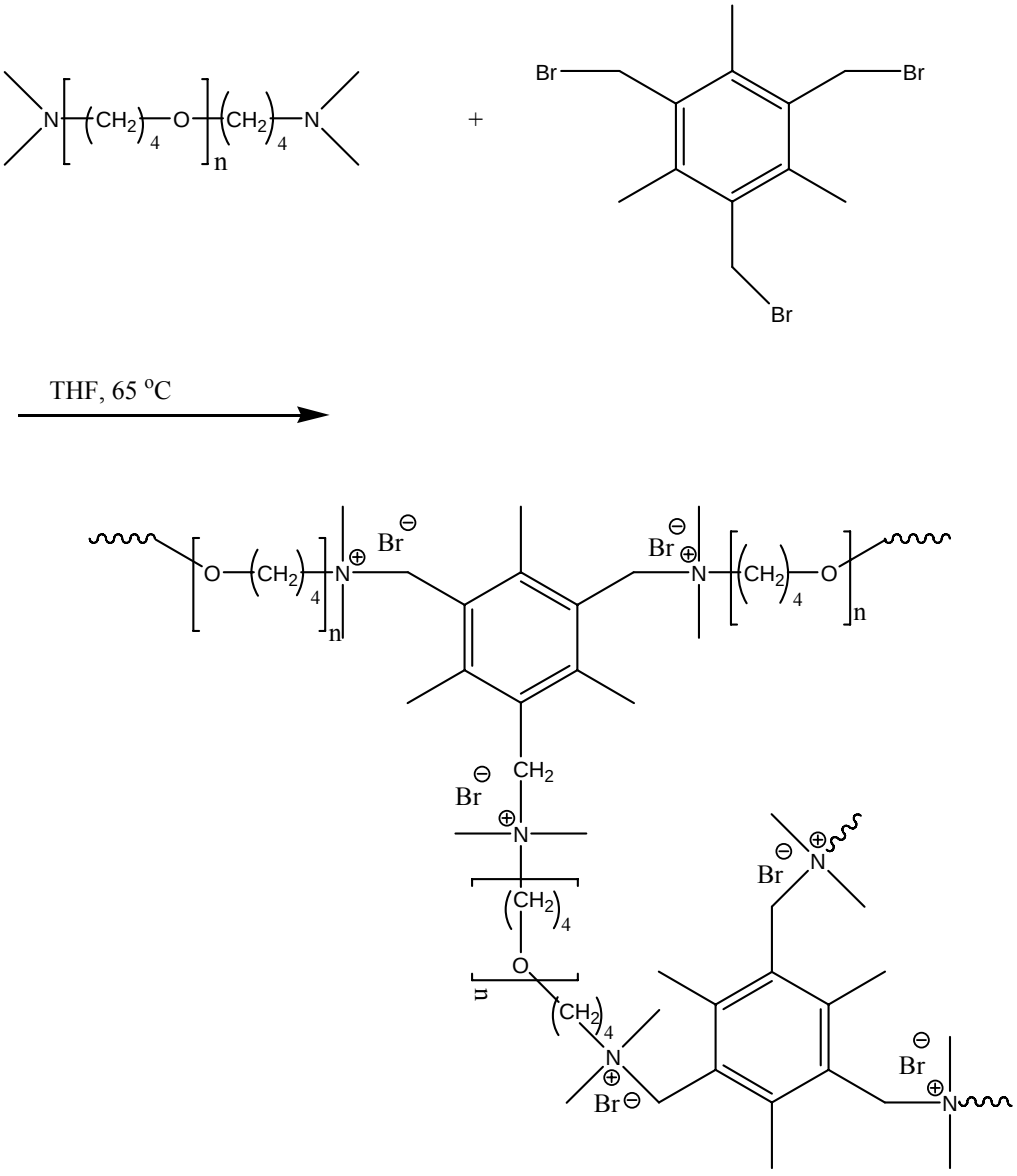

Scheme 3.2: Highly branched ionene synthetic scheme

Table 3.1: Summary of DSC data from highly branched and linear ionenes

Sample ID	Architecture	BAPTMO M_n (g/mol)[a]	BAPTMO M_n (g/mol)[b]	T_g (^oC)	T_m (^oC)
LI-2k	linear	1,700	2,100	-78	28
LI-7k	linear	5,500	6,400	-78	26
HBI-2k	highly branched	2,100	2,100	-75	30
HBI-7k	highly branched	5,700	6,900	-78	33

[a] ^{1}H NMR spectroscopy
[b] Titration with HCl

Dynamic mechanical analysis (DMA) was used to probe the dependence of storage modulus (E') and tan δ on temperature for linear and highly branched ionenes. Two molecular weights were chosen to determine the effect of distance, below and above the molecular weight for entanglement of PTMO (M_c = 2,500 g/mol), between branch points on the properties of the highly branched ionenes. The initial storage moduli below -70 ^{o}C of all samples were approximately 10^9 Pa, which are typical for glassy polymers (Figure 3.1).[159] A decrease in the storage modulus, E', was observed at about -50 ^{o}C and attributed to the glass transition of the PTMO. A peak in the tan δ curve occurred at this temperature, -60 ^{o}C, as well. Both LI-2k and HBI-2k ionenes with 2,000 g/mol PMTO had a smaller peak in tan δ for the PTMO T_g due to the restriction of mobility from the connecitivity from the ionic associations for each architecture. Branching and lower PTMO molecular weight had similar effects on the intensity of the tan δ peak for the PTMO T_g. In both cases, when comparing the linear and highly branched ionenes with the same PTMO molecular weight, the tan δ peak was reduced for the highly branched

architectures. The gradual increase in E' as the tempeartature was raised from -60 to 50 ^{o}C was attributed to the melting and crystallization of the PTMO.

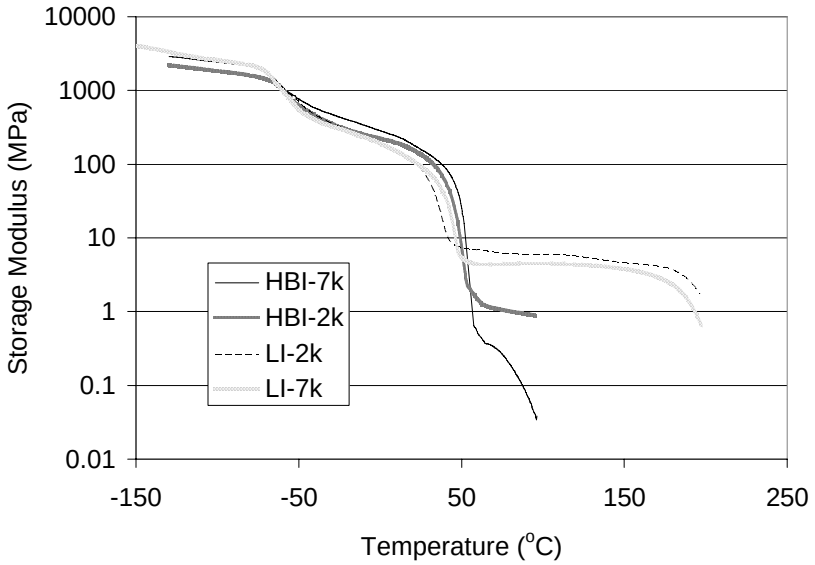

Figure 3.1: Dynamic mechanical analysis of highly branched and linear ionenes based on 2,000 and 7,000 g/mol PTMO

The linear ionenes each had a transition that was associated with PTMO melting i.e. ~15 ^{o}C for LI-2k and ~35 ^{o}C for LI-7k. The difference in the endotherm transition was attributed to the differences in crystallinity for each ionene. The plateau moduli over this temperature range (-60 to 50 ^{o}C) were similar for all architectures and soft segment lengths. The crystalline phase of PTMO in both the highly branched and linear ionenes began melting at approximately 50 ^{o}C, which was revealed in the decrease in E' for both the highly branched and linear ionenes. Interestingly, earlier linear ionenes with an aromatic chain extender (1,4-dibromo-*p*-xylene) melted at much lower temperatures (~0 ^{o}C) compared to the linear ionenes reported herein (~50 ^{o}C).[151] It was proposed that

earlier synthetic methodologies employed PTMO soft segments that led to further alkylation during dimethylamine endcapping. Further alkylation is proposed to lead to an increase in polydisperisty of the soft segment corresponding to lower melting temperatures. HBI-7k exhibited the most dramatic decrease in E' after the crystalline regions of the PTMO melted. HBI-7k had the lowest storage modulus due to a combination of a greater distance between cations, which corresponded to a decrease in the concentration of cations, and the incorporation of branching. A similar effect on the storage modulus was observed previously with the addition of zinc stearate as a plasticizer for PTMO-based ionenes.[152] HBI-2k was found to have a plateau in storage modulus after the crystalline region of the PTMO melted; however, the storage modulus plateau for HBI-2k was lower than for LI-2k. However, the significant plateau in E' for HBI-2k indicated that the increased concentration of ionic sites when compared to HBI-7k strengthened the ionic association and provided a rubbery plateau at high temperatures. The plateau in storage modulus of the ionenes was attributed to the presence of ionic aggregates. A SAXS interdomain spacing of 7-12 nm was determined for PTMO-based ionenes.[160] The presence of the ionic aggregates was confirmed with SAXS and TEM in these earlier studies.[161] The mechanical behavior of segmented ionenes is frequently attributed to aggregation of ionic groups. Higher E' for HBI-2k at 50 to 200 ^{o}C compared to HBI-7k was attributed to the higher concentration of ionic groups in HBI-2k, which was consistent with previous findings.[151] While there was a rubbery plateau for HBI-2k, the plateau in E' after 50 ^{o}C was much lower than for the linear analog. E' appeared approximately constant for the LI-7k from approximately 50 to 200 ^{o}C. The rubbery plateau modulus was slightly higher for LI-2k than for LI-7k due

to the increased concentration of ionic aggregates. Whether the PTMO was above or below the molecular weight for entanglement appeared to be much less influential on the thermal properties of the ionenes than the distance between ionic groups. Only a slight influence of the longer PTMO soft segment was observed in the rubbery plateau for linear ionenes and a deleterious effect on rubbery plateau was observed for the longer distance between ionic groups in the highly branched ionenes.

DSC of all the samples showed the T_g of PTMO at approximately -78 ^oC for the linear and highly branched polymers. The T_g was close to that of PTMO. The melting transition observed in the DSC was attributed to melting of PTMO. The amount of crystallization as determined using the change in enthalpy was approximately the same, which indicated that the branching had not disrupted the crystallinity in the highly branched ionenes.

The TGA of the ionenes indicated that the degradation temperature at 5 % weight loss was comparable for other linear ionenes.[162, 163] For the LI-7k, the temperature at 5 % weight loss was 240 ^oC and 276 ^oC for LI-2k (Figure 3.2). The highly branched ionenes had similar degradation temperatures to linear ionenes. HBI-7k had 5 % weight loss at 256 ^oC, and the HBI-2k degraded to 5% weight loss at 238 ^oC. The highly branched ionenes degraded at similar temperatures to the linear analogs. Both linear and highly branched ionenes were synthesized with approximately a 1:1 molar ratio of reactive halide to diamine. The similar content of quaternary amines, where dequaternization is the primary mechanism for the degradation of ionenes, led to similar temperatures of degradation at 5 % weight loss.

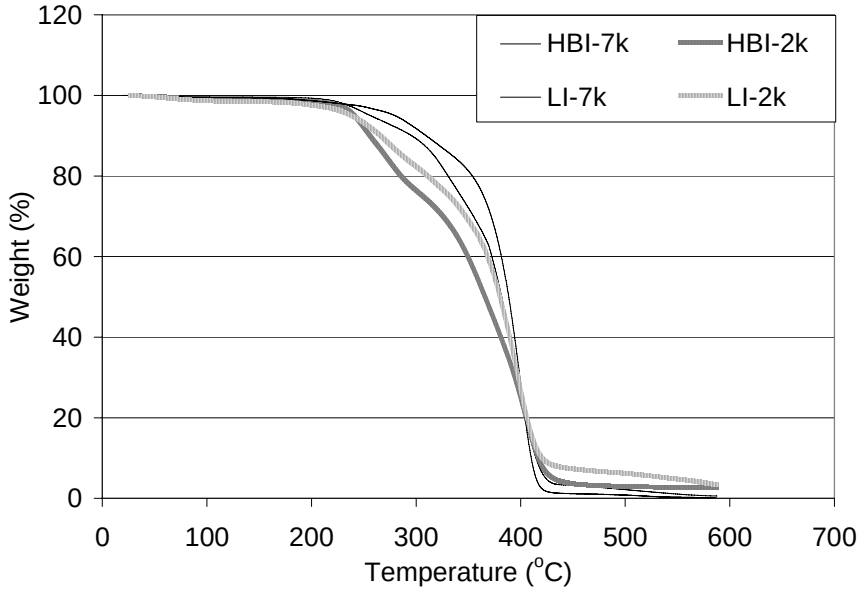

Figure 3.2: TGA of linear and highly branched ionenes

However, over the 150 °C range of approximately 250 to 400 °C from 5 % weight loss and char, the LI-7k and HBI-7k degraded at higher temperatures than LI-2k and HBI-2k. With a lower concentration of quaternary amines in the backbone, LI-2k and HBI-2k degraded at higher temperatures. It was also found that the highly branched ionenes degraded at lower temperatures than the linear analogs. The thermal degradation of hyperbranched polymers was shown to occur at lower temperatures previously.[124] It was proposed that the electron donating nature of the neighboring methyl groups adjacent to unreacted methylbromide groups contributed to the faster degradation of the highly branched polymers compared to the linear.

While the melt rheology of the ionenes led to only qualitative results because the molecular weights were not determined, there were some interesting trends. The

complex viscosity was determined for all of the ionenes at 80 ^{o}C. The complex melt viscosity has implications for the processsibility of the ionenes, which are not thermally stable at high temperatures due to de-quaternization of the amines.[141] While the thermal stability is a function of the chemical structure of the ionenes, aromatic halides are some of the most thermally stable of ionenes synthesized via the Menschutkin reaction.[141] The complex viscosity of the linear ionenes was approximately the same at 80 ^{o}C over the frequency range probed (0.1 to 10 Hz) (Figure 3.3). Shear-thinning was observed for the linear ionenes and a slope of approximately 1 was found for the log η^* vs. ω curves. The highly branched ionenes had lower melt viscosities than the linear analogs. While the absolute molecular weights were unknown, it was interesting to note that the linear ionenes had virtually the same complex viscosity. HBI-2k exhibited shear-thinning over the range of frequencies investigated (Figure 3.3b). The complex viscosity was more than a magnitude lower for HBI-2k than for the linear analog, LI-2k. HBI-7k exhibited a greater reduction in complex viscosity than HBI-2k. Compared to LI-7k, the complex viscosity of HBI-7k was more than two orders of magnitude (Figure 3.3b). Shear-thinning was observed for HBI-7k. The lower complex viscosity of the highly branched ionenes when compared with the linear analogs was in agreement with the observed E' that was higher for the linear ionenes than the highly branched ionenes. While crystallinity did not appear to be disturbed, ionic aggregation clearly was altered as evidenced by the flow behavior, which did not exhibit the typical slope of ~1.0 for crosslinked systems, at low temperature (80 ^{o}C) for the highly branched ionenes. The storage modulus was constant and much higher for the linear ionenes than the highly branched ionenes. This was consistent with the DMA of linear ionenes, where a

substantial change in E' was not observed from 50 to 200 ^{o}C. Also, HBI-7k exhibited a lower storage modulus than HBI-2k, which was expected due to the observed low storage modulus of HBI-7k in the DMA. The reduced concentration of ionic aggregates coupled with the disruption of aggregates with branching resulted in the HBI-7k having the lowest plateau in storage modulus, complex viscosity, and storage modulus at low temperature.

Figure 3.4 depicts the mechanical behavior of the ionenes. There was considerable difficulty with slippage of the linear ionenes at high elongations in the Instron. Therefore, there was a smaller sample set for the linear ionenes than the highly branched (LI-7k, 2 samples; LI-2k 1 sample). Both linear ionenes showed tremendous mechanical properties, which was reported previously for different compositions.[151] The upturn in the stress-strain curve for the linear ionenes was attributed to strain-induced crystallization of the PTMO soft segments (Figure 3.4).[151] LI-2k and LI-7k have ultimate tensile strengths greater than 35 MPa, but the tensile strength of LI-2k is slightly lower than that of LI-7k (LI-2k, 37.4 MPa; LI-7k, 40.1 MPa). The linear ionenes have elongations at break that exceed 1000%, but LI-2k was slightly lower than LI-7k (LI-2k, 1086%; LI-7k, 1233%). The Young's modulus for LI-2k was averaged from 6 samples (5 of which experienced slippage at high elongation). The Young's modulus for LI-2k was lower, 4.5 MPa, than LI-7k, 8.9 MPa. However, both linear ionenes had tremendous tensile strength and elongation at break. The ionic aggregates in these ionenes as well as the strain-induced crystallization of the PTMO soft segment imparted the excellent mechanical properties. The mechanical behavior of the highly branched ionenes was averaged over 3 samples (Figure 3.4).

a)

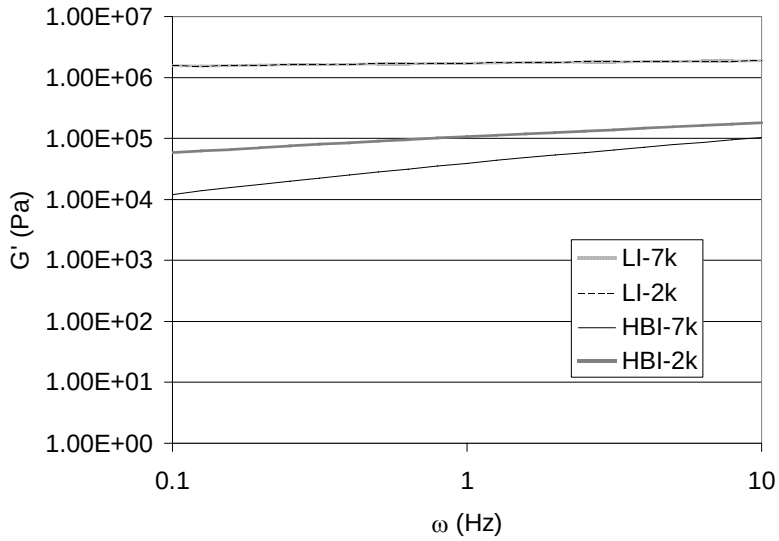

b)

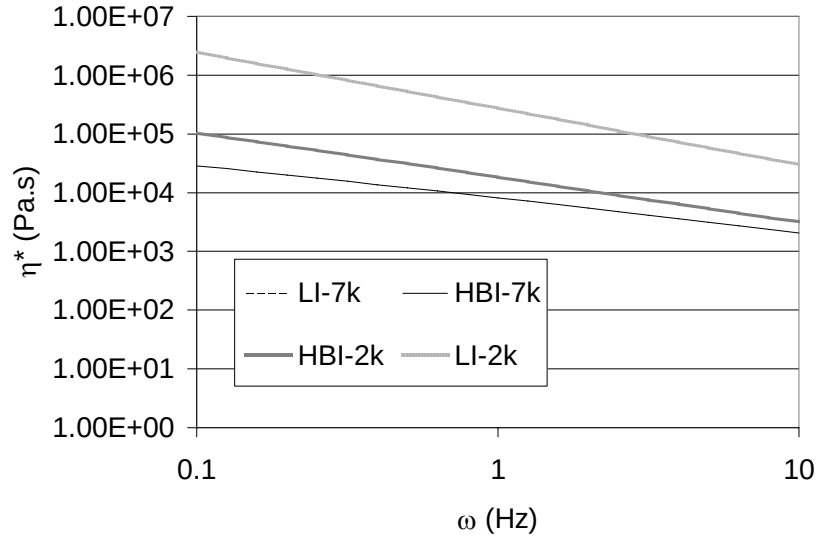

Figure 3.3: Melt rheological behavior of linear and highly branched ionenes. LI-7k and LI-2k overlap in both plots. a) storage modulus versus frequency b) complex viscosity versus frequency at 80 ^{o}C

HBI-7k had higher elongation at break (545%) compared with HBI-2k (437%), which was attributed to a weaker "network" due to the longer distance between ionic groups (i.e. higher molecular weight PTMO) (Table 3.2). With a lower concentration of ionic groups in the backbone, which was a reduction in the number of pseudo-crosslinks, HBI-7k had a lower Young's modulus (0.74 MPa) than the HBI-2k (0.86 MPa). However, the Young's modulus was quite low for both highly branched ionenes. A higher number of ionic associations in the highly branched ionene based on the lower molecular weight PTMO led to a greater ultimate tensile strength (1.69 MPa) for HBI-2k compared with HBI-7k (1.13 MPa). The lower Young's moduli of the highly branched ionenes compared to the linear counterparts were a good indication that the ionic associations of the highly branched ionenes were disrupted with branching, because the Young's modulus is independent of molecular weight. The mechanical properties of the highly branched ionenes were reduced compared to the impressive tensile behavior of linear, segmented ionenes. Linear, segmented ionenes have ultimate tensile strengths of >30 MPa and elongations at break in excess of 1000%. Loveday et al. found that the regular spacing of the ionic groups along the backbone of the ionene was crucial for good mechanical properties.[150] The mechanical properties from the polyurethane ionenes synthesized in that study are comparable to those found for highly branched ionenes.

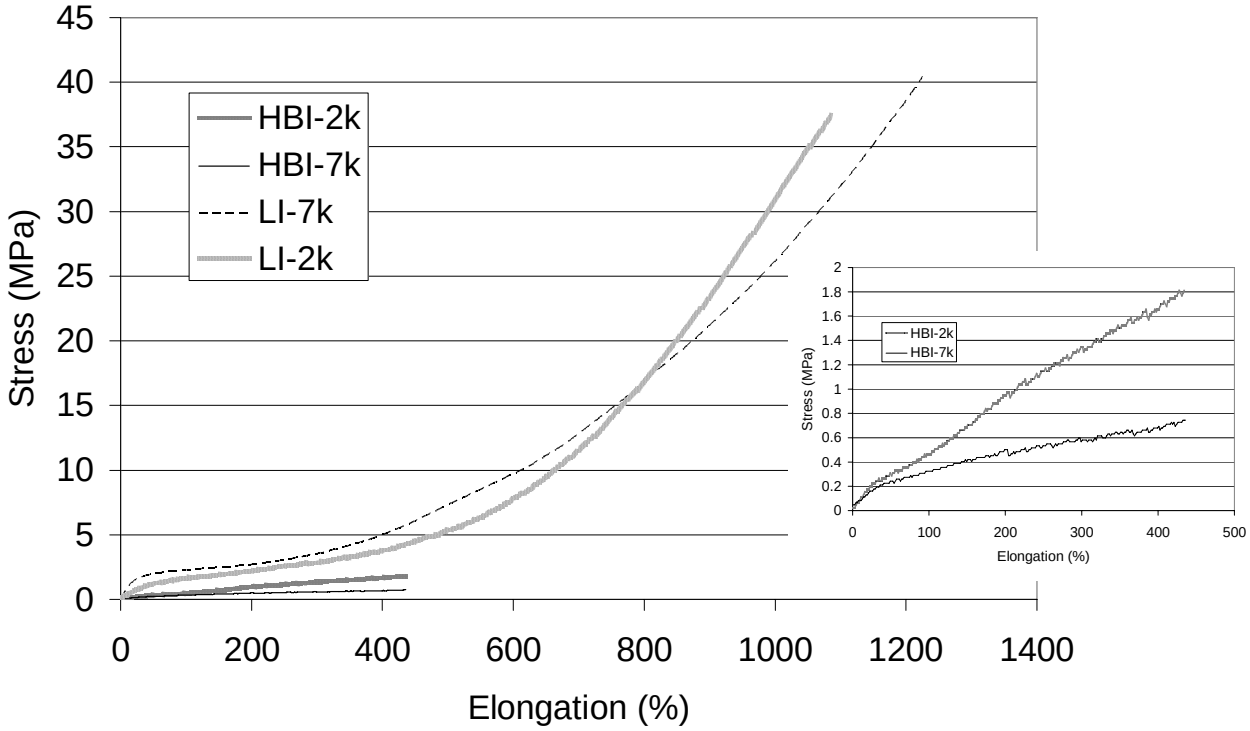

Figure 3.4: Tensile behavior of linear and highly branched ionenes at 25 ^{o}C. Inset: comparison of highly branched polymers

The presence of some ionic aggregation was consistent with results from DMA, melt rheology, and tensile properties. Work on model poly(urethane urea)s, where non-covalent interactions lead to microphase separation in linear systems, indicated that branching can severely disrupt the long range order of microphases from non-covalent interactions.[164, 165] The reduced but constant plateau in storage modulus of HBI-2k was indicative that some microphase separation was present in the HBI-2k system, but it was not to the same extent as the linear analog. The mechanical properties of HBI-2k were reduced when compared to the mechanical properties for the linear analogs. Further

investigation of8 the microphase separation of the highly branched and linear ionenes including AFM and SAXS is underway.

Table 3.2: Mechanical properties of linear and highly branched ionenes

Sample	Young's modulus (MPa)	Ultimate tensile strength (MPa)	Elongation at break (%)
LI-2k*	4.5 ± 2.0	30.7	1086
LI-7k	8.9 ± 0.28	40.1 ± 9.2	1233 ± 0.13
HBI-2k	0.86 ± 0.05	437 ± 62	1.69 ± 0.32
HBI-7k	0.74 ± 0.26	545 ± 119	1.13 ± 0.27

*One sample reported for ultimate tensile strength and elongation at break due to problems with slippage in the Instron

3.4 Conclusions

Linear and highly branched ionenes based on PTMO with molecular weights of 2,000 and 7,000 g/mol were synthesized via a modified Menschutkin reaction. The branching in the ionic groups effectively reduced the influence of ionic aggregates on the system. The plateau in storage modulus of the branched ionenes was significantly reduced due to the introduction of the branched ionenes. Typically, a shift in the T_g from the typical soft segment T_g with the disruption of microphase separation occurs. However, the T_g of the linear ionenes was comparable to the highly branched T_g. While there was no evidence of the reduction in the DSC, the loss in plateau in storage modulus after the PTMO T_m for the highly branched ionenes and the dramatic reduction in mechanical properties indicated that the ionic aggregates were effectively disrupted in the HBI-7k and somewhat disrupted in HBI-2k. The narrow molecular weight distribution PTMO soft segments aided in the microphase separation and excellent mechanical properties of the linear ionenes (ultimate tensile strength >35 MPa, elongation at break > 1000%). The influence of the molecular weight between entanglements for the soft segment was masked with the subsequent reduction in concentration of the ionic groups.

Further studies on the nature of microphase disruption in the highly branched ionenes (e.g. AFM, SAXS) are ongoing.

3.5 Acknowledgements

This material is based upon work supported by the U.S. Army Research Laboratory and the U.S. Army Research Office under grant number DAAD19-02-1-0275 Macromolecular Architecture for Performance (MAP) MURI. The authors thank Dr. Charles Leir for his helpful discussions.

3.6 References

1. Trukhanova, E. S.; Izumrudov, V. A.; Litmanovich, A. A.; Zelikin, A. N. *Biomacromolecules* **2005** 6, 3198-3201.

2. Hadek, V.; Noguchi, H.; Rembaum, A. *Macromolecules* **1971** 4, 494-499.

3. Lupinski, J. M.; Kopple, K. D.; Hertz, J. J. *J. Polym. Sci., Polym. Symp.* **1967** 16, 1561-1578.

4. Dieterich, D.; Keberle, W.; Witt, H. *Angew. Chem., Int. Ed. Engl.* **1970** 9, 40-50.

5. Tsutusi, T.; Tanaka, R.; Tanaka, T. *J. Polym. Sci., Polym. Phys. Ed.* **1976** 14, 2273-2284.

6. Menschutkin, N. *Z. Phys. Chem.* **1890** 5, 589.

7. Rembaum, A.; Baumgartner, W.; Eisenberg, A. *J. Polym. Sci., Polym. Lett.* **1968** 6, 159-171.

8. Wang, J.; Meyer, W. H.; Wegner, G. *Macromol. Chem. Phys.* **1994** 195, 1777-1795.

9. Leir, C. M.; Stark, J. E. *J. Appl. Polym. Sci.* **1989** 38, 1535-1547.

10. Eisenberg, A. *Macromolecules* **1971** 4, 125-128.

11. Rembaum, A. *Appl. Polym. Symp.* **1973** 22, 299-317.

12. Casson, D.; Rembaum, A. *Macromolecules* **1972** 5, 75-81.

13. Toutianoush, A.; Saremi, F.; Tieke, B. *Mat. Sci. Eng. C* **1999** 8-0, 343-352.

14. Hong, J.-D.; Jung, B.-D.; Kim, C. H.; Kim, K. *Macromolecules* **2000** 33, 7905-7911.

15. Han, H.; Vantine, P. R.; Nedeltchev, A. K.; Bhowmik, P. K. *J. Polym. Sci.: Part A: Polym. Chem.* **2006** 44, 1541-1554.

16. Yen, S. P. S.; Casson, D.; Rembaum, A. *Polym. Sci. Tech.* **1973** 2, 291-312.

17. Bayoudh, S.; Laschwesky, A.; Wischerhoff, E. *Colloid Polym. Sci.* **1999** 277, 519-527.

18. Loveday, D.; Wilkes, G. L.; Bheda, M. C.; Shen, Y. X.; Gibson, H. W. *Pure Appl. Chem.* **1995** A32, 1-27.

19. Feng, D.; Venkateshwaran, L. N.; Wilkes, G. L.; Leir, C. E.; Stark, J. E. *J. Appl. Polym. Sci.* **1989** 37, 1549-1565.

20. Venkateshwaran, L. N.; Leir, C. E.; Wilkes, G. L. *J. Appl. Polym. Sci.* **1991** 43, 951-966.

21. Kotzev, A.; Laschewsky, A.; Adriaensens, P.; Gelan, J. *Macromolecules* **2002** 35, 1091-1101.

22. Dragan, S.; Cazacu, M.; Toth, A. *J. Polym. Sci.: Part A: Polym. Chem.* **2002** 40, 3570-3578.

23. Tsutusi, T.; Tanaka, R.; Tanaka, T. *J. Polym. Sci., Polym. Phys. Ed.* **1975** 13, 2091-2102.

24. Davis, A.; Golden, J. *Makromol. Chem.* **1965** 81, 38-50.

25. Voit, B. *J. Polym. Sci.: Part A: Polym. Chem.* **2005** 43, 2679-2699.

26. Hawker, C. J.; Farrington, P. J.; Mackay, M. E.; Wooley, K. L.; Frechét, J. M. J. *J. Am. Chem. Soc.* **1995** 117, 4409-4410.

27. Kim, Y. H. *J. Polym. Sci.: Part A: Polym. Chem.* **1998** 36, 1685-1698.

28. Hong, Y.; Coombs, S. J.; Cooper-White, J. J.; Mackay, M. E.; Hawker, C. J.; Malmstrom, E.; Rehnberg, N. *Polymer* **2000** 41, 7705-7713.

29. Unal, S.; Lin, Q.; Mourey, T. H.; Long, T. E. *Macromolecules* **2005** 38, 3246-3254.

30. Unal, S.; Oguz, C.; Yilgor, E.; Gallivan, M.; Long, T. E.; Yilgor, I. *Polymer* **2005** 46, 695-696.

31. Unal, S.; Yilgor, I.; Yilgor, E.; Sheth, J. P.; Wilkes, G. L.; Long, T. E. *Macromolecules* **2004** 37, 7081-7084.

32. McKee, M. G.; Park, T.; Unal, S.; Yilgor, I.; Long, T. E. *Polymer* **2005** 46, 2011-2015.

33. Fornof, A. R.; Long, T. E. *Unpublished data* **2006**.

34. Czupik, M.; Fossum, E. *J. Polym. Sci., Part A: Polym. Chem.* **2003** 41, 3871-3881.

35. Campbell, D.; Pethrick, R. A.; White, J. R., In *Polymer Characterization: Physical Techniques*. Second ed.; Stanley Thornes (Publishers) Ltd: London, 2000.

36. Ikeda, Y.; Murakami, T.; Yuguchi, Y.; Kajiwara, K. *Macromolecules* **1998** 31, 1246-1253.

37. Feng, D.; Wilkes, G. L.; Leir, C. E.; Stark, J. E. *J. Macromol. Sci.-chem.* **1989** A26, 1151-1181.

38. Meyer, W. H.; Dominguez, L., In *Polymer Electrolyte Reviews--2 Ch. 6 Structure and Properties of Ionene Polymers*. Elsevier Applied Science: New York, 1989.

39. Grassl, B.; Galin, J. C. *Macromolecules* **1995** 28, 7035-7045.

40. Fossum, E.; Tan, L.-S. *Polymer* **2005** 46, 9686-9693.

41. Sheth, J. P.; Wilkes, G. L.; Fornof, A. R.; Long, T. E.; Yilgor, I. *Macromolecules* **2005** 38, 5681-5685.

Chapter 4: Degree of Branching of Highly Branched Polyurethanes Synthesized via the *Oligomeric* A_2 Plus B_3 Methodology: ^{13}C NMR Spectroscopic Investigations

(Fornof, A.R.; Glass, T.E.; Long, T.E. *Macromol. Chem. Phys.* **2006**, *Accepted*)

4.1 Abstract

The *oligomeric* A_2 plus monomeric B_3 synthetic methodology provided highly branched, poly(ether urethane)s based on trimethylol propane (B_3) and isocyanate endcapped polyethers. ^{13}C NMR spectroscopic assignments for the branched polyurethanes were verified using model urethane-containing compounds based on trimethylol propane and a monofunctional isocyanate (either cyclohexyl or phenyl isocyanate). Derivatization of hydroxyl endgroups with trifluoroacetic anhydride enhanced the ^{13}C NMR resolution in spectra for branched polyurethanes. The ^{13}C NMR resonance for the linear unit exhibited a broad shoulder due to quaternary carbons that were attributed to cyclic species in the highly branched polyurethanes. The classical degree of branching calculation revealed the efficiency of the B_3 monomer for branching; however, an equation that incorporated the linear contribution of the A_2 oligomer provided a more accurate degree of branching for highly branched polyurethanes.

Keywords: Highly branched, degree of branching, polyurethanes, hyperbranched

4.2 Introduction

Flory's theoretical predictions involving AB_x monomer polycondensation and the formation of hyperbranched polymers received sparse attention until the synthesis of hyperbranched polyphenylenes in the early 1990s.[5, 59] Fréchet et al. subsequently demonstrated the AB_2 step-growth polymerization of soluble hyperbranched polyurethanes using a blocked isocyanate and a hydroxyl group with careful synthetic methods.[166] During the same year, Kumar and Ramakrishnan used a Curtius-type rearrangement of dihydroxybenzoylazide in a one-pot synthesis of hyperbranched polyurethanes. A number of other synthetic strategies followed for the synthesis of hyperbranched polyurethanes.[31, 167]

The low molar mass A_2 plus B_3 route re-emerged in recent years as an alternative to functionally nonsymmetrical AB_x monomers for hyperbranched polymers.[168-170] Emrick et al. used this synthetic strategy for the synthesis of hyperbranched polyethers.[171] A major advantage of the A_2 plus B_3 approach is the commercial availability of A_2 and B_3 monomers due to symmetrical functionality.[172] For example, the use of an oligomeric A_2 with a trifunctional B_3 was recently demonstrated in our laboratories and provides highly branched polymers with segments of sufficient length for entanglement leading to enhanced mechanical properties.[16, 170] Hyperbranched and dendritic polymers typically have short distances between branch points, which do not enable entanglements, and our earlier efforts demonstrated the need to balance degree of branching and distance between branch points.[9]

Hawker et al. incorporated non-entangled linear units into AB_x monomer structure to synthesize hyperbranched poly(ethylene glycol) (n = 1, 2 or 5).[16] It was suggested that these hyperbranched polyethers, which had varying segment lengths between branch points, were suitable as ionic conductors. The segment lengths between branch points for these polyethers were well below the critical molar mass for entanglement, and as expected, waxy solids were achieved. However, an improvement was observed in the ionic conductivity of the hyperbranched polyethers compared to linear analogs. [171 ,64]

Hawker et al. proposed a calculation of the degree of branching (DB) for hyperbranched polymers, as defined from Flory's description of AB_2 condensation

$$DB = (D + T)/(D + T + L) \qquad \text{Equation (1)}$$

where D is the number of dendritic units, T is the number of terminal units, and L is the number of linear units.[36] A number of alternate equations were proposed for special cases. For example, Hölter et al. proposed an equation,

$$DB = 2D/(2D + L) = (D + T - N)/(D + T + L - N) \qquad \text{Equation (2)}$$

that was independent of the molecular weight of the hyperbranched polymer or sparsely branched polymers, where N is the number of hyperbranched molecules.[67] At high molecular weights, N becomes negligible, and the degrees of branching calculated from Equation (1) and (2) are equal. Most recently, Long et al. suggested a variation for the calculation of the degree of branching in the presence of oligomeric reagents,

$$DB = (D + T)/(D + L + T + n) \qquad \text{Equation (3)}$$

where n is the degree of polymerization of the oligomeric A_2 or B_3 reactant.[173]

Our efforts herein employ poly(ethylene glycol) (PEG) as an A_2 oligomer. An A_2 oligomer rather than a monomer permits longer uninterrupted ethylene oxide units for

increased chain mobility and possibly increased conductivity. Highly branched, PEG-based polyurethanes are also film-forming, which is useful for solid polymer electrolyte applications.[174] Equation (1) was used to evaluate the degree of branching for poly(ether urethane)s that were synthesized via the *oligomeric* A_2 plus monomeric B_3 route. A treatment of the data, which incorporates the number of monomeric units from the oligomeric A_2 into the total degree of branching, is proposed herein. In addition, this is the first time that the degree of branching of a highly branched or hyperbranched polyurethane was revealed using ^{13}C NMR spectroscopy.

4.3 Experimental

4.3.1 Materials

Bayer kindly supplied 2,200 and 4,200 g/mol poly(propylene glycol) (PPG, Acclaim^{TM}), which has low unsaturation and a high degree of difunctionality. Poly(tetramethylene glycol) (PTMO) (Terathane 2000) and poly(ethylene glycol) (PEG) of two different molecular weights (600 and 2,000 g/mol) were obtained from Aldrich and dried at 80 °C at reduced pressure overnight prior to use. Bayer AG provided dicyclohexylmethane-4,4'-diisocyanate (HMDI), which was used as received. 1,4-Butanediol was purchased from Aldrich and dried over 3 Å molecular sieves. Cyclohexyl isocyanate (CHI), phenyl isocyanate (PI), and dibutyltin dilaurate (DBTDL) were obtained from Aldrich and used as received. Chromatographic grade tetrahydrofuran (THF) was purchased from Reagents, Inc. and used without further purification.

4.3.2 Synthesis of model compounds

Trimethylol propane (0.5367 g, 4.0 mmol) and cyclohexyl isocyanate (1.001 g, 8.0 mmol) or phenyl isocyanate (0.9530 g, 8.0 mmol) were added to a 50-mL, round-bottomed flask. The reaction mixture was magnetically stirred and 100 ppm dibutyltin dilaurate, DBTDL, was added as a catalyst. The reaction was allowed to proceed for 1 h at 80 °C. The reaction mixtures were precipitated in hexanes to remove any unreacted isocyanate and dried at reduced pressure at 80 °C. Flash column chromatography was used to separate the three possible products of the isocyanate and trimethylol propane reaction with a gradient of hexane and ethyl acetate as the mobile phase.

4.3.3 Synthesis of linear polyurethanes

Linear polyurethanes were synthesized in a conventional two-step process.[136] The prepolymer was formed from the reaction of an oligomeric diol (4.30 g, 7.2 mmol of PEG 600 g/mol) and HMDI (14.0 g, 18 mmol) in bulk at 80 °C for 1 h with 100 ppm DBTDL catalyst. After complete reaction, tetrahydrofuran (9 mL) was used to dissolve the prepolymer. A 50 wt% solution of the chain extender, 1,4-butanediol (0.98 g, 11 mmol), in THF was added dropwise to the prepolymer to form the linear polyurethane. This reaction was cooled to room temperature after approximately 8 h when FTIR confirmed the quantitative disappearance of isocyanate groups.

4.3.4 Synthesis of highly branched polyurethanes

The prepolymers were formed in an identical fashion as described for the linear polyurethane. The prepolymer was dissolved to form a 30 wt% solution in THF and added dropwise to a 10 wt% solution in THF of the B_3 monomer, TMP, at 80 °C. The

reaction was allowed to proceed for 8 h or until FTIR spectroscopy indicated complete conversion of isocyanate. The reaction was diluted with THF as needed to ensure a low viscosity solution.

4.3.5 Derivatization of endgroups

The highly branched polyurethane (0.39 g, 0.03 mmol) was dissolved in 15 mL of dry THF at 3 wt%. Trifluoroacetic anhydride (6.0 g, 30 mmol) was added at room temperature to the magnetically stirred solution under a nitrogen atmosphere. The reaction was allowed to proceed for 1 h. THF and excess trifluoracetic anhydride were removed at 25 °C with reduced pressure.

4.3.6 Polymer characterization

Size exclusion chromatography (SEC) was used to determine molecular weights with a Waters 717 autosampler, Waters 2410 refractive index detector, a Wyatt Technology mini-DAWN triple-angle light scattering detector, and a Viscotek viscometer. Quantitative ^{13}C NMR spectroscopy was performed on the highly branched polyurethanes under ambient conditions on a Varian Unity at 100 MHz. Quantitative ^{13}C NMR of the highly branched polyurethanes included inverse gated proton decoupling to minimize the nuclear Overhauser enhancements as well as included long recycle delays (6 s) in $CDCl_3$ with approximately 60 mmol chromium acetylacetonate. The ^{13}C DEPT 45 NMR spectroscopic analysis of the model compounds was performed on a Varian Inova at 100 MHz. FTIR was performed on a MIDAC M-1700 with Durascope single bounce diamond ATR. Accurate mass of the model compounds was determined on a JMS-HX110 dual focusing mass spectrometer. Fast atom bombardment was used with a

nitrobenzyl alcohol matrix, poly(ethylene glycol) standard, and a signal-to-noise ratio of 5000. A CH Instruments electromechanical analyzer was used at a high frequency of 100,000 Hz and a low frequency of 1 Hz with an amplitude of 0.25 V for the determination of the ionic conductivity. Two copper discs with a diameter of 1.9 cm were used as the electrodes. The bulk resistance was determined from analysis of the Impedance Plane plot, and ionic conductivity was calculated.[105]

4.4 Results and Discussion

Highly branched polyurethanes with polyether soft segments were synthesized via the oligomeric A_2 plus monomeric B_3 route. Polyethers were chosen as the soft segment for potential application in electromechanical devices.[175] Unlike Nafion, polyethers are ionically conductive with the addition of a metal salt in the absence of water.[176, 177] A variety of polyethers (i.e. PEG, PTMO, PPG) were ionically conductive in the presence of a metal salt; however, PEG has the highest ionic conductivity.[79, 178-180] Previous efforts to introduce branching in PEG-based polymers for solid polymer electrolyte applications have included the synthesis of comb-burst poly(ethylene glycol) and the incorporation of small amounts of hyperbranched PEG-based poly(urethane urea)s with linear poly(urethane urea)s.[64, 181]

The hard segment of the highly branched poly(ether urethane)s was comprised of dicyclohexylmethane-4,4'-diisocyanate (HMDI) and trimethylol propane (TMP). An isocyanate end-capped prepolymer was synthesized through the reaction of two equivalents of HMDI and one equivalent of polyether. Polyether oligomers of various degrees of polymerization (n from 14 to 69) were chosen to vary the distance between branch points. In order to avoid gelation, the prepolymer was added to a solution of

TMP (B_3) in THF (Scheme 4.1). TMP was previously used in the synthesis of hyperbranched poly(3-ethyl-3-hydroxymethyloxetane) and branched polyesters.[37, 130, 182]

The degree of branching (DB) is a descriptive term for hyperbranched and highly branched polymers, providing a general understanding of the branching efficiency. For a perfectly dendritic polymer, DB is equal to one according to Equation (1).[36]

Scheme 4.1: Synthesis of highly branched polyurethanes with TMP B3 branching agent

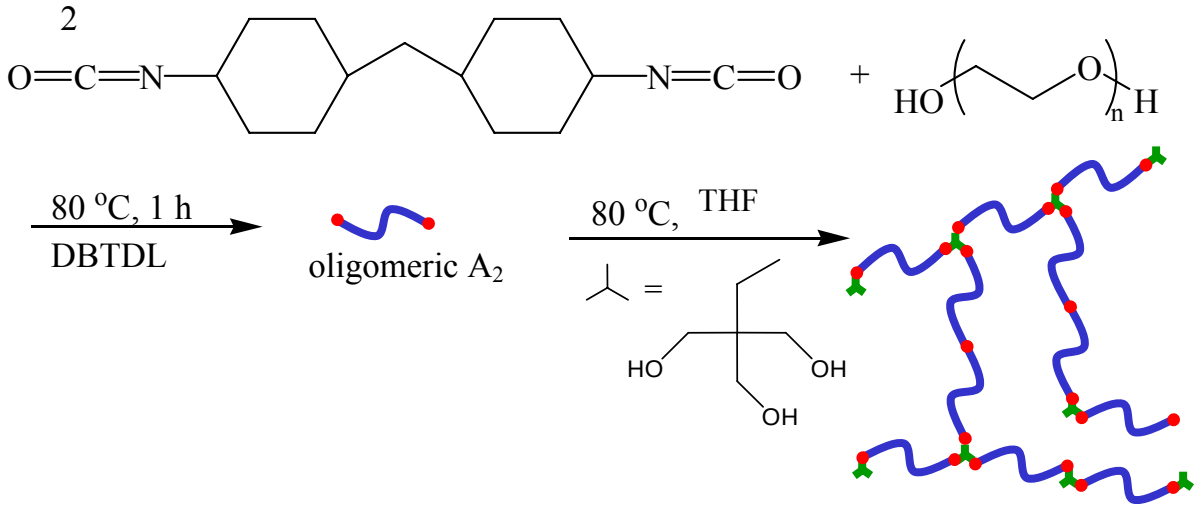

In this work, a straightforward ^{13}C NMR spectroscopic approach to determine the degree of branching for highly branched polyurethanes is presented. Several regions including the carbonyl (150-160 ppm), methyl (5-10 ppm) , and methylene (20-25 ppm) regions of the ^{13}C NMR spectrum were analyzed to identify the dendritic, linear, and terminal units that exhibited distinct resonances. However, the quaternary carbon of the TMP branching agent was the only resonance that was suitable to determine the degree of branching of the highly branched, poly(ether urethane)s. Well-resolved resonances that

were assigned to the quaternary carbon for the linear, dendritic, and terminal groups in the ^{13}C NMR spectra were observed.

Model compounds were prepared to ascertain if the urethane linkage adjacent to the TMP quaternary carbon showed well resolved resonances for the linear, dendritic, and terminal groups (Scheme 4.2). Cyclohexyl isocyanate was reacted with TMP to produce model compounds for ^{13}C NMR spectroscopic assignments, where trisubstituted represents dendritic, disubstituted is equivalent to linear, and monosubstituted corresponds to terminal groups in the highly branched products. However, thin layer chromatography (TLC) after column chromatographic separation was problematic due to the lack of UV absorption. Despite the absence of convincing TLC data, ^{13}C NMR spectroscopic analysis of the model compound mixture clearly showed three distinct resonances in several regions of the ^{13}C NMR spectrum. The methyl resonance that was assigned to the trimethylol propane appeared in the range of 8.0 to 6.5 ppm (Figure 4.1a). The model compounds showed three distinct resonances in this region; however, the corresponding polymer resonances were not as well-resolved. Three resonances were discernable in the region of 24 to 18 ppm (Figure 4.1b) and assigned to the methylene adjacent to the methyl group of the branching agent. However, the ^{13}C NMR spectrum of the polymer did not reveal three distinct resonances and significant overlap occurred in this region. The carbonyl region (160-154 ppm) was also probed, and three well-resolved resonances were observed in the model compounds (Figure 4.1c).

Scheme 4.2: Synthesis of model compounds

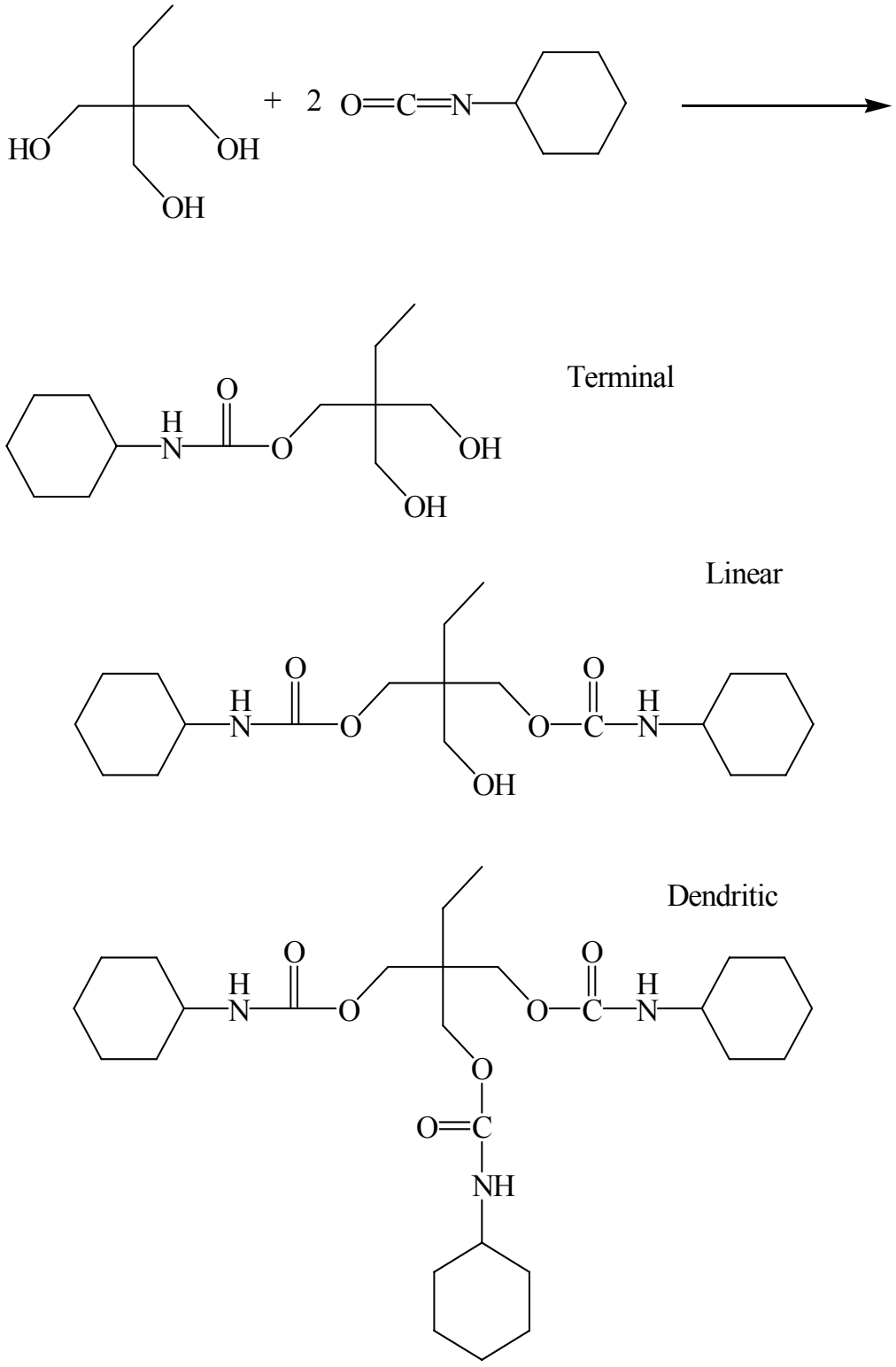

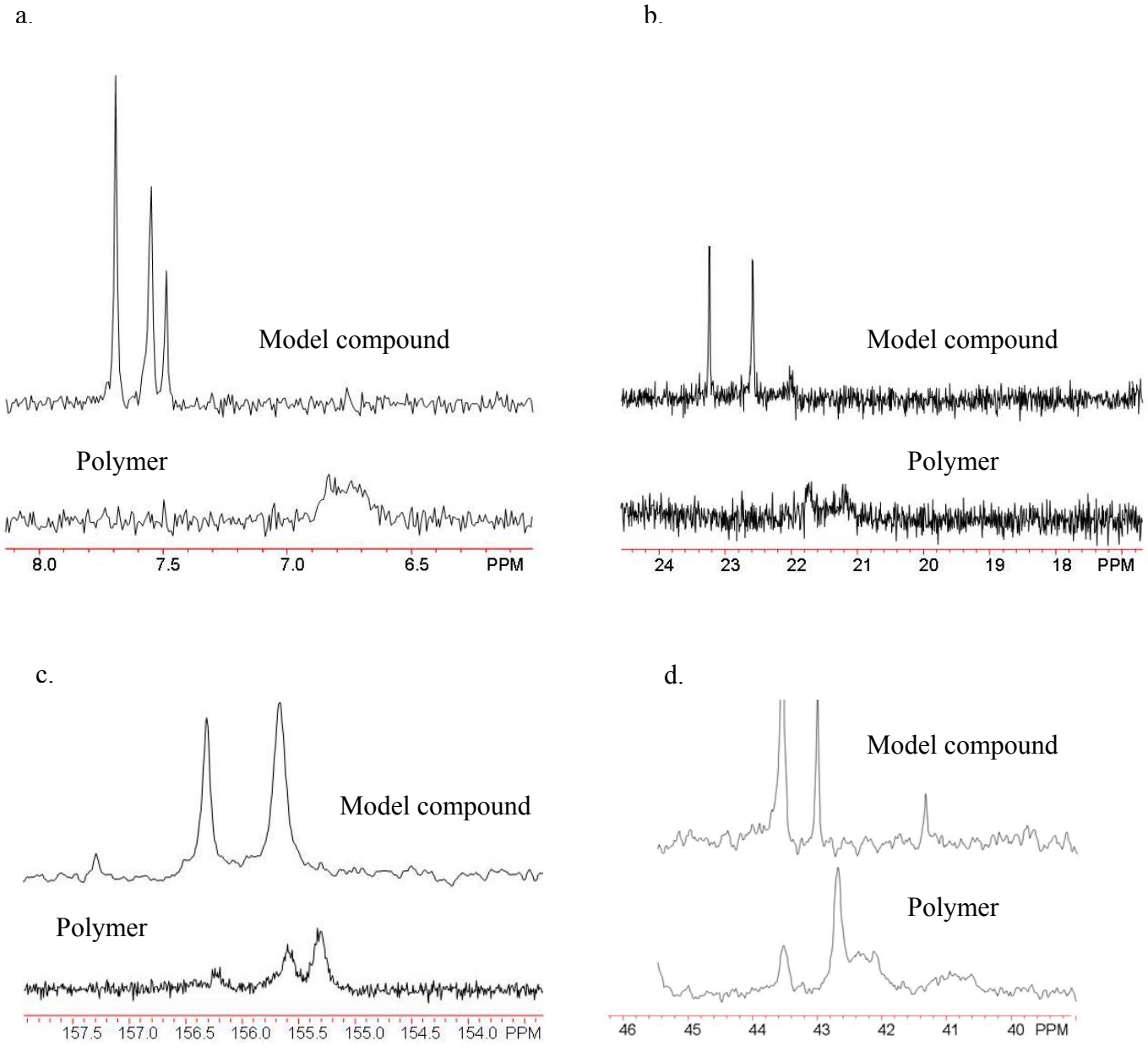

Figure 4.1: Resonances from 13C NMR spectroscopy of model compounds derived from cyclohexyl isocyanate compared with the polyurethane a.) methyl region, b.) methylene region, c.) carbonyl region, d.) quaternary carbon region

In the carbonyl region of the polymer, four resonances were expected, i.e. dendritic, terminal, linear, and carbonyls adjacent to the polyether, which had resulted from the prepolymer reaction. However, these resonances were not resolved, which made the carbonyl region unsuitable for determination of the degree of branching. In the quaternary carbon region, 45-40 ppm, three well-resolved resonances were observed for the model compounds (Figure 4.1d). Three well-resolved resonances were also observable in the polymer. Thus, the ^{13}C NMR resonances that were assigned to the quaternary carbon were pursued for the determination of the degree of branching.

In order to assess the chemical shift for the linear, terminal, and dendritic units, an alternate model compound was synthesized using phenyl isocyanate. As expected, the phenyl urethane absorbed UV light, and the three products were easily separated using column and thin layer chromatography. Mass spectroscopy confirmed the presence of a single compound for each fraction. The predicted and observed masses were in close agreement with the proposed structures (masses predicted: 373.18, 254.14; masses observed: 373.18, 254.14, respectively). The ^{13}C NMR spectrum of the phenyl isocyanate-based model compounds indicated that the resonance associated with the quaternary carbon moved downfield with increasing substitution (Figure 4.2). This agrees with our earlier assignments for polyesters that were also prepared using the *oligomeric* A_2 plus B_3 strategy.[173]

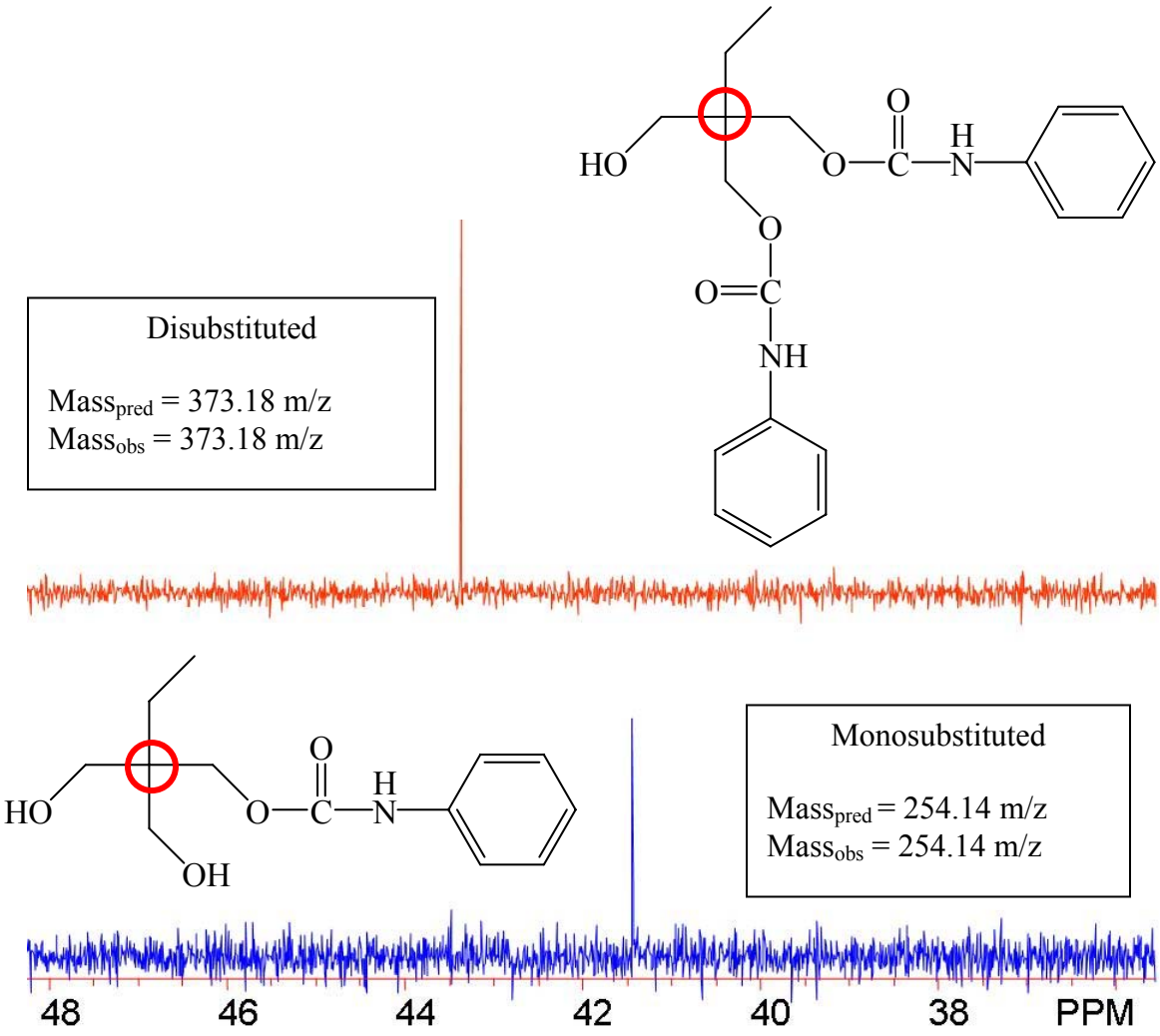

Figure 4.2: Quaternary carbon region of the 13C NMR of the phenyl isocyanate-based model compounds and mass spectroscopy data

The quantitative ^{13}C NMR spectrum of the highly branched polyurethane revealed terminal, linear, and dendritic resonances in the quaternary carbon region (Figure 4.3), but the terminal group resonance was particularly weak. It is well recognized that quaternary carbons are relatively weak resonances in ^{13}C NMR spectra, and in this case, the large distance between branch points further diluted the number of quaternary carbons in the polyurethane.[183] In order to overcome the low resolution, the hydroxyl endgroups

were quantitatively reacted with trifluoroacetic anhydride, which resulted in trifluoroester endgroups. This reaction was frequently used in the earlier literature to enhance the resolution in ^{13}C NMR spectra of polymers with hydroxyl or ester endgroups.[45, 182, 184, 185] The quantitative ^{13}C NMR spectrum of the trifluoroester endcapped, highly branched polyurethane showed significant improvement in the resolution resulting in an improved signal-to-noise ratio for the terminal groups (Figure 4.4).

A broadening of the resonance for the linear unit in the polymer relative to the model compounds was observed in the ^{13}C NMR spectrum of the highly branched polyurethane. In order to confirm that the broadening of the linear resonance was attributable to a quaternary carbon, a ^{13}C DEPT 45 NMR experiment was performed to further analyze the 45-40 ppm region of the ^{13}C NMR spectrum. In a ^{13}C DEPT 45 spectrum, only protonated carbon signals appear.[183] The ^{13}C DEPT 45 confirmed that the signal in the 45-40 ppm region of the ^{13}C NMR spectrum (Figure 4.5) was due solely to quaternary carbons since other resonances were not observed in this region. It was presumed that the shoulder in the resonance for the linear unit was due to the presence of cyclics in the highly branched polyurethane since it is widely recognized that cyclics form in most A_2 plus B_3 syntheses.[85]

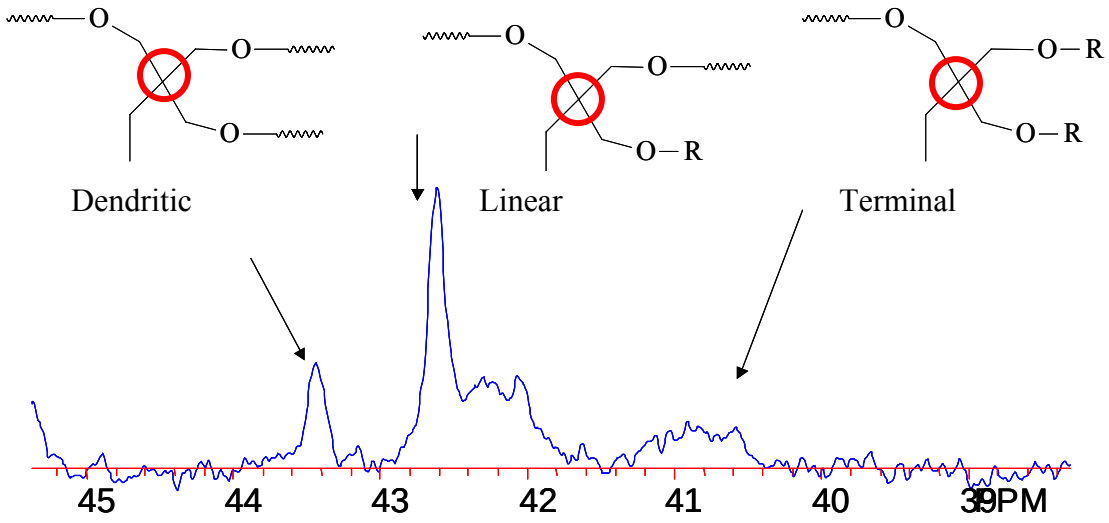

Figure 4.3: Quantitative 13C NMR spectrum of the highly branched polyurethane

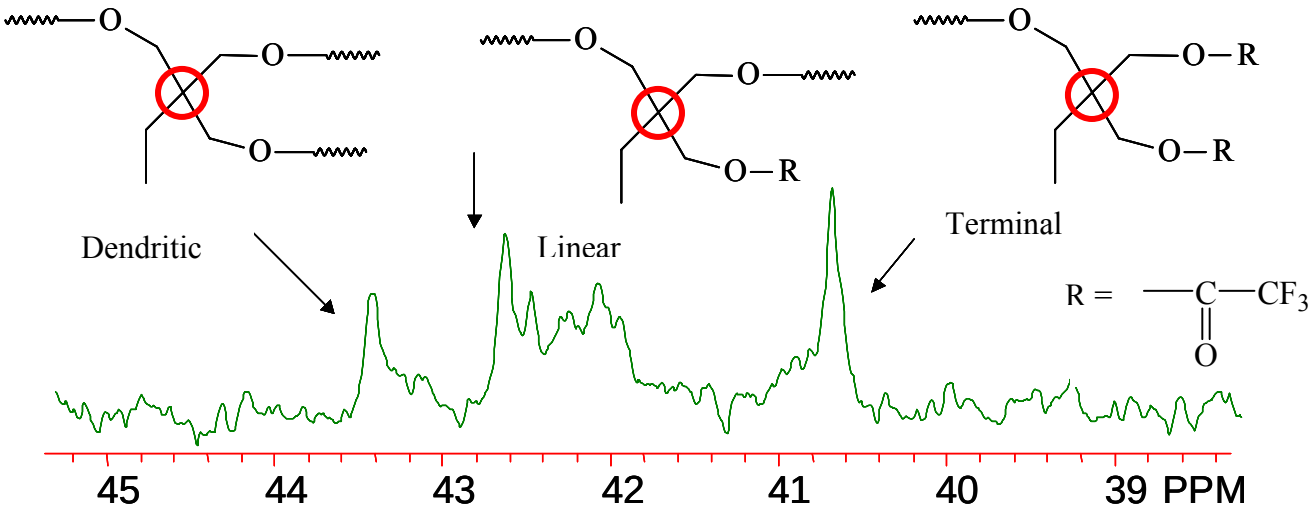

Figure 4.4: Quantitative 13C NMR spectrum of the trifluoroester endcapped highly branched polyurethane

As mentioned earlier, there are several avenues to calculate the degree of branching for a highly branched polymer. Fréchet et al. proposed Equation (1) for a traditional hyperbranched polymer synthesized from an AB_2 monomer.[36] In an AB_2 based hyperbranched polymer, every monomer offers a potential branch point. For a highly branched polymer, the oligomeric A_2 contributes linear oligomeric sequences, which are incapable of branching. In order to account for these oligomeric sequences in the degree of branching determination, Long et al. subsequently introduced Equation (3) for *oligomeric* A_2 plus monomeric B_3 polymerization, where the sum of the dendritic, linear and terminal units is normalized to 1.[173] The degree of polymerization for an *oligomeric* A_2 is then added to the sum of D, L, and T (or 1 in all cases) in the denominator for the case of one to one stoichiometry of the *oligomeric* A_2 and monomeric B_3. As expected, incorporation of the linear units from the *oligomeric* A_2 in the degree of branching calculation significantly reduced the degree of branching as compared to the DB determined with Equation (1).[173] An alternate equation was proposed in order to ensure that the number of repeat units from the A_2 group relative to the dendritic, linear, and terminal groups was incorporated:

$$(D + T)/(D + T + L + L') \qquad \text{Equation (4)}$$

where D, L, and T are dendritic, linear and terminal groups. L' is the linear unit from the oligomeric A_2, which was integrated relative to the other resonances in the ^{13}C NMR spectrum. This allowed a calculation of the molar ratio of the branching units relative to the total number of monomeric units in the highly branched polymer, whether or not the monomeric units were capable of branching. In this equation, the sum of D, T, and L is

not required to equal one. The only requirement is that D, T, L, and L' in the NMR spectrum are integrated relative to the same resonance. While Equation (3) is useful when it is not possible to quantitatively determine the linear contribution of the oligomeric A_2, Equation (4) is useful when all resonances, D, L, T, and L', are determinable. Equation (4) is not a reflection of the efficiency of branching. For every dendritic unit, three oligomeric A_2 units are incorporated into the polymer. An investigation of the degree of branching using both Equation (1) and Equation (4) was necessary to determine the efficiency of the branching agent (B_3) and the percentage of repeating units that contribute to branching for an *oligomeric* A_2 plus monomeric B_3 polymerization.

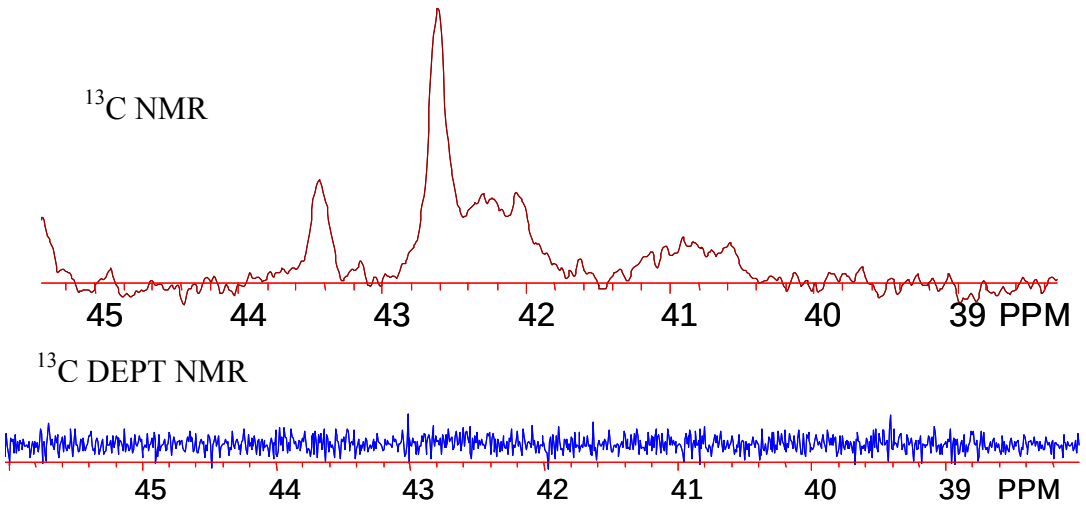

Figure 4.5: Edited 13C DEPT NMR spectrum indicating the presence of quaternary carbons in the 45-40 ppm region of the 13C NMR spectrum of the highly branched polyurethanes

Table 4.1: Degree of branching results highly branched poly(ether urethane)s

Sample	Oligomeric Diol	n[a]	Diol MW (g/mol)	M_w[b] (g/mol)	M_w/M_n	DB_1 (%)	DB_4 (%)
1	PEG	14	600	40,400	2.31	35	6.2
2	PEG	14	600	37,400	2.76	36	8.0
3	PEG	14	600	25,400	2.57	38	6.6
4	PTMO	28	2000	53,400	1.77	30	5.5
5	PTMO	28	2000	84,700	2.51	34	5.4
6	PPG	34	2000	21,300	2.69	42	3.7
7	PEG	45	2000	41,900	1.62	50	2.7
8	PEG	45	2000	26,600	1.70	36	3.5
9	PPG	69	4000	45,200	1.64	36	1.2

[a] Number of repeating units in oligomeric diol

[b]Determined with MALLS detector

DB of the highly branched polyurethanes was dependent on the degree of polymerization of the A_2 oligomer (Table 4.1), and, as expected, Equation (4) revealed lower DB values than Equation (1). The polydispersity of the highly branched polyurethanes was relatively narrow (Table 4.1). The lower polydispersity was attributed to residual narrow molecular weight distribution polyol in the polyurethane, which could reduce the overall polydispersity (Figure 4.6). The chromatogram dramatically shifted from long elution time, or low molecular weight, to short elution time, approximately 20

min, or high molecular weight. Also, the lower efficiency of branching than predicted for a statistical reaction accounts for lower polydispersities, and with a greater linear contribution, the distribution of molecular weights was reduced. One possibility is that the long, linear segments of the *oligomeric* A_2 sterically hindered the branching unit causing a larger contribution of linear units than statistically predicted.[67] Others have observed a decrease in the degree of branching due to steric hinderance.[117]

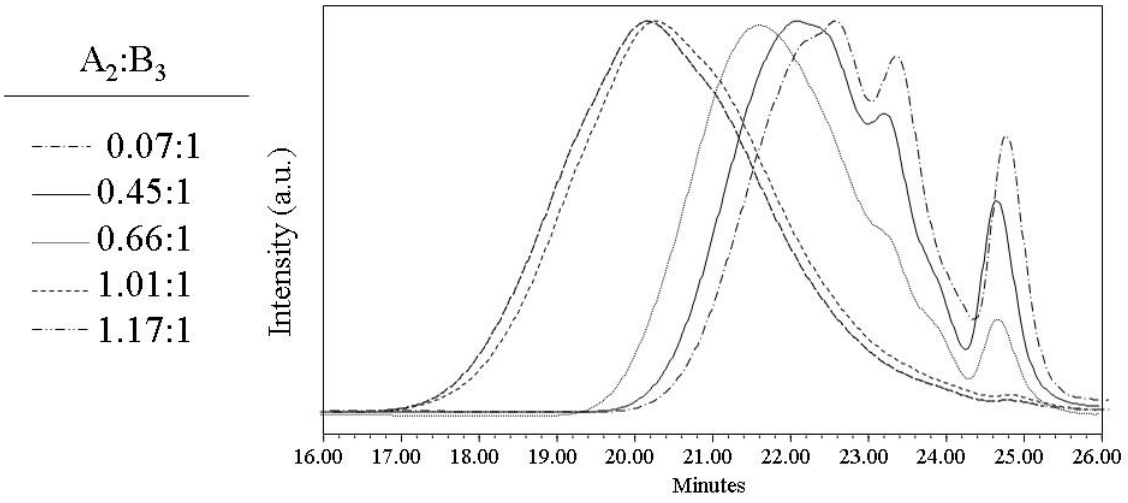

Figure 4.6: SEC chromatograms for increasing addition of A2

However, previous efforts with the *oligomeric* A_2 plus B_3 synthetic strategy revealed expected degrees of branching.[173]

Increasing the PEG segment length from 600 to 2,000 g/mol (sample 8, Table 4.1) caused a decrease in the DB from Equation (4), DB_4, to 3.5% compared to 6.6% for the equivalent molecular weight 600 g/mol PEG-based, highly branched polyurethane (sample 3). The DB from Equation (1), DB_1, for the 600 g/mol PEG-based polyurethane

(35%) was approximately the same as the 2,000 g/mol PEG-based polyurethane (36%). The equivalent DB_1 values indicated that these polymers have a similar efficiency of branching. However, DB_4 indicated that there are significantly fewer branch points relative to total monomeric units for the 2,000 g/mol PEG-based polyurethane (3.5% DB) when compared to the 600 g/mol PEG-based polyurethane (6.6% DB). The lower DB_4 for the polyurethane based on the longer soft segment length was expected, because of the greater dilution of branch points with the longer oligomeric A_2. The intrinsic viscosity across the molecular weight distribution and the Mark-Houwink exponent, a, of the 600 g/mol PEG-based, highly branched polyurethane (sample 3, Table 4.1) was lower (a = 0.49) than for the 2000 g/mol PEG-based analog (a = 0.59, Figure 4.7), which was consistent with DB_4 for the pair of highly branched polyurethanes. The Mark-Houwink exponent is typically in the range of 0.6 to 1.0 for linear polymers.[30] Both of the highly branched polyurethanes exhibited Mark-Houwink constants, which were consistent with the expected values for branched polymers.[1]

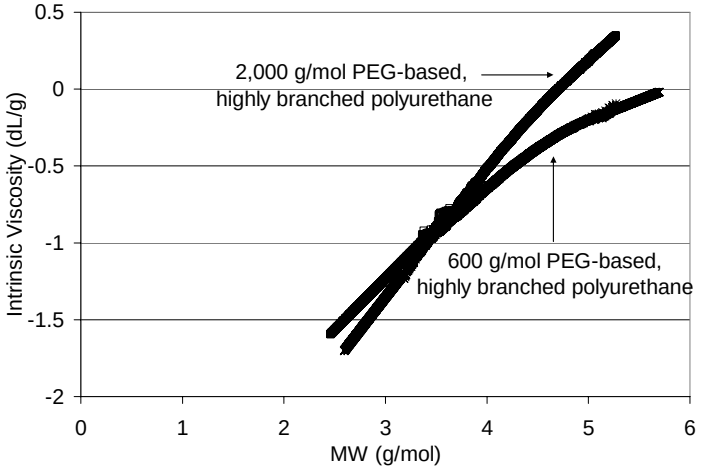

Figure 4.7: Intrinsic viscosity across the molecular weight distribution for two PEG-based, highly branched polyurethanes (■ , 2,000 g/mol PEG; *, 600 g/mol PEG).

Highly branched polyurethanes were synthesized with higher amounts of the oligomeric A_2 relative to monomeric B_3 in order to observe the change in the degree of branching with an increase in molecular weight (Table 4.2). As the stoichiometric ratio of A_2 to B_3 was increased from 0.25:1 to 1:1, the degree of polymerization increased. The efficiency of branching, which is represented with DB_1, improved as the ratio of A_2 to B_3 increased. DB_4 indicated a reduction in the degree of branching with an increase in the addition of A_2. In the earlier literature, it was theoretically predicted that DB would increase with addition of A_2, which leads to higher molecular weight.[74] However, the *oligomeric* A_2 plus monomeric B_3 system differs, because the formation of each dendritic unit results in the addition of three *oligomeric* A_2 units. Therefore, the number of monomeric units, which do not contribute to branching, greatly outweighs the increase in total branching groups and the DB_4 decreases. DB_4 decreased from 6.8 to 5.5% over the range of 0.25:1 to 1:1 for the stoichometric ratio of A_2:B_3 for PTMO-based polyurethanes. As theoretically predicted, the efficiency of branching increased over the same range of stoichometric ratios of A_2:B_3 (0.25:1 to 1:1) from 27 to 34%. However, it is important to note that PTMO-based polyurethanes as well as the PEG and PPG-based polyurethanes typically resulted in DB_1 values well below the predicted 50% for a hyperbranched polymer. A greater incorporation of linear units caused this lower branching efficiency. One possibility for the lower DB_1 than predicted is that the *oligomeric* A_2 sterically hindered the branching agent.

A decrease in DB_4 was also observed for an increase in the degree of polymerization of the oligomeric A_2 units (Figure 4.8) for all highly branched polyurethanes discussed. While the efficiency of branching was similar for most of the highly branched

polyurethanes, the dendritic units were diluted with the incorporation of segments from the oligomeric A_2. Therefore, the DB_4 accurately reflected this dilution and the actual degree of branching for the highly branched polymers synthesized with a variety of polyethers.

Table 4.2: Influence of increasing addition of A2 from 2,000 g/mol PTMO on degree of branching for highly branched polyurethanes

Sample	A_2 added (mol %)	M_w (g/mol)	M_w/M_n	DB_1 (%)	DB_4 (%)
8	25	9,900	1.47	27	6.8
9	50	12,000	1.47	28	6.9
10	95	53,400	1.77	30	5.9
11	100	84,700	2.51	34	5.5

[a]Determined with MALLS detector

As mentioned earlier, the poly(ether urethane) are useful as electromechanical devices including actuators, sensors, and transducers.[105, 186] A highly branched, 600 g/mol PEG-based polyurethane (Sample 2, M_w = 37,400, PDI = 2.76) was doped with a metal salt, lithium perchlorate, in a ratio of eight ethylene oxide units to one lithium perchlorate. The ionic conductivity of the highly branched polyurethane was determined with impedance spectroscopy (Figure 4.9). The bulk resistance was determined from the Impedance Plane plot, and the ionic conductivity was calculated, $1.43*10^{-7}$ S/cm. Previous studies indicated that linear PEG-based polyurethanes have conductivities around 10^{-7} S/cm for a comparable ethylene oxide to lithium ratio.[186] The conductivities of the linear polyurethanes and highly branched polyurethanes appear similar, and the branched polymer has the potential for improved processability for fabrication of

electromechanical devices. However, more experiments are planned to determine the effect of temperature, branching, distance between branch points, and varied dopant levels on the ionic conductivity of the highly branched polyurethanes.

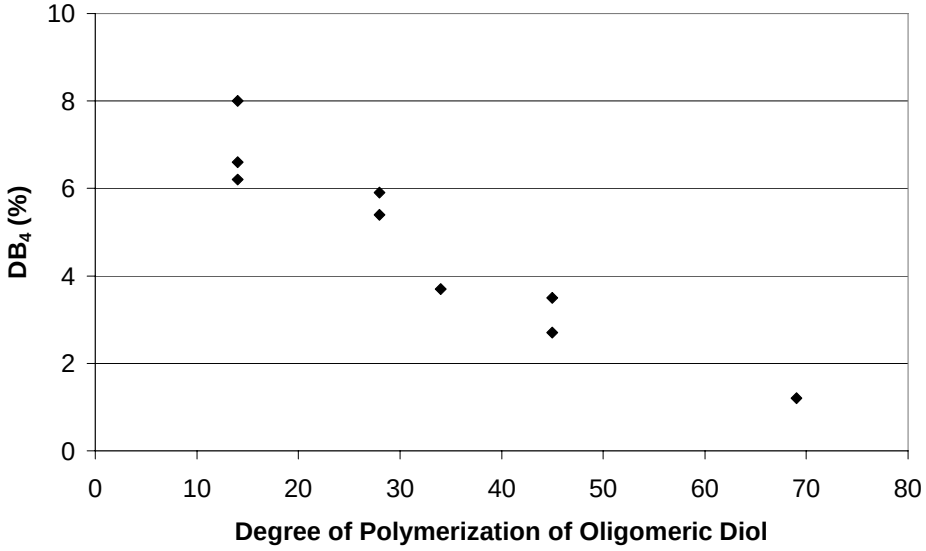

Figure 4.8: Trend of decreasing DB (%) as calculated by equation (4) with increasing molecular weight of the oligomeric A_2 group

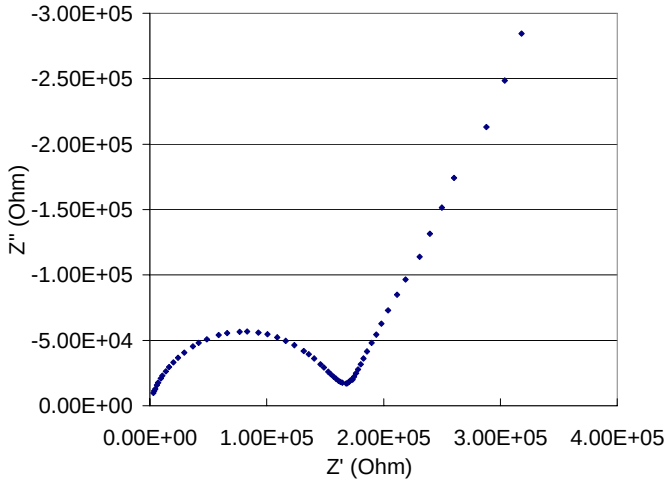

Figure 4.9: Impedance plane plot of highly branched polyurethane doped with 8:1 lithium perchlorate

4.5 Conclusions

Highly branched, poly(ether urethane)s were synthesized via an oligomeric A_2 plus monomeric B_3 polymerization and reaction with trifluoroacteic acid produced trifluoroester endgroups. Quantitative ^{13}C NMR spectroscopic analysis based on the quaternary carbon of the TMP B_3 monomer provided the number of linear units from the branching agent, linear units from the *oligomeric* A_2, dendritic, and terminal units in the highly branched polyurethanes. Model compounds confirmed the assignments of the resonances from the quaternary carbons in the ^{13}C NMR spectrum between 40 and 45 ppm. A revised DB_4 was proposed to reflect the increase in molecular weight between branch points for the *oligomeric* A_2 plus monomeric B_3 highly branched polymers. An increase in the soft segment molecular weight from 600 g/mol to 2,000 g/mol led to a decrease in the DB_4 from 6.6% to 3.5%, and the Mark-Houwink constants increased from 0.49 to 0.59. The DB_4 indicated degrees of branching for the highly branched polyurethanes ranging from 1.2 to 8.0%, which agreed well with the increased distance between branch points due to the *oligomeric* A_2.

4.6 Acknowledgements

The authors thank Mr. Bill Bebout for his help with mass spectroscopy, Dr. Mark Anderson and Mr. David Roach for their help with ionic conductivity measurements. The authors greatly appreciate the input of Dr. Cheryl Heisey on this work. The authors thank Dr. Matthew G. McKee for his helpful discussions. This material is based upon work supported in part by the U.S. Army Research Laboratory and the U.S. Army

Research Office under grant number DAAD19-02-1-0275 Macromolecular Architecture for Performance (MAP) MURI.

4.7 References

[1] Flory, P. J. *J. Am. Chem. Soc.* **1952**, *74*, 2718-2723.

[2] Kim, Y. H.; Webster, O. W. *J. Am. Chem. Soc.* **1990**, *112*, 4592-4593.

[3] Spindler, R.; Fréchet, J. M. J. *Macromolecules* **1993**, *26*, 4809-4813.

[4] Hong, L.; Cui, Y.; Wang, X.; Tang, X. *J. Polym. Sci., Part A: Polym. Chem.* **2002**, *40*, 344-350.

[5] Gao, C.; Yan, D. *Macromolecules* **2003**, *36*, 613-620.

[6] Kienle, R. H.; van der Meulen, P. A.; Petke, F. E. *J. Am. Chem. Soc.* **1939**, *61*, 2258-2268.

[7] Kienle, R. H.; Hovey, A. G. *J. Am. Chem. Soc.* **1929**, *51*, 509-519.

[8] Emrick, T.; Chang, H.-T.; Fréchet, J. M. J. *Macromolecules* **1999**, *32*, 6380-6382.

[9] Emrick, T.; Chang, H.-T.; Fréchet, J. M. J. *J. Polym. Sci., Part A: Polym. Chem.* **2000**, *38*, 4850-4869.

[10] Lin, Q.; Long, T. E. *Macromolecules* **2003**, *36*, 9809-9816.

[11] Unal, S.; Yilgor, I.; Yilgor, E.; Sheth, J. P.; Wilkes, G. L.; Long, T. E. *Macromolecules* **2004**, *37*, 7081-7084.

[12] Suneel; Buzza, D. M. A.; Groves, D. J.; McLeish, T. C. B.; Parker, D.; Keeney, A. J.; Feast, W. J. *Macromolecules* **2002**, *35*, 9605-9612.

[13] Hawker, C. J.; Chu, F.; Pomery, P. J.; Hill, D. J. T. *Macromolecules* **1996**, *29*, 3831-3838.

[14] Hawker, C. J.; Lee, R.; Fréchet, J. M. J. *J. Am. Chem. Soc.* **1991**, *113*, 4583-4588.

[15] Hölter, D.; Burgath, A.; Frey, H. *Acta Polymer.* **1997**, *48*, 30-35.

[16] Hölter, D.; Frey, H. *Acta Polymer.* **1997**, *48*, 298-309.

[17] Unal, S.; Lin, Q.; Mourey, T. H.; Long, T. E. *Macromolecules* **2005**, *38*, 3246-3254.

[18] Jiang, G.; Maeda, S.; Yang, H.; Wang, C.; Saito, Y.; Tanase, S.; Sakai, T. *J. Electrochem. Soc.* **2004**, *151*, 1886-1890.

[19] Dieterich, D.; Schmelzer, H. G. Polyurethane Handbook; Hanser/Gardner Publications, Inc.: Cincinnati, 1993.

[20] Huang, X.; Ren, T.; Tian, L.; Hong, L.; Zhu, W.; Tang, X. *J. Mater. Sci.* **2004**, *39*, 1221-1225.

[21] Shahinpoor, M.; Kim, K. J. *App. Phys. Letters* **2002**, *80*, 3445-3447.

[22] Harrison, W. L.; Hickner, M. A.; Kim, Y. S.; McGrath, J. E. *Fuel Cells* **2005**, *5*, 201-212.

[23] Shahinpoor, M. *Electrochim. Acta* **2003**, *48*, 2343-2353.

[24] Lee, S.-M.; Chen, C. Y.; Wang, C.-C. *Electrochim. Acta* **2003**, *48*, 3699-3708.

[25] van Heumen, J. D.; Stevens, J. R. *Macromolecules* **1995**, *28*, 4268-4277.

[26] Ferry, A.; Jacobson, P.; van Heumen, J. D.; Stevens, J. R. *Polymer* **1996**, *37*, 737-744.

[27] Watanabe, M.; Sanui, K.; Ogata, N. *Macromolecules* **1986**, *19*, 815-819.

[28] Itoh, T.; Ichikawa, Y.; Uno, T.; Kubo, M.; Yamamoto, O. *Solid State Ionics* **2003**, *156*, 393-399.

[29] Smith, T. J.; Mathias, L. J. *Polymer* **2002**, *43*, 7275-7278.

[30] Magnusson, H.; Malmström, E.; Hult, A. *Macromol. Rapid Commun.* **1999**, 453-457.

[31] Malmström, E.; Hult, A. *Macromolecules* **1996**, 1222-1228.

[32] Malmström, E.; Johansson, M.; Hult, A. *Macromolecules* **1995**, *28*, 1698-1703.

[33] Malmström, E.; Trollsas, M.; Hawker, C. J.; Johansson, M.; Hult, A. *PMSE* **1997**, *77*, 151-152.

[34] Breitmaier, E.; Voelter, W. Carbon-13 NMR Spectroscopy; VCH: New York, 1987.

[35] Kenwright, A. M.; Peace, S. K.; Richards, R. W.; Bunn, A.; MacDonald, W. A. *Polymer* **1999**, *40*, 2035-2040.

[36] Girardon, V.; Correia, I.; Tessier, M.; Marechal, E. *Eur. Polym. J.* **1998**, *34*, 363-380.

[37] Rajan, M.; Cotiuga, I.; Ma, Y.; Picchioni, F.; Agarwal, U. S. *e-Polymers* **2003**, *46*, 1-7.

[38] Kricheldorf, H. R.; Schwarz, G. *Macromol. Rapid Commun.* **2003**, *24*, 359-381.

[39] Ishida, Y.; Sun, A. C. F.; Jikei, M.; Kakimoto, M. *Macromolecules* **2000**, *33*, 2832-2838.

[40] Jikei, M.; Kakimoto, M. *Prog. Polym. Sci.* **2001**, *26*, 1233-1285.

[41] McKee, M. G.; Unal, S.; Wilkes, G. L.; Long, T. E. *Prog. Polym. Sci.* **2005**, *30*, 507-509.

[42] Schmaljohann, D.; Voit, B. *Macromol. Theory Simul.* **2003**, *12*, 679-689.

[43] Hong, L.; Shi, L.; Tang, X. *Macromolecules* **2003**, *36*, 4989-4994.

Chapter 5: Rheological Behavior and Ionic Conductivity of Highly Branched Poly(ether urethane)s for Electromechanical Devices

5.1 Abstract

The *oligomeric* A_2 plus B_3 synthetic strategy was employed to produce highly branched polyurethanes suitable for electromechanical devices. Highly branched polymers synthesized via the *oligomeric* A_2 plus B_3 strategy offer significant branching density and longer distances between branch points when compared to a hyperbranched topology. The highly branched polyurethanes were synthesized with polyether soft segments (PEG or PTMO), which are ionically conductive when in the presence of a metal salt. The melt and solution viscosities of these highly branched polyurethanes were significantly lower than linear analogs. For a given molecular weight with different degrees of branching, the relationship between the degree of branching and rheological behavior was investigated. A higher hard segment content caused an increase in the complex viscosity despite a higher degree of branching. Addition of lithium perchlorate to the highly branched poly(ether urethane) caused an increase in the zero shear rate viscosity and relaxation time due to the interaction of the salt with multiple polyether segments. The highly branched polyurethane demonstrated significantly higher ionic conductivity compared to the linear analog. The improved conductivity was attributed to greater mobility of the highly branched polyurethane.

5.2 Introduction

Hyperbranched polymers have emerged as viable candidates for diverse application due to the synergy of rheological performance and functionality. Rheological modification is a frequently cited application for dendritic and hyperbranched polymers.[166, 187] Hyperbranched polymers were introduced approximately fifteen years ago as an inexpensive alternative to dendritic polymers.[28] Since dendritic polymers are often quite challenging and expensive to synthesize, hyperbranched polymers were introduced as cost effective alternatives.[29] AB_x monomers, where $x \geq 2$, are typically used in the synthesis of hyperbranched polymers.[36, 59, 131] The A_2 plus B_3 route uses relatively inexpensive, commercially available monomers; however, rigorous synthetic techniques are required to avoid crosslinking such as order of monomer addition, dilute solutions, and slow monomer addition.[7, 158, 188]

Previous studies probed the rheological behavior of hyperbranched polymers prepared via the AB_x and A_2 plus B_3 synthetic routes.[7, 10] Earlier efforts primarily focused on rheological studies of hyperbranched and dendritic polymers in dilute solution.[6-8] Recently, several studies have concentrated on the melt rheological behavior of hyperbranched and dendritic polymers.[189] The power law relationship between zero shear rate viscosity, η_0, and weight average molecular weight, M_w, received significant attention in these studies. The power law scaling for the η_0-M_w relationship was typically ~1.0, which is the predicted power law scaling for unentangled, linear polymers. This power law relationship was valid for hyperbranched polymers with molecular weights greater than 10^6 g/mol.[10, 89, 190] Kunamaneni et al. investigated hyperbranched

polystyrenes and crossover of the dynamic moduli in the terminal region was not observed in these systems.[82] Hyperbranched polymers typically do not exhibit an overlap of loss and storage moduli in the terminal region because this intersection correlates to the longest relaxation time of the polymer, which is an indication of entanglements.[103, 130, 191] Hyperbranched polymers were previously synthesized for melt rheological studies using both traditional AB_2 and other recently introduced synthetic routes including self-condensing group transfer copolymerization.[9, 103, 130] Each synthetic strategy has benefits, which range from ease of synthesis to the control of molecular weight distribution. Our laboratory recently proposed an *oligomeric* A_2 plus B_3 route for synthesis of highly branched polymers.[1, 7, 15, 16] An *oligomeric* A_2 provides linear segments between branch points for enhanced mechanical properties, while retaining many of the benefits of a high degree of branching including improved processability and higher functional chain end concentration.[7, 16]

Polyethers are widely recognized as ionic conductors in the presence of metal salts, because the polyether solvates the salt. Additional low molar mass diluents are not required for ionic conductivity in polyethers, which is an advantage over other materials frequently used for solid polymer electrolytes, including water swollen Nafion. Polyurethanes with polyether as the soft segment have emerged as a class of polymers with potential as solid polymer electrolytes due to the incorporation of ionically conductive polyethers and improved mechanical properties.[105, 174, 192] Semi-crystallinity reduces the molecular mobility of the polyethers and acts as a barrier to high ionic conductivities for poly(ether urethane)s. Efforts to improve the mobility of the soft segment have included introduction of hyperbranched polyurethanes to a matrix of linear

of poly(ether urethane)s.[105, 186] Blends of hyperbranched and linear poly(ether urethane)s offered enhanced ionic conductivity in poly(ether urethane)s compared to neat linear poly(ether urethane)s.

The melt rheological behavior of highly branched polyurethanes synthesized via the *oligomeric* A_2 plus B_3 methodology was determined to more fully understand the influence of highly branched architectures on viscoelastic properties. The impact of the improved mobility of the highly branched polyurethane when compared to the linear analog of equivalent molecular weight on ionic conductivity was determined. The complex viscosity and specific solution viscosity of the highly branched polymers were compared to linear analogs, and the influence of branching on dynamic rheological behavior was investigated for equivalent molecular weights. The length of the polyether soft segment was adjusted to determine the effect of hard segment content on the melt rheology. Highly branched and linear polyurethanes were doped with lithium perchlorate, which is a salt frequently used for electromechanical device applications. The salt introduces temporary physical crosslinks, and the effect of salt on the complex viscosity and relaxation times of the linear and highly branched polyurethanes was determined.[192, 193]

5.3 Experimental

5.3.1 Materials

Polyethylene glycol (PEG) of 600 and 2000 g/mol number average molecular weights and Terathane (PTMO) of 2000 g/mol were obtained from Aldrich and dried at

80 °C under reduced pressure for 18 h prior to use. Bayer AG provided dicyclohexylmethane-4,4'-diisocyanate (HMDI), which was used as received. Lithium perchlorate was purchased from Alfa Aesar and dried for 24 h at 80 °C under reduced pressure prior to use. 1,4-Butanediol was purchased from Aldrich and dried over 3 Å molecular sieves. Dibutyltin dilaurate (DBTDL) catalyst were obtained from Aldrich and used as received. Chromatographic grade tetrahydrofuran (THF) was purchased from Reagents, Inc. and used without further purification.

5.3.2 Synthesis of linear polyurethanes

Linear polyurethanes were synthesized in a conventional two-step process.[136] The prepolymer was formed from the reaction of an oligomeric diol (e.g. 4.3 g, 7.2 mmol of PEG 600 g/mol) and HMDI (14 g, 18 mmol) in bulk at 80 °C for 1 h with 100 ppm DBTDL catalyst. After complete reaction, tetrahydrofuran (11.3 mL) was used to dissolve the prepolymer. A 50 wt% solution of the chain extender, 1,4-butanediol (0.98 g, 11 mmol), in THF was added dropwise to the prepolymer to form the linear polyurethane. This reaction was cooled to room temperature after approximately 8 h when FTIR confirmed the quantitative disappearance of isocyanate groups.

5.3.3 Synthesis of highly branched polyurethanes

The prepolymers were formed in an identical fashion as described for the linear polyurethane. The prepolymer was dissolved to form a 30 wt% solution in THF and added dropwise to a 10 wt% solution in THF of the B_3 monomer, TMP, at 80 °C. The reaction was allowed to proceed for 8 h or until FTIR spectroscopy indicated complete

conversion of isocyanate. The reaction was diluted with THF as needed to ensure a low viscosity solution.

5.3.4 Addition of salt to polyurethane

Approximately 10 wt% polyurethane was dissolved in THF. Once the polymer was completely dissolved, the lithium perchlorate was added in an 8:1 ratio of ethylene oxide units to lithium (EO:Li) and allowed to dissolve. The homogeneous solution was poured into Teflon molds, and the films were dried at 25 °C for 24 h, 80 °C for 24 h, and 80 °C under reduced pressure for 24 h.

5.3.5 Polymer Characterization

Molecular weights were determined at 40 °C, 1 mL/min in THF (ACS grade) with a Waters SEC with a 717 autosampler, 2410 refractive index detector, and a Wyatt Mini-DAWN MALLS detector. FTIR was performed on a MIDAC M-1700 FTIR with Durascope single bounce diamond ATR. Melt rheology measurements were performed on an AR 1000 TA Instruments rheometer with 8 or 25 mm parallel plates and 5 % strain in oscillatory mode at a gap of 1 mm. The zero-shear rate viscosities were determined with a Carreau-Yasuda model. The reptation times were calculated from the inverse of the frequency at which the loss and storage modulus intersected. Solution rheology was performed on a Bohlin rheometer at 25 °C with concentric cylinder geometry in steady shear with dimethylformamide, DMF, as the solvent. A CH Instruments electromechanical analyzer was used at a high frequency of 100,000 Hz and a low frequency of 1 Hz with an amplitude of 0.25 V for the determination of the ionic conductivity. Two copper discs with a diameter of 1.9 cm were used as the electrodes.

The bulk resistance was determined from analysis of the Impedance Plane plot, and ionic conductivity was calculated.[105]

5.4 Results and Discussion

Poor mechanical properties of hyperbranched and dendritic polymers is attributed to a lack of chain entanglements.[112] Hyperbranched polymers are frequently cited as potential additives such as rheological modifiers, where a small amount of the branched polymer is added to a linear polymer to reduce melt viscosity.[10] The reduction in the number of entanglements in hyperbranched polymers was previously reported based on rheological studies.[9] A comparison of the rheological behavior of highly branched polymers and linear analogs provided insight into the nature and effect of branching and distance between branch points.

Highly branched poly(ether urethane)s were synthesized via the *oligomeric* A_2 plus monomeric B_3 polymerization.[7, 15, 16, 165] The tailored distance between branch points place the highly branched *oligomeric* A_2 plus B_3 topology between hyperbranched and linear architectures. The lower melt and solution viscosities of these highly branched poly(ether urethane)s are expected to influence processibility. Linear poly(ether urethane)s with equivalent hard segment content and weight average molecular weights were synthesized via traditional step-growth methodologies for comparison with the highly branched counterparts. Two complimentary equations were used to accurately describe the branching agent efficiency (Equation 1) and the degree of branching (Equation 2) of highly branched polymers. Hawker et al. proposed the classical degree of branching, DB, equation for hyperbranched polymers Equation (1), where every repeating unit is a potential branch point, does not describe the DB of highly branched

polymers well as highly branched polymers contain linear segments that do not contribute to branching. However, Equation (1) does describe the efficiency of branching in highly branched systems because the dendritic, D, and terminal, T, units that contribute to a completely branched system are divided by the sum of all units from the branching agent including the linear units, L:[36]

$$DB = (D + T)/(D + T + L) \qquad \text{Equation (1)}$$

Equation (2) was recently proposed to describe the DB for highly branched systems.[157] In Equation (2), the numerator is the sum of the units that contribute to a wholly branched architecture as in Equation (1), and the linear units, L', from the *oligomeric* A_2 are included in the denominator:

$$DB = (D + T)/(D + T + L + L') \qquad \text{Equation (2)}$$

Equation (2) accounts for all of the repeating units in the highly branched polymer and accurately reflects the dilution of branching in the highly branched polyurethanes. The number of D, T, L, and L' units were determined with ^{13}C NMR spectroscopy, as described elsewhere.[157]

The efficiency of branching and degree of branching were well described as DB_1 and DB_2, respectively (Tables 5.2 and 5.3). The branching efficiency for the polyurethanes was less than the predicted 50% for hyperbranched polymers. The lower branching efficiency was attributed to steric hindrance of the branching agent, which led to a greater linear contribution.

A linear and a highly branched polymer of the same hard segment content (57 wt%), soft segment composition (600 g/mol PEG), and molecular weight (50,000 g/mol)

were prepared with different chain extenders. The linear polymer was prepared with a difunctional chain extender, 1,4-butanediol, and the highly branched polymer was synthesized with TMP as the trifunctional branching agent. The complex melt viscosity, η^*, of the highly branched polyurethane was orders of magnitude lower than the η^* of the comparable linear polyurethane (Figure 5.1). The onset of shear thinning was not apparent for the highly branched polymer over the 0.001 to 1.0 Hz shear rate range while shear thinning occurred at shear rates even lower than 0.001 Hz with the linear analog. The observation of shear thinning in the melt viscosity of the linear polymer was confirmed as the tan δ reached a constant value over the frequency range. A constant tan δ was not observed with the highly branched polymer until the frequency was increased to 10 to 100 Hz. The constant tan δ was an indication of pure gelation scaling. Interestingly, this behavior was also seen with a randomly branched polyester with linear segments between branches.[194]

A series of highly branched polyurethanes with increasing A_2 to B_3 ratio from 0.25:1 to 1:1 (DB_2 from 6.9 to 5.4) was synthesized (Table 5.1). The relationship between weight average molecular weight and zero shear rate viscosity followed a power law relationship, where η_0 scaled with $M_w^{3.9}$ (Figure 5.2). The well-known η_0-M_w relationship scales to the power 3.4 for entangled linear polymers. The η_0 of the highly branched polyurethanes had a slightly stronger dependence on M_w than theoretically predicted for entangled linear polymers. A much higher power law dependence than 3.4 or 3.9 is expected for entangled, long chain branches.

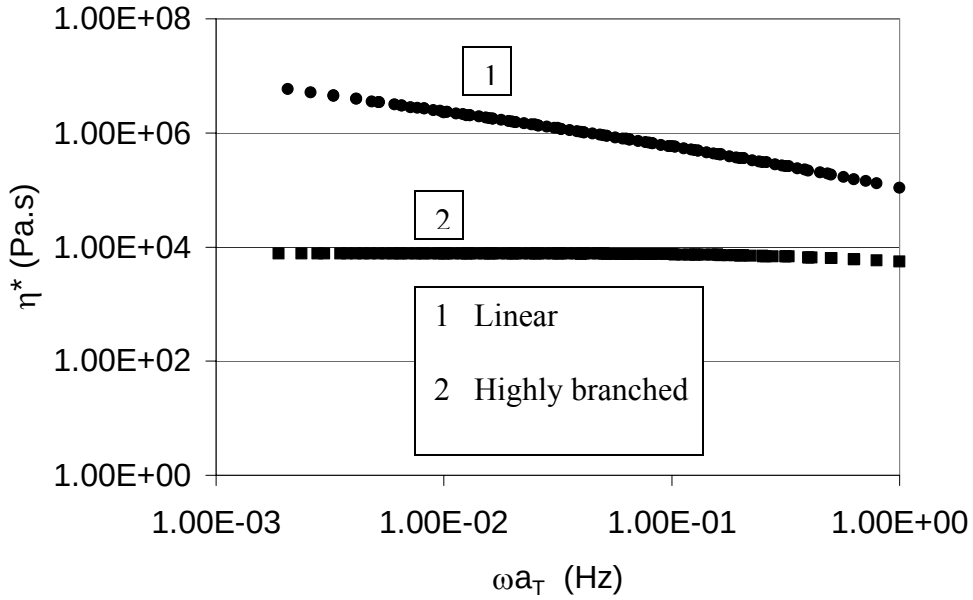

Figure 5.1: Lower complex viscosity of highly branched oligomeric A_2 plus B_3 compared with linear analog

The similarity of the η_0-M_w relationship to entangled linear polymer indicated the highly branched polyurethanes did not have substantial entanglements in the branches but some backbone entanglement was preserved. The slightly higher exponent (3.9 vs. 3.4) was attributed to intermolecular hydrogen bonding, which may have increased the apparent molecular weight of the polyurethanes in the melt. However, only four samples were used to determine this dependence and more samples are required for a definitive determination of the η_0-M_w relationship for highly branched polyurethanes. The distance between branch points and the hard segment content were varied to determine the effect of these parameters on the viscoelastic behavior of the highly branched polyurethanes. Three polyurethanes were synthesized with varying levels of branching (DB_2 = 0, 6.2, and 8%) and equivalent molecular weight (Table 5.2). The melt viscosity was shown to increase systematically with a decrease in the degree of branching *for equivalent*

molecular weights (Figure 5.3). Previous literature refers to the dependence of viscometric parameters on branch length, degree of branching, or the contraction factor, g'.[1, 194] The increase in the zero-shear rate viscosity as determined with the Carreau model showed a strong power law dependence (6.19) on g' (Figure 5.4a). The power law dependence of these parameters on g' indicated that the melt viscosity of the polyurethanes was adjusted easily with a change in the degree of branching, which had implications for the processing of these polymers. It is possible to visualize the change in the degree of branching with constant molecular weight as adjusting the branch length, where the lower degree of branching corresponds to a higher branch molecular weight, M_{br}. Previous studies of the relationship between g' and η_0 or more generally, between branching and rheological behavior, focused on polymers with different molecular weights.

Table 5.1: Increasing ratio of A2 : B3 led to increased molecular weight and zero shear rate viscosity.

Sample	Ratio of $A_2 : B_3$	M_w (g/mol)	η_0 (Pa.s)
1	0.25 : 1.0	9,820	34
2	0.50 : 1.0	12,000	124
3	0.95 : 1.0	53,400	26,710
4	1.0 : 1.0	84,700	195,900

Most literature on the influence of branching on melt behavior has focused on the η_0-M_w relationship, which was shown in Figure 5.2 for these polymers. Previous literature indicated a stronger power law dependence of η_0 on M_w for long-chain branching, which

was not observed in this case. [91, 194, 195] A drastic decrease in η_0 was observed when DB_2 increased from 0 to 8% (Table 5.2). The number and integrity of entanglements were reduced as more branch points were incorporated along the polyurethane backbone causing a decrease in η_0. However, from the $\eta_0 \sim M_w^{3.9}$ relationship, entanglements do appear to persist in the highly branched polyurethanes. It was also found that the reptation time, τ_{rep}, the time required for the polymer to move through its confining tube, was drastically reduced with increased branching (Figure 5.4b). The reduced reptation time indicated the branching was short chain, as long chain branching results in longer reptation times.[196, 197]

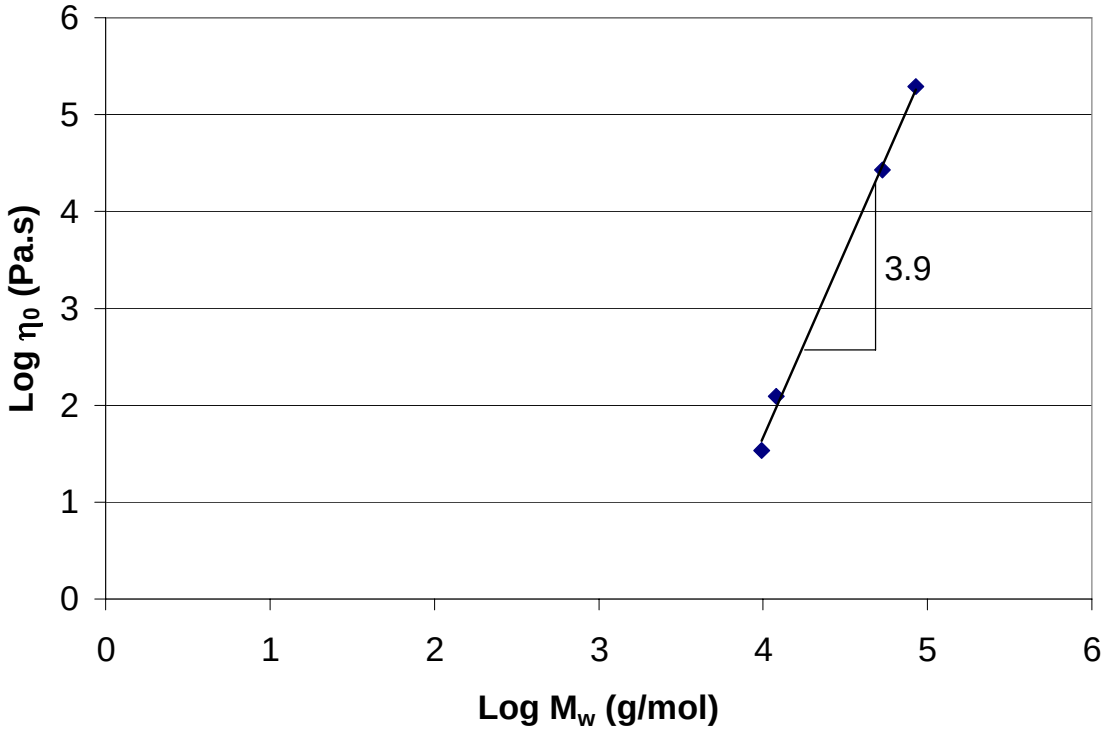

Figure 5.2: Dependence of η_0 on Mw for a highly branched polyurethane series. The η_0—M_w relationship is similar to the 3.4 theoretical prediction for linear polymers.

Oligomeric soft segments of two different molecular weights, 600 and 2000 g/mol, were used to obtain highly branched polyurethanes with a hard segment content of 57 and 36 wt%, respectively. The first pair of highly branched polyurethanes (samples 7 and 8) had a molecular weight of about 25, 000 g/mol (Table 5.3). The highly branched polyurethane with the 600 g/mol PEG soft segment and 57 wt% hard segment (sample 7) had a higher DB_2 (6.6 %) than sample 8 (3.5%), the polymer with the lower 36 wt% hard segment incorporation. The higher DB_2 was expected for the highly branched polyurethane with shorter distances (lower 600 g/mol molecular weight PEG soft segment) between branch points. The polyurethane with higher hard segment content (57 wt%) and greater DB_2 (6.6%) (Sample 7) had the higher η_0, as well. As shown earlier (Table 5.2), a higher degree of branching at equivalent molecular weight led to a drastic reduction in η_0. However, in this case, the increased incorporation of hard segment dominated the effects of increased branching and resulted in an increase in η_0.

Table 5.2: Influence of branching in polyurethanes on rheological behavior.

Sample	Topology	M_w (g/mol)[a]	DB_1 (%)[b]	DB_2 (%)[b]	g'[c]	τ_{rep} (s)	η_0 (Pa.s) ($*10^3$)
4	Linear	36,800	N/A	N/A	0.86	480	1,070
5	HB	37,400	35	6.2	0.38	0.25	27.3
6	HB	40,400	36	8.0	0.24	0.24	4.73

[a] MALLS
[b] ^{13}C NMR spectroscopy
[c] Viscometric detector

The higher hard segment content may have led to an increase in intermolecular hydrogen bonding of the polyurethane chains, and therefore, an increase in the apparent molecular weight, which would account for the increase in η_0.

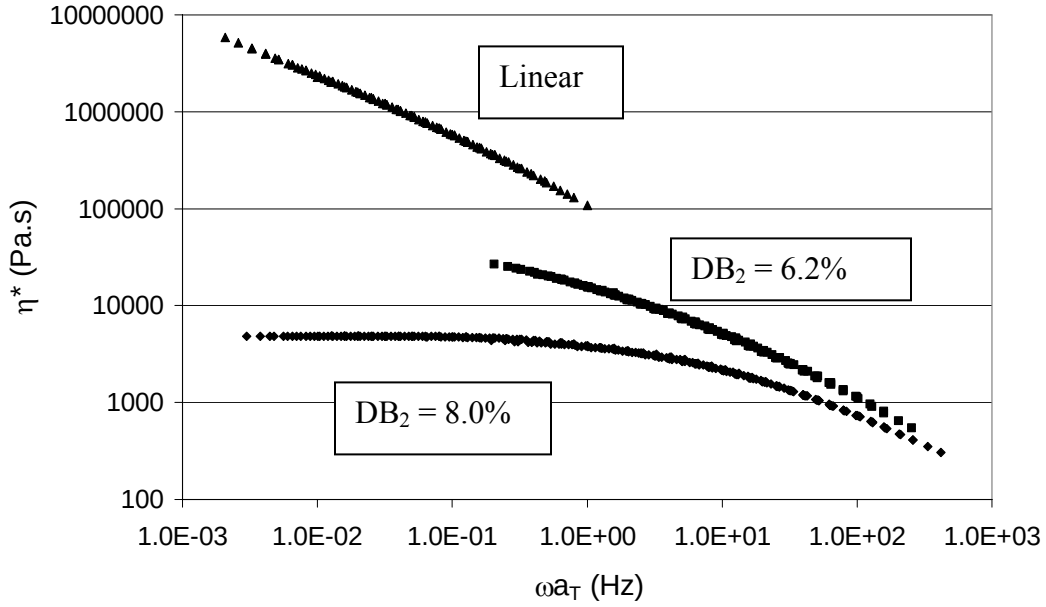

Figure 5.3: Systematic decrease in melt viscosity with increase degree of branching

A pair of highly branched polyurethanes with differing hard segment content and equivalent molecular weight of about 50,000 g/mol was also synthesized (samples 9 and 10). The highly branched polyurethane with the shorter soft segment length (600 g/mol) had a DB_2 of 5.4% (sample 9) while the highly branched polyurethane with the longer soft segment length had a DB_2 of 1.6% (sample 10). Again, the polyurethane with the higher DB_2 and greater hard segment content had the higher η_0 (sample 9). However, the difference between η_0 values of samples 9 and 10 was much less than between samples 7 and 8. Interestingly, the 6.6% DB_2 of the higher hard segment polyurethane from the 25,000 g/mol pair (sample 7) was about twice as large as the 3.5% DB_2 of the polyurethane with a hard segment content of 36 wt% (sample 8). In the 50,000 g/mol pair of highly branched polyurethanes, the higher hard segment content polyurethane

(sample 9) had a 5.4% DB_2, which is about three times larger than the 1.6% DB_2 for corresponding polyurethane with a lower hard segment content (sample 10). This result indicated that perhaps the increase in η_0 with increased incorporation of hard segment can be overcome with an increased DB_2.

Previous studies have shown that high molecular weight hyperbranched polymers do not entangle due to the high number of branch points.[9] Highly branched polymers have longer distances between branch points relative to hyperbranched polymers, which may enable significant entanglement. Indeed, complex melt viscosity and dynamic modulus data indicated there may be entanglements present in the highly branched polyurethanes. Shear-thinning was observed in the melt rheology indicating the disruption of entanglements (Figure 5.2). The loss and storage moduli intersect in the terminal region, and relaxation times were calculated from this intersection (Figure 5.5). Typically, the loss and storage moduli of hyperbranched polymers or unentangled, low molecular weight polymers do not intersect in the terminal region.[9] Entanglements in the melt typically result in a plateau in the storage modulus over a large range of frequencies.[109] While the storage modulus did not plateau over the frequency range probed, the slope was greatly reduced at higher frequencies. The lack of a plateau in G' was attributed to a wide range of relaxations due to the broad polydispersity (PDI = 2.51) of the highly branched polyurethanes (Figure 5.6).

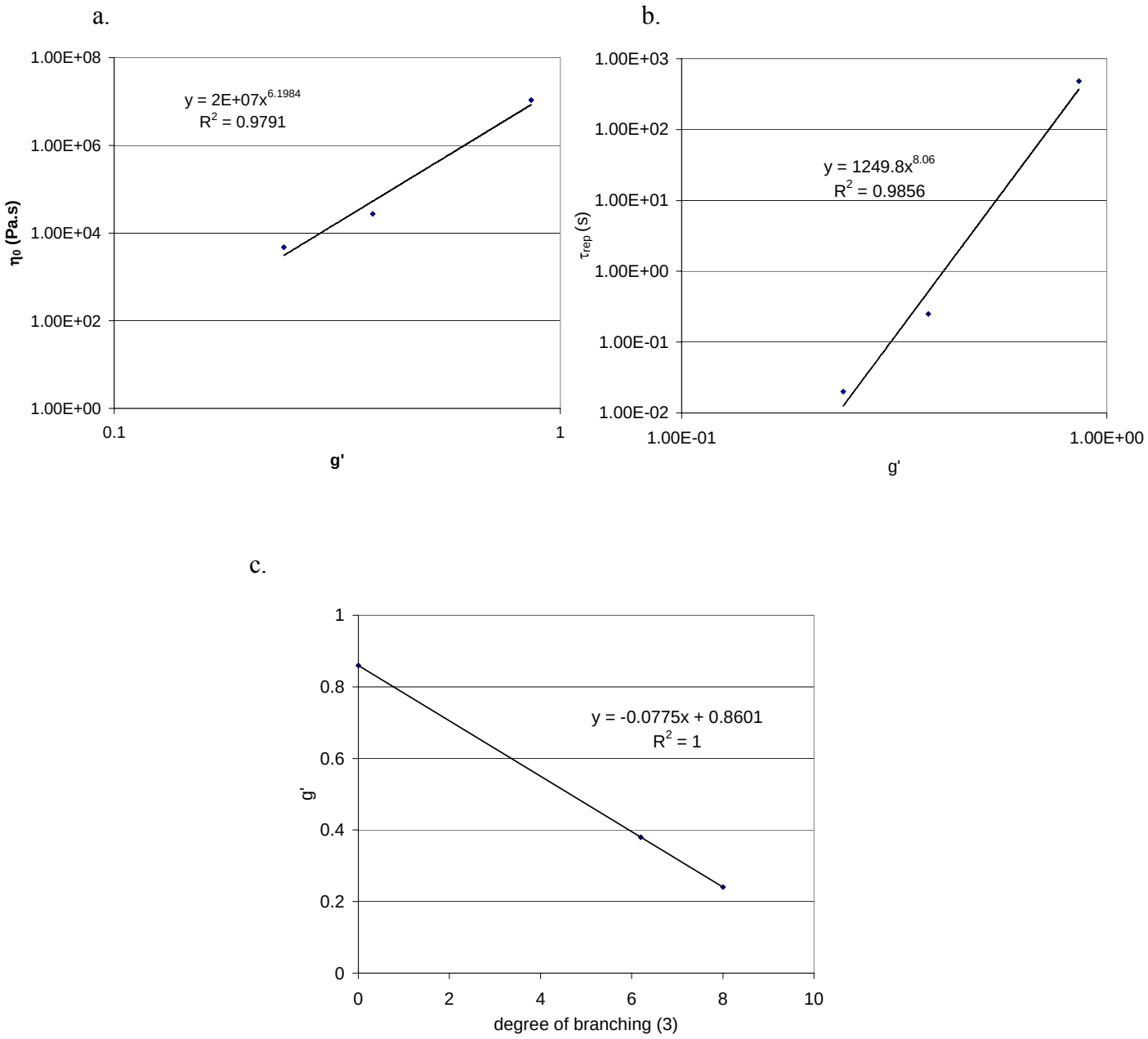

Figure 5.4: Exponential dependence of (a) zero shear rate viscosity and (b) longest relaxation time on the contraction factor, g'. Significant (R2 = 1) relationship (c) between the contraction factor, g', and DB2.

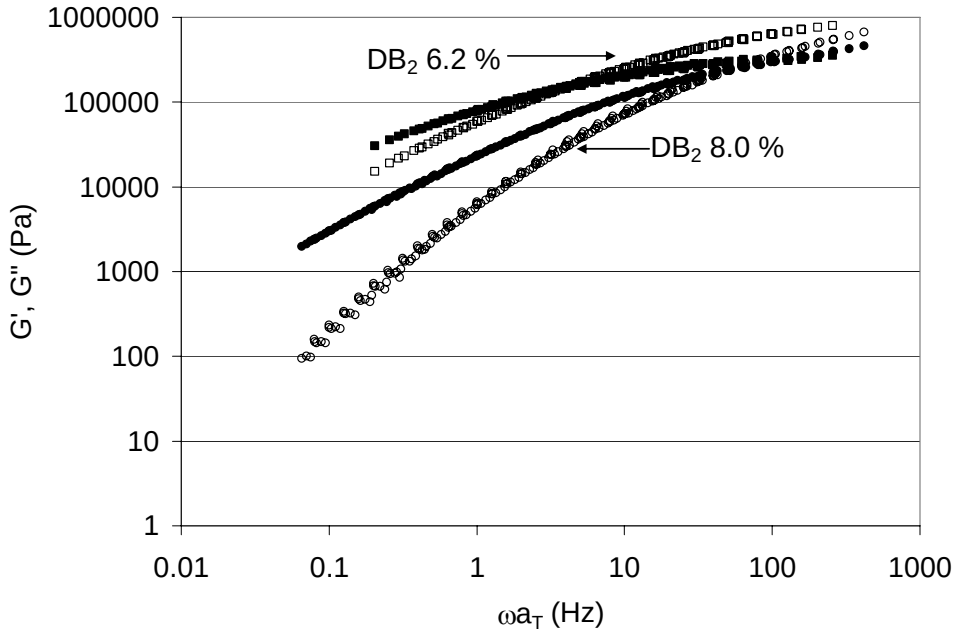

Figure 5.5: Dynamic moduli of highly branched polyurethanes with DB2 of 6.2% (squares) and 8.0% (circles). Intersection of G'(open symbols) and G" (closed symbols) is related to the relaxation time.

While all of these points typically indicate that entanglements are present in polymeric systems, hydrogen bonding must also be considered when interpreting these rheological behaviors. Therefore, solution rheology was investigated to elucidate the role of entanglements on the rheological behavior of highly branched polyurethanes without the interference of hydrogen bonding. Polyurethanes are well-known to undergo monodentate hydrogen bonding in the hard segment, which aids in the microphase separation of these elastomeric materials.[198] The elastomeric properties from hydrogen bonding in the hard segment are desirable for the application of highly branched

polyurethanes in electromechanical devices.[199, 200] However, separating the effects of hydrogen bonding and entanglements on rheology required the use of a solvent that disrupts hydrogen bonding. DMF was chosen for these rheological measurements as DMF disrupts hydrogen bonding of the polyurethane and has a low volatility. A number of chain interactions from the dilute to concentrated regimes are observed with the scaling of the log-log plot of η_{sp} versus concentration over a wide range of solution concentrations.[201] The semi-dilute unentangled and the semi-dilute entangled regimes were observed over the concentration range probed for these polyurethanes. The viscosity in these regimes was within the sensitivity limits of the rheometer used.

Table 5.3: Influence of higher hard segment content on zero shear rate viscosity

Sample	M_w[a] (g/mol)	PEG MW (g/mol)	HS content (%)	DB_1 (%)	DB_2 (%)	η_0 (Pa.s)
7	25,400	600	57	38	6.6	12,730
8	26,600	2000	36	36	3.5	1,500
9	51,700	600	57	42	5.4	21,000
10	45,300	2000	36	48	1.6	8,980

[a] MALLS

The solution rheology of a linear and highly branched polymer based on a 600 g/mol PEG as the soft segment with 57 wt% hard segment and about 40,000 g/mol M_w, was investigated. With equivalent molecular weight, hard segment content, and soft segment composition, the difference between these two polymers was solely architecture. The DB_2 for the branched polyurethane was 6.2% and the branching efficiency or DB_1 was 35%. The η_0 were determined for several concentrations in the semi-dilute unentangled and semi-dilute entangled regime (Figure 5.7). At all concentrations, η_{sp} of

the highly branched polyurethane was higher than the linear counterpart. The entanglement concentration, C_e, was determined from the intersection of the semi-dilute unentangled and entangled regimes.[201] The C_e for the linear polyurethane, 9 wt%, occurred at a slightly lower concentration than for the highly branched polyurethane, 11 wt%. The increase in C_e was attributed to a lower hydrodynamic radius for the highly branched polyurethane, which required a higher concentration for entanglement. The increase in C_e with distance between branch points was shown previously in AB plus AB_2 type systems, pom poms,[202, 203] and for randomly branched polyesters with significantly lower degrees of branching.[1] The determination of the entanglement concentration for highly branched polyurethanes indicated that the highly branched polyurethanes indeed do have entanglements despite the incorporation of a large number of branch points.

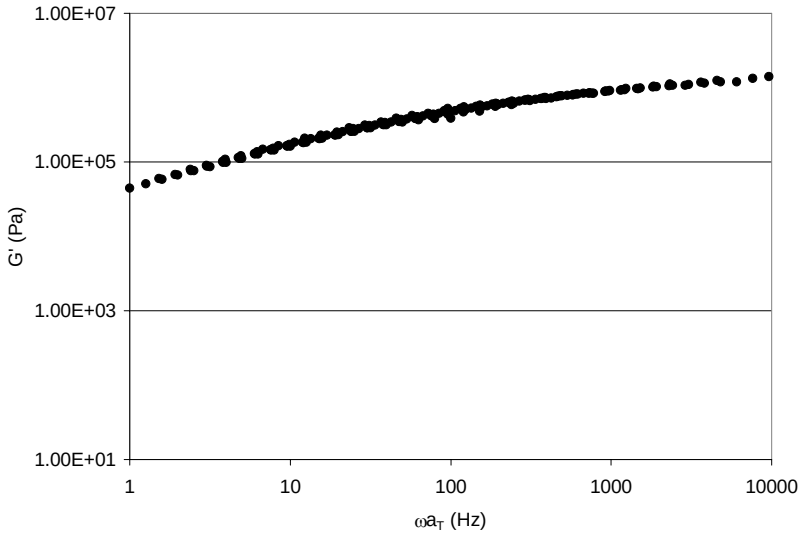

Figure 5.6: Master plot of storage modulus of a highly branched polyurethane at Tref = 80 ^{o}C Lack of a plateau in the storage modulus of highly branched polyurethanes was attributed to the high 2.51 polydispersity.

One application for poly(ether urethane)s may be in electromechanical devices.204 For this application a metal salt must be added to render the polyurethane ionically conductive.205 The metal salt dopant, in this case lithium perchlorate, interacts with the polyether segments and acts as a temporary physical crosslink.192 The complex viscosities of both a highly branched and linear polyurethane were determined for a dopant level of 8 ethylene oxide units to 1 lithium. Complex viscosities for both topologies increased significantly with the addition of salt (Figure 5.8). While η* of the highly branched polyurethane changed more than the linear analog, the complex viscosity of the highly branched polyurethane was still less than the doped, linear polyurethane. The dynamic moduli of both polyurethanes were also found to increase on lithium perchlorate addition. The relaxation times also increased significantly with the addition of the dopant (Figure 5.8). The increase in relaxation time and melt viscosity are consistent with the suggestion that lithium perchlorate acted as a physical crosslinking agent and reduced the chain mobility. The greater increase in melt viscosity for the highly branched polyurethane was attributed to interaction of the lithium perchlorate with the preponderance of chain ends.

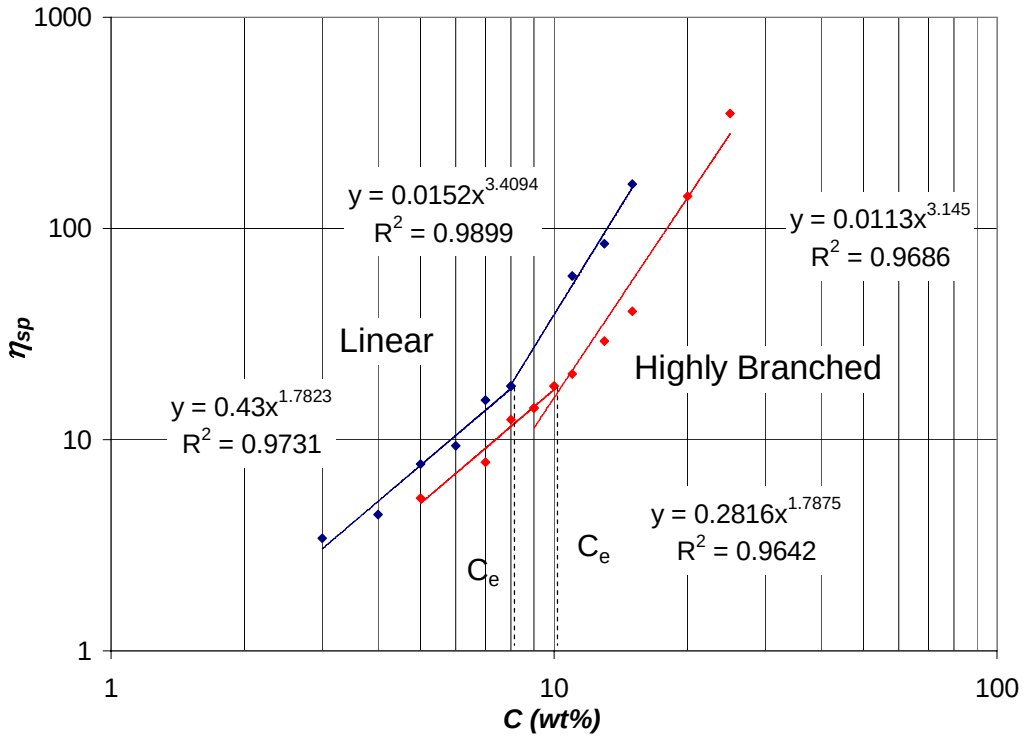

Figure 5.7: Comparison of the specific viscosity for a linear and highly branched polyurethane of equal hard segment content (57%), soft segment composition (600 g/mol PEG), and molecular weight (40,000 g/mol) over a wide concentration range in DMF. The intersection of the semi-dilute unentangled and semi-dilute entangled regime indicates the entanglement concentrations. The slopes of the semi-dilute unentangled

regime for both polymers were 1.78 and 3.1 and 3.5 for the semi-dilute entangled concentration regime for the highly branched and linear polymers, respectively.

The ionic conductivity of the polyurethanes doped at 8 ethylene oxide units to 1 lithium was determined with impendence measurements. The hard segment content was 57 wt% for the highly branched and linear polyurethanes, the soft segment was based upon 600 g/mol PEG, and the M_w for both polymers was approximately 40,000 g/mol (Samples 4 and 5). The ionic conductivity for both architectures of the PEG-based polyurethanes was found to follow an Arrhenius type trend with temperature, where $\sigma = A \exp[-E_a/RT]$ (Figure 5.9). Arrhenius behavior, where A is a constant and E_a is the activation energy, was observed previously for ion transport, which was decoupled from the segmental movement of the polymer.[178] The Arrhenius type behavior indicated that the primary mode of ion transport was through ion hopping.[79] Transport through ion hopping in polyurethanes is typically associated with the salt concentration being above a critical concentration to transition from coupling of the ion transport to the segmental motion of the polymer backbone to ion hopping. The activation energy for the linear and highly branched polyurethanes were nearly equivalent at 1.39 J for the linear and 1.36 J for the highly branched polymer, which indicated that the energy required for activated ion hopping in both systems was similar.

The ionic conductivity of the highly branched polyurethane was significantly higher than the ionic conductivity of the linear analog. The linear polyurethane even at temperatures well over 50 degrees higher had an ionic conductivity approximately four orders of magnitude lower ($3.6*10^{-10}$ S/cm, 99 ^{o}C) than the highly branched polyurethane

($3.19*10^{-6}$ S/cm, 40 ^{o}C). The conductivity of the linear polyurethane was too low at 25 ^{o}C to reliably determine the ionic conductivity. Previous studies, where hyperbranched poly(urethane urea)s were blended with linear poly(urethane urea)s, demonstrated that the addition of a branched structure resulted in an increase in the ionic conductivity.[105, 186] The enhanced ionic conductivity was attributed to a decrease in the crystallinity of the soft segment, which lead to an increase in the segmental mobility of the PEG soft segment in that case. The reduced melt viscosity of the highly branched polyurethane, which was discussed earlier, indicated that the highly branched polyurethane had greater mobility when compared with the linear analog. The improved ionic conductivity of the highly branched polyurethane was attributed to the greater mobility of the PEG-based polyurethane.

a.

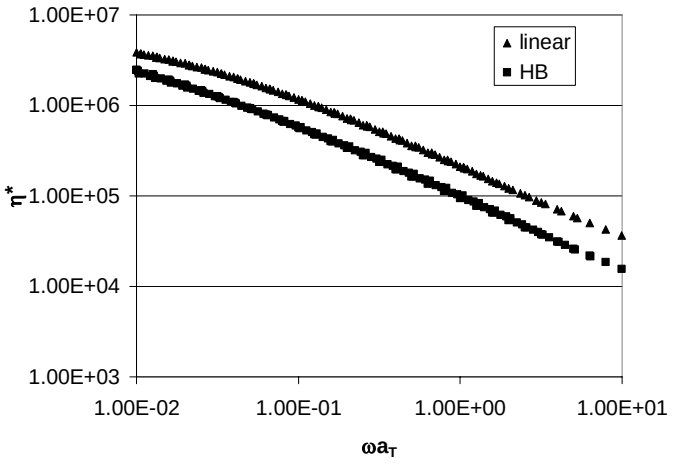

b.

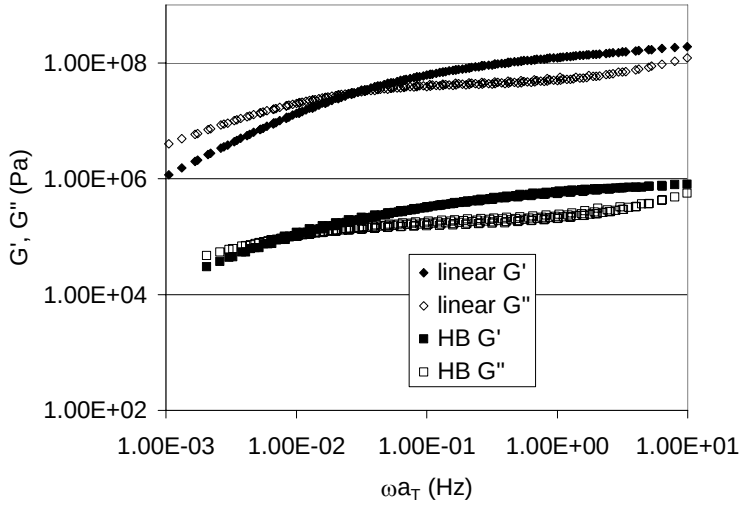

Figure 5.8: Melt rheology of linear and highly branched (HB) polyurethanes with 8:1 ethylene oxide : lithium perchlorate doping level. a) melt complex viscosity at T_{ref} = 80 oC b) dynamic modulus data

Higher hard segment content was shown previously to decrease the overall bulk conductivity of poly(urethane urea)s.[206] The hard segment content of the highly branched and linear PEG-based polyurethanes was equivalent (57 wt%); however, the branch points in the highly branched polyurethanes were located in the hard segment. The incorporation of branching in the hard segment of polyurethanes was shown previously to adversely affect the microphase separation of the polyurethanes.[165] The disruption of the hard segment packing was also considered a possible source of the improved ionic conductivity of the highly branched polyurethane.

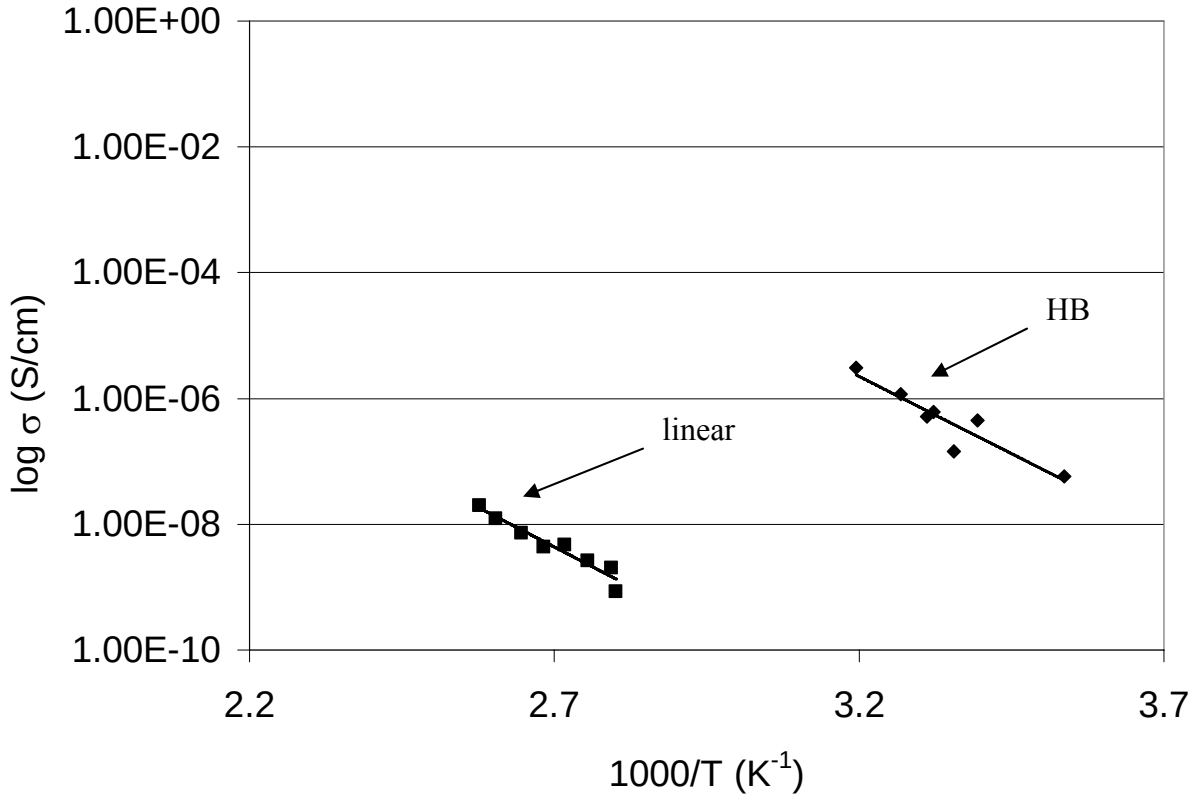

Figure 5.9: Ionic conductivity for PEG 600 g/mol-based polyurethane

5.5 Conclusions

Highly branched polyurethanes were synthesized using an oligomeric A_2 plus B_3 method for melt and solution rheology studies. The complex viscosities of the highly branched polyurethanes were orders of magnitude lower than for linear analogs. This significant reduction in melt viscosity with branching has implications for improved processability. The reduction in melt viscosity correlated with a reduction in relaxation time for the highly branched polyurethanes. The power law relationship between η_0 and M_w was slightly stronger (3.9) than the theoretical prediction for linear polymers (3.4), and this increase was attributed to an increase in the apparent molecular weight of the polyurethanes in the melt due to intermolecular hydrogen bonding. However, more experiments are required to confirm this trend. Small changes in the degree of branching at equivalent molecular weight drastically reduced η_0 due to the reduction in entanglements. Increasing the hard segment at equivalent molecular weight content caused an increase in η_0 despite a simultaneous higher degree of branching. The melt rheological data was complicated with the potential hydrogen bonding of the highly branched polyurethanes, and solution rheology was performed with a solvent that disrupted the hydrogen bonding to conclusively determine that entanglements were present in the highly branched polyurethanes. The 11 wt% entanglement concentration determined for the highly branched polyurethanes in the solution rheology experiments indicated the highly branched polymers were entangled. The specific viscosity of the highly branched polyurethanes was lower at all of the concentrations tested relative to linear analogs. The higher viscosity was attributed to the larger hydrodynamic volume of

the linear polymers. The ionic conductivity of the highly branched polyurethane was significantly higher than that for the linear analog. The increased ionic conductivity was attributed to greater mobility of the ions in the highly branched polyurethane matrix as observed in the melt viscosity.

5.6 Acknowledgements

This material is based upon work supported by the U.S. Army Research Laboratory and the U.S. Army Research Office under grant number DAAD19-02-1-0275 Macromolecular Architecture for Performance (MAP) MURI. The authors thank Dr. Cheryl Heisey for her helpful discussions.

5.7 References

1. Spindler, R.; Fréchet, J. M. J. *Macromolecules* **1993** 26, 4809-4813.

2. Kwak, S.-Y.; Ahn, D. U. *Macromolecules* **2000** 33, 7557-7563.

3. Voit, B. *J. Polym. Sci.: Part A: Polym. Chem.* **2005** 43, 2679-2699.

4. Voit, B. *J. Polym. Sci.: Part A: Polym. Chem.* **2000** 38, 2505-2525.

5. Hawker, C. J.; Lee, R.; Fréchet, J. M. J. *J. Am. Chem. Soc.* **1991** 113, 4583-4588.

6. Trollsas, M.; Atthoff, B.; Claesson, H.; Hedrick, J. L. *Macromolecules* **1998** 31, 3439-3445.

7. Kim, Y. H.; Webster, O. W. *J. Am. Chem. Soc.* **1990** 112, 4592-4593.

8. Scheel, A.; Komber, H.; Voit, B. *Macromol. Symp.* **2004** 210, 101-110.

9. Lin, Q.; Long, T. E. *Macromolecules* **2003** 36, 9809-9816.

10. Czupik, M.; Fossum, E. *J. Polym. Sci.: Part A: Polym. Chem.* **2003** 41, 3871-3881.

11. Hawker, C. J.; Farrington, P. J.; Mackay, M. E.; Wooley, K. L.; Frechét, J. M. J. *J. Am. Chem. Soc.* **1995** 117, 4409-4410.

12. Scherrenberg, R.; Coussens, B.; van Vilet, P.; Edouard, G.; Brackman, J.; de Brabander, E. *Macromolecules* **1998** 31, 456-461.

13. Mourey, T. H.; Turner, S. R.; Rubenstein, M.; Frechét, J. M. J.; Hawker, C. J.; Wooley, K. L. *Macromolecules* **1992** 25, 2401-2406.

14. Uppuluri, S.; Keinath, S. E.; Tomalia, D. A.; Dvornic, P. R. *Macromolecules* **1998** 31.

15. Gretton-Watson, S. P.; Alpay, E.; Steinke, J. H.; Higgins, J. S. *Ind. Eng. Chem. Res.* **2005** 44, 8682-8693.

16. Karchenko, S. B.; Kannan, R. M. *Macromolecules* **2003** 36, 407-415.

17. Luciani, A.; Plummer, C. J. G.; Nguyen, T.; Garamszegi, L.; Månson, J.-A. E. *J. Polym. Sci.: Part B: Polym. Phys.* **2004** 42, 1218-1225.

18. Kunamaneni, S.; Buzza, D. M. A.; De Luca, E.; Richards, R. W. *Macromolecules* **2004** 37, 9295-9297.

19. Ferry, J. D., In *Viscoelastic Properties of Polymers*. Second ed.; John Wiley & Sons, Inc.: New York, 1970.

20. Simon, P. F. W.; Müller, A. H. E.; Pakula, T. *Macromolecules* **2001** 34, 1677-1684.

21. Magnusson, H.; Malmström, E.; Hult, A.; Johansson, M. *Polymer* **2002** 43, 301-306.

22. Suneel; Buzza, D. M. A.; Groves, D. J.; McLeish, T. C. B.; Parker, D.; Keeney, A. J.; Feast, W. J. *Macromolecules* **2002** 35, 9605-9612.

23. Unal, S.; Lin, Q.; Mourey, T. H.; Long, T. E. *Macromolecules* **2005** 38, 3246-3254.

24. Unal, S.; Oguz, C.; Yilgor, E.; Gallivan, M.; Long, T. E.; Yilgor, I. *Polymer* **2005** 46, 695-696.

25. Unal, S.; Yilgor, I.; Yilgor, E.; Sheth, J. P.; Wilkes, G. L.; Long, T. E. *Macromolecules* **2004** 37, 7081-7084.

26. McKee, M. G.; Park, T.; Unal, S.; Yilgor, I.; Long, T. E. *Polymer* **2005** 46, 2011-2015.

27. Huang, X.; Ren, T.; Tian, L.; Hong, L.; Zhu, W.; Tang, X. *J. Mater. Sci.* **2004** 39, 1221-1225.

28. Jiang, G.; Maeda, S.; Yang, H.; Wang, C.; Saito, Y.; Tanase, S.; Sakai, T. *J. Electrochem. Soc.* **2004** 151, 1886-1890.

29. Watanabe, M.; Sanui, K.; Ogata, N. *Macromolecules* **1986** 19, 815-819.

30. Hong, L.; Shi, L.; Tang, X. *Macromolecules* **2003** 36, 4989-4994.

31. Matsumiya, Y.; Balsara, N. P.; Kerr, J. B.; Inoue, T.; Watanabe, H. *Macromolecules* **2004** 37, 544-553.

32. Dieterich, D.; Schmelzer, H. G., In *Polyurethane Handbook*. 2nd ed.; Hanser/Gardner Publications, Inc.: Cincinnati, 1993; p 25-37.

33. Hong, Y.; Coombs, S. J.; Cooper-White, J. J.; Mackay, M. E.; Hawker, C. J.; Malmstrom, E.; Rehnberg, N. *Polymer* **2000** 41, 7705-7713.

34. Hawker, C. J.; Farrington, P. J.; Mackay, M. E.; Wooley, K. L.; Fréchet, J. M. J. *J. Am. Chem. Soc.* **1995** 117, 4409-4410.

35. Sheth, J. P.; Unal, S.; Yilgor, E.; Yilgor, I.; Beyer, F.; Long, T. E.; Wilkes, G. L. *Polymer* **2005** 46, 10180-10190.

36. Sheth, J. P.; Wilkes, G. L.; Fornof, A. R.; Long, T. E.; Yilgor, I. *Macromolecules* **2005** 38, 5681-5685.

37. Fornof, A. R.; Glass, T. E.; Long, T. E. *In Progress* **2006**.

38. Lusignan, C. P.; Mourey, T. H.; Wilson, J. C.; Colby, R. H. *Phys. Rev. E* **1999** 60, 5657-5669.

39. McKee, M. G.; Wilkes, G. L.; Colby, R. H.; Long, T. E. *Macromolecules* **2004** 37, 1760-1767.

40. Graessley, W. W.; Masuda, T.; Roovers, J. E. L.; Hadjichristidis, N. *Macromolecules* **1976** 9, 127-141.

41. Hess, C.; hirt, P.; Opperman, W. *J. Appl. Polym. Sci.* **199** 74, 728-734.

42. Liu, C.; Li, C.; Chen, P.; He, J.; Fan, Q. *Polymer* **2004** 45, 2803-2812.

43. Doerpinghaus, P. J.; Baird, D. G. *J. Rheol.* **2003** 47, 717-736.

44. Rubenstein, M.; Colby, R. H., In *Polymer Physics*. Oxford University Press: New York, 2003.

45. Dietrich, D.; Hespe, H., In *Polyurethane Handbook*. 2nd ed.; Hanser/Gardner Publications, Inc.: Cincinnati, OH, 1993; p 37-53.

46. Watanabe, M.; Sanui, K.; Ogata, N. *Macromolecules* **186** 19, 815-819.

47. Shilov, V. V.; Shevchenko, V. V.; Pissis, P.; Kyritsis, A.; Georgoussis, G.; Gomza, Y. P.; Nesin, S. D.; Klimenko, N. S. *J. Non-Cryst. Solids* **2000** 275, 116-136.

48. de Gennes, P.-G., In *Scaling Concepts in Polymer Physics*. Elsevier: New York, 1979.

49. Sendijarevic, I.; Liberatore, M. W.; McHugh, A. J.; Markoski, L. J.; Moore, J. S. *J. Rheol.* **2001** 45, 1245-1258.

50. Juliani; Archer, L. A. *Macromolecules* **2002** 35, 6953-6960.

51. Ferry, A.; Jacobsson, P.; van Heumen, J. D.; Stevens, J. R. *Polymer* **1996** 37, 737-744.

52. Du, Y.-L.; Wen, T.-C. *Mater. Chem. Phys.* **2001** 71, 62-69.

53. van Heumen, J. D.; Stevens, J. R. *Macromolecules* **1995** 28, 4268-4277.

54. Lee, S.-M.; Chen, C. Y.; Wang, C.-C. *Electrochim. Acta* **2004** 49, 4907-4913.

55. Seki, M.; Sato, K. *Macromol. Chem.* **1992** 193, 2971-2982.

56. Sheth, J. P.; Wilkes, G. L.; Fornof, A. R.; Long, T. E.; Yilgor, I. *Macromolecules* **2005** 38, 5681-5685.

Chapter 6: Synthesis and Characterization of Triglyceride-Based Polyols and Tack-Free Coatings via the Air Oxidation of Soy Oil

(Fornof, A.R.; Onah, E.; Ghosh, S.; Frazier, C.; Sohn, S.; Wilkes, G.L.; Long, T.E. *J. Appl. Polym. Sci.* **2006**, *Accepted*)

6.1 Abstract

The effect of time and temperature on the air oxidation of soybean oil in the absence of catalysts or added initiators was investigated. It was possible to divide the air oxidation of soybean oil into three regimes. The first regime of air oxidation resulted in insignificant change in the hydroxyl number. During this regime, it was proposed that natural antioxidants, which are present in raw soybean oil, were consumed and peroxide formation occurred. A drastic increase in hydroxyl number due to the formation and subsequent decomposition of peroxides marked the second regime of air oxidation. In the third regime of air oxidation, free radical crosslinking of the soybean oil occurred, and an insoluble gel was formed. The three regimes of air oxidation were used as a guide for the preparation of soy-based polyols and crosslinked polymers. Crosslinked, tack-free coatings were prepared from a metal catalyzed oxidation of soybean oil, where soybean oil and ambient oxygen were the only reactants. Higher temperatures (125 °C) were more efficient than lower (50 °C) for obtaining high gel fractions and tack-free coatings. Cure of the coatings was expedited with exposure of the coating to UV irradiation after initial heating.

Keywords: oxidation, renewable resources, coatings

6.2 Introduction

Renewable resources have received increased attention as potential alternatives to traditional petroleum-based monomer feedstocks.[196, 207] Synthetic approaches that range broadly from incorporating various triglycerides into polyurethane networks to utilizing enzymes as catalysts for polycondensations were targeted for the use of renewable resources as replacements for traditional feedstocks.[208, 209] Soybean oil is an abundant and inexpensive vegetable oil, and these agriculture-based triglycerides are considered green feedstocks. Multiple sites of chemical reactivity are intrinsic in soybean-based triglycerides, which makes this renewable resource particularly attractive as a potential alternative to petroleum-based monomers. [210-212] Previous investigations of soybean oil as a potential monomer have utilized well-established synthetic organic methodologies to modify the internal unsaturated sites.[118] Various synthetic strategies for the introduction of specific reactive functionalities including epoxide[213], hydroxyl[214], and aldehyde[215] groups were developed.[215-219] The applications for soy-based monomers have included rigid polyurethane foams and photo-crosslinkable monomers for adhesives. [213, 220-222] Polymers with shape memory attributes were synthesized via the cationic polymerization of soybean oil and crosslinked with divinylbenzene.[223] Halogenated soy-based polyols derived from epoxidized soybean oil were used in the synthesis of polyurethanes, and the effects of pendant halogens that are adjacent to the reactive hydroxyls were investigated.[214]

While the synthesis of monomer feedstocks was primarily explored with traditional synthetic approaches, oxidation of lipids and fats has also gained significant interest due to its important role in several areas including human health with its implications for aging, cancer, and heart disease as well as in food spoilage and monomer feedstocks. [224-227] Due to this broad applicablility, lipid oxidation has received significant interest in the literature. Extensive studies of the mechanism of autoxidation of lipids elucidated the initiation and subsequent steps of this free radical reaction. Air oxidation involves free radical intermediates due to the abstraction of allylic hydrogens and the subsequent formation of a delocalized free radical. These free radicals react with ambient oxygen and other triglycerides to form polyols and a host of other products. Multiple products were reported earlier from the catalyzed autoxidation of soybean oil, including hydroxyl-containing compounds.[228] Several kinetic stages of autoxidation were described for fats under constant pressure. [229] The extent of oil oxidation is frequently assessed using a variety of techniques, which include iodine value, color, refractive index, percentage of free fatty acids, total polar compounds, and hydroxyl number, which is the milligrams of potassium hydroxide equivalent to the hydroxyl groups of one gram of sample.[123, 230-233] These time-consuming techniques require large amounts of organic solvents and precise measurements for reproducible results. Changes in the longitudinal and transverse relaxation times from ^{1}H NMR were compared with the increase in free fatty acid percentage and total polar materials of oxidized soybean oil.[86]

Renewable resources have received notable attention as important components of coatings, especially as drying oils in alkyd and other resins.[136, 234, 235] Moreover, the synthesis of novel coatings from derivatized renewable resources was highlighted in a

recent review.[218, 236] Coatings utilized for a variety of applications including anti-corrosion and waterborne coatings have successfully incorporated modified soybean oil as a component.[234, 237]

The air oxidation in the absence of catalyst, which represents the simplest reaction in term of reactants, i.e. air and soybean oil, has not received significant attention for the synthesis of monomer feedstocks. These reactions also produce polyols, which are suitable for subsequent polymer synthesis. The focus of this research was to investigate the free radical air oxidation of soybean oil and subsequent polyol formation. Synthetic strategies for preparing high hydroxyl number soy polyol monomer feedstocks were developed as a function of time and temperature. In this study, air at a constant flow rate was distributed to the soybean oil. For the first time in this work, three regimes of air oxidation were identified using ^{1}H NMR spectroscopy, viscosity, and hydroxyl number determination as complementary characterization techniques to monitor the oxidation of soybean oil. In this paper, the relationship between hydroxyl number, an analytical technique that requires several titrations, and the doubly allylic resonance in the ^{1}H NMR spectrum was determined for oxidized soybean oil. The use of ^{1}H NMR spectroscopy for determination of the extent of oxidation provided a straightforward analysis of oxidized soybean oil.

Emergence of the three regimes of soybean oil air oxidation provided a framework for the more well-defined synthesis of renewable resource-based raw materials. Soy polyols with high hydroxyl number were produced for use in the synthesis of polyesters, polyurethanes, and multifunctional acrylates when the second regime of air oxidation was targeted. The third regime of air oxidation, which includes significant

branching and crosslinking, produced interesting polymeric networks. Crosslinked coatings synthesized from raw soybean oil were also investigated in this work.

6.3 Experimental

6.3.1 Statistical Design of Experiments

A central composite statistical design of experiments (DOE) was developed for the investigation of the air oxidation of soybean oil. The factors assigned for this DOE were temperature, time, and air flow rate. Temperatures ranging from 77 to 110 °C, reaction times ranging from one to six days, and air flow rates from 10 to 40 L min^{-1} were investigated. The responses modeled for this design of experiments were hydroxyl number, viscosity, and doubly allylic and singly allylic ^{1}H NMR resonances with Stat-Ease software. The Design-Expert version 6.0.1 was used and the central composite design was chosen to model these experiments.

6.3.2 Air Oxidation

The soybean oil was heated to the appropriate temperature in a 250-mL, round-bottomed flask, which was stirred with a magnetic stir bar, and equipped with a dispersion tube that delivered air for the allotted time. The air used in the soybean oil oxidation was kept at ambient temperature prior to entering the reaction flask. For example, 100 mL of raw soybean oil in a 250-mL, two-neck, round-bottomed flask was heated to 110 °C while air was delivered to the sample via a dispersion tube at 25 L min^{-1} for three days. For the high pressure reactions, a Parr reactor charged with 100 mL of raw soybean oil was held at constant temperature and pressure. The reaction was vigorously stirred with the mechanical stirrer in the reactor. The sample was allowed to

cool to room temperature after the reaction was completed and analyzed with ^{1}H NMR spectroscopy, hydroxyl number determination, and viscosity measurements. The allylic protons were found at 2.01 ppm and the doubly allylic protons were found at 2.79 ppm utilizing a Varian Unity 400 MHz NMR at ambient conditions with *d*-chloroform as the NMR solvent. The normalized doubly allylic resonance was calculated from division of the integration of the doubly allylic resonance for the oxidized sample by the integration of the raw soybean oil. The statistical design of experiments software (Stat-Ease) was utilized to model the system. Thermogravimetric analysis (TGA) was conducted on a TA Instruments High Res TGA 2950 thermogravimetric analyzer under an oxygen flow rate of 60 mL min^{-1}. An ASI ReactIR 1000 (Mettler-Toledo, Inc., Columbus, OH) was used for the *in-situ* FTIR spectroscopic investigations. Size exclusion chromatography (SEC) was performed at 40 °C in tetrahydrofuran at 1 mL min^{-1} with three 5-μm PLgel columns in series and utilizing a Waters 717 autosampler and Waters 2410 refractive index detector. UV-Vis spectra were collected with an Analytical Instrument Systems, Inc. spectrometer equipped with fiber optics light guides, a DT1000CE light source and an Ocean Optics USB2000 UV-Vis detector. Viscosity measurements of 100% soybean oil were performed with a TA Instruments AR 1000 rheometer. The geometry used was a 40 mm cone (1.59 degrees) and plate at a gap of 44 microns in rotational mode at 25 ^{o}C.

6.3.3 Hydroxyl Number Determination

Hydroxyl number is defined as the milligrams of potassium hydroxide equivalent to the hydroxyl groups of one gram of sample. The hydroxyl number was determined utilizing the procedure outlined in American Oil Chemists' Society (AOCS) Tx 1a-66. The procedure includes the use of pyridine and n-butyl alcohol as solvents. Acetic

anhydride was reacted with the hydroxyl groups of the soy polyol. Excess acetic anhydride was quenched with water and back titrated with 1.0 N KOH in ethanol with phenolphthalein as the indicator. The acid number was determined using the acid value procedure according to AOCS Cd 3d-63. Isopropyl alcohol and toluene were used to dissolve the soy polyol, and the acid was immediately titrated with 0.1 N KOH in ethanol using phenolphthalein to indicate the endpoint.

6.3.4 Film Formation

Thin films were formed from a 5 w/v % mixture of raw soybean oil and cobalt(II) ethyl hexanoate (65 wt % solution in mineral oil). The low viscosity mixture was thoroughly blended and drawn in a controlled manner with a doctor blade across a glass microscope slide to create a 100-μm layer. These films were heated in an oven for a given period of time at 50, 100, or 125 °C. Some films were also exposed to UV irradiation from an Oriel UV reactor. A TA.XT2i Texture Analyzer (Texture Technologies Corp., Scarsdale, NY/Stable Micro Systems, Godalming, Surrey, UK) was used to perform the tack tests according to ASTM D 2979. The parameters included a probe speed of 10 mm s^{-1}, 1.42 psi applied pressure, and a residence time of 0.1 s. Gel fractions were determined after soxhlet extraction in refluxing tetrahydrofuran for 24 h. The soxhlets were dried under vacuum for 48 h prior to the determination of gel fraction. Glass transition temperatures were determined under nitrogen on a Perkin-Elmer Pyris 1 cryogenic instrument at a heating rate of 10°C/min. The T_g was reported as the transition midpoint during the second heat. The TGA was performed on a TA Instruments High Res TGA 2950 thermogravimetric analyzer under nitrogen at a heating rate of 10 °C/min to a maximum temperature of 600 °C.

6.4 Results and Discussion

Soybean oil is widely used in a variety of well-known applications such as drying oils.[205, 235, 238, 239] Soybean oil is an abundant and inexpensive vegetable oil with multiple sites of reactivity including ester and olefinic sites. In this work, the interest lies in exploiting air oxidation, which is the most inexpensive and simple reaction in terms of reactants (air and soybean oil), as a method for the production of high hydroxyl number soy polyols. Significant work previously investigated the impact of metal catalysts and added initiators on the synthesis of polyols derived from vegetable oils. [240-242] This is the first systematic study of triglyceride air oxidation in the absence of catalysts[243] The three regimes of air oxidation of soybean oil, which differ significantly in content and application from the kinetic stages previously determined[229, 243], are defined through this work. The knowledge gained from these experiments was utilized to produce tack-free films with soybean oil and atmospheric oxygen.

6.4.1 High molecular weight polyols

Initiation of the autoxidation of unsaturated triglycerides occurs via the abstraction of an allylic hydrogen. The free radical process that follows is uncontrolled and propagation occurs simultaneously with termination reactions such as radical coupling. Multiple products are formed from this free radical reaction [Scheme 1].

Several trends were observed during the investigation of soybean oil oxidation, which were used to define three regimes of oxidation. Isothermal thermogravimetric analysis (TGA) of the soybean oil under oxygen atmosphere at 150 °C indicated a long

period of inactivity or an "induction" period followed with an increase in mass and rapid degradation of the soybean oil [Figure 6.1]. Mikula et al. have shown similar behavior for bleached and deodorized soybean oil at high temperatures (>195 °C).[244] The temperature of oxidation was found as a crucial parameter for balancing the time required to overcome the induction period and avoiding the subsequent, rapid degradation of the soybean oil. Thus, both time and temperature were important variables for the synthesis of high hydroxyl number soy polyols.

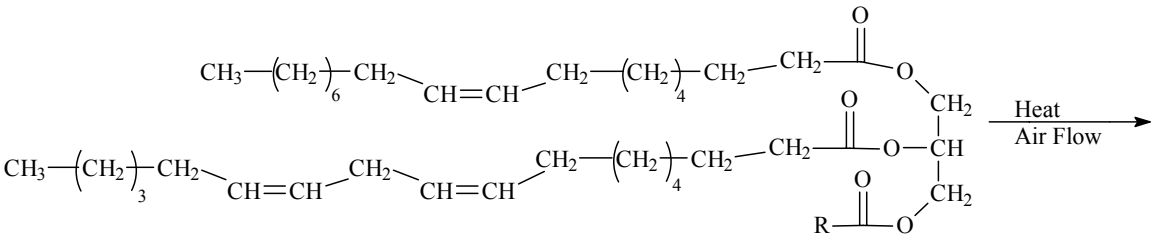

R = fatty acid chain

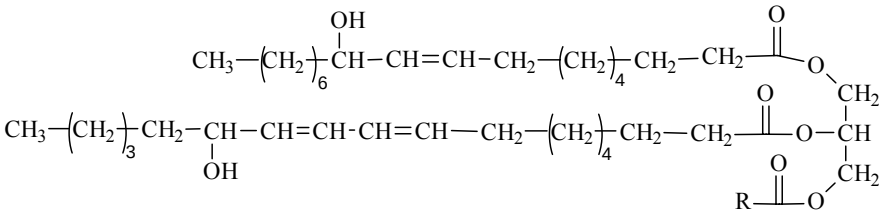

Aldehydes, Ketones, Epoxides, Acids, etc.

Scheme 6.1. Air oxidation of triglyceride yields hydroxyl groups replacing allylic protons.

The first regime was defined as the period when insignificant change in the hydroxyl number of the soybean oil occurred. Initiation and consumption of natural antioxidants that are present in the raw soybean oil (e.g. vitamin E) occurred during this time.[243] The first regime of air oxidation was modeled with a statistical design of experiments (DOE), which was performed with Stat-Ease software. The disappearance of allylic and doubly

allylic hydrogens, which are abstracted during the initiation of air oxidation, were monitored with ^{1}H NMR spectroscopy (2.01 ppm and 2.79 ppm, respectively). An increase in reaction time and temperature lead to a decrease in the normalized doubly allylic resonance (Eqn 1) and an increase in the hydroxyl number [Figure 6.2].

$$NDA = DA/DA_0 \qquad \text{(Eqn 1)}$$

where NDA = normalized doubly allylic resonance, DA = the integration of the doubly allylic ^{1}H NMR resonance of an oxidized soy polyol, and DA_0 = the integration of the same resonance for the control or unoxidized soybean oil. The doubly and singly allylic resonances followed a similar decreasing trend with oxidation. The doubly allylic resonance was chosen for comparison with the hydroxyl number, because the resolution of the doubly allylic resonance was better when compared to other resonances in the ^{1}H NMR spectrum. A significant, linear relationship between hydroxyl number and normalized doubly allylic resonance was found (r^2 = 0.98) [Figure 6.3]. From this relationship, an indication of the degree of oxidation was provided without performing multiple titrations that are required for hydroxyl number determination. The integration of the doubly allylic resonance from ^{1}H NMR was successfully used as an indicator of hydroxyl functionality for these soy polyols. While the increase in hydroxyl number is directly related to the decrease in the normalized doubly allylic resonance, it was not assumed that each abstracted doubly allylic hydrogen resulted in the formation of a hydroxyl group. Rather the relationship between the hydroxyl number and doubly allylic resonance was determined as potentially useful for fast analysis of the extent of oxidation.

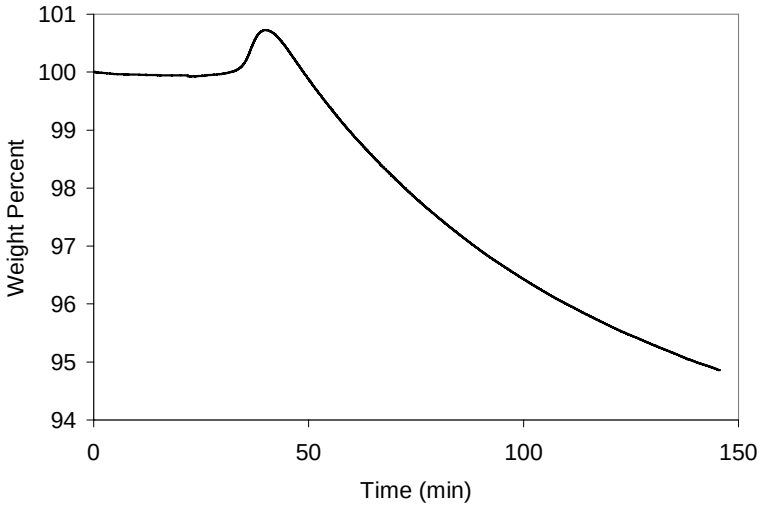

Figure 6.1. Isothermal TGA of raw soybean oil at 150 °C under oxygen.

Rapid oxidation of the soybean oil occurred in the second regime of air oxidation. This corresponded to the increase in mass or uptake of oxygen in the TGA [Figure 6.1]. A significant and rapid increase in the hydroxyl number was a feature of the second regime of air oxidation and was accompanied with a decrease in the normalized doubly allylic resonance in the ^{1}H NMR spectrum [Figure 6.4 and Table 6.1]. Radical-radical coupling, which indicated that propagation was occurring in this regime, was shown through the broadening of the polydispersity from 1.01 to 15.9 after 3.5 days at 110 °C [Table 1]. As radical-radical coupling occurred and the dispersity broadened, there was also an increase in the weight average molecular weight of the soy polyol [Table 1].

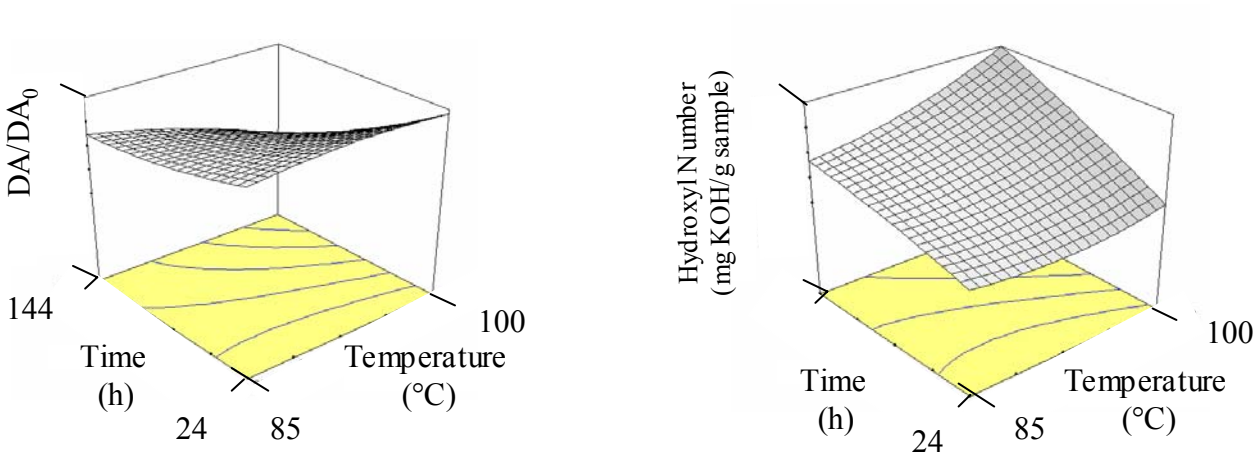

Figure 6.2. 3-D plots of temperature and time dependence of first regime of oxidation for normalized doubly allylic resonance integration and hydroxyl number.

This rapid increase in polydispersity over a relatively short period of time indicated the swift nature of the propagation. This narrow window for the synthesis of soluble, high functionality (> 75 mg KOH/g) soy polyols highlights the usefulness of the accurate definition of this regime. An increase in the high molar mass fractions of the soy polyol produced an increase in the melt viscosity as well during this regime of air oxidation. Viscosity is quite sensitive to the higher molar mass fractions of polymers and oligomers [Figure 6.5].[245] The increase in viscosity was undesirable from a processing standpoint, but it was unavoidable with the air oxidation route for the production of soy polyols. Continued reaction at high temperatures resulted in crosslinking of the soybean oil. A

network is a product of the termination step and an indication of the third regime of air oxidation. The resulting insolubility of the crosslinked soybean oil prohibited many common characterization techniques. The definition of regime two was critical when targeting the synthesis of more well-defined soy polyols.

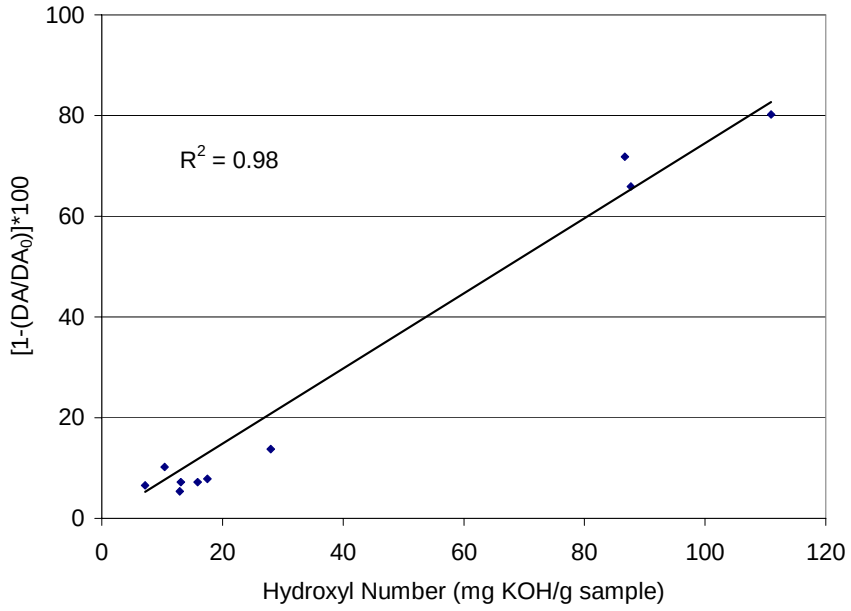

Figure 6.3. Significant relationship between the normalized integration of the doubly allylic resonance and hydroxyl number.

To determine the impact of increased air pressure on the oxidation of soybean oil, the reaction was performed in a Parr reactor at elevated pressure. Several reactions were performed to determine the effect of pressure on the oxidation of soybean oil. Reactions were allowed to proceed for one day at 110 ^{o}C at pressures ranging from 15 to 75 psi. An increase from atmospheric pressure to 25 psi lead to an initial drop in normalized doubly allylic resonance indicating greater oxidation at this modest increase in pressure.

However, for the rest of the series, little difference was observed for the increase in pressure [Figure 6.6]. When the normalized doubly allylic resonances were compared for one day at 60 psi versus one day in a round-bottomed flask with a constant air flow rate of 25 L/min, it was found that the soybean oil under pressure was only slightly more oxidized than the soybean oil subjected to air flow (NDA: 0.83, 0.93, respectively).

Table 6.1. Molecular weight and hydroxyl number data for soybean oil oxidized at 110 °C

Sample	Time (d)	M_w[a] (g/mol)	M_w/M_n[a]	Hydroxyl Number (mg KOH/g)
1	0	1,100	1.01	N/A
2	1	1,300	1.02	7 +/- 2.4
3	3	1,400	1.02	10 +/- 2.5
4	3.5	44,000	15.3	110 +/- 2.4

[a] From RI, versus polystyrene standards

Several high pressure reactions that ranged in length from one to 15 days were performed at 75 psi of air pressure. However, an insignificant difference of the normalized doubly allylic resonance was observed after one day of heating [Figure 6.7].

As described in Henry's law, there is a relationship between the vapor pressure and the mole fraction of the solute. In these high pressure reactions, a specific pressure was charged and remained unchanged for the duration of the experiment. Equilibrium between the gas and liquid was most likely reached, and the extent of oxidation was limited. When the reaction was continued for three to four days, the reaction with air flow through the sample was significantly more oxidized than that under a constant pressure (NDA: 0.20, 0.83, respectively) for the same reaction temperature and time.

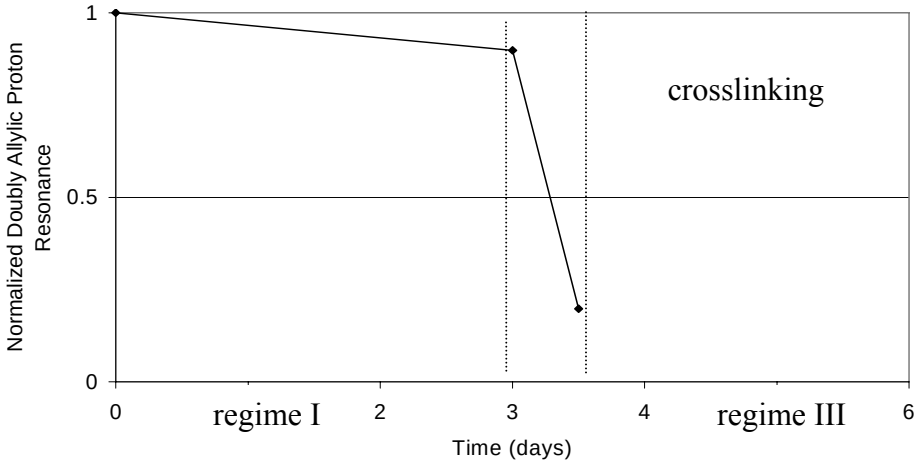

Figure 6.4. Decrease in normalized doubly allylic resonance from ^{1}H NMR spectra indicating an increase in hydroxyl number of soy polyols.

Thus, the technique of passing air through the soybean oil with a dispersion tube was used for the efficient production of high hydroxyl number soy polyols.

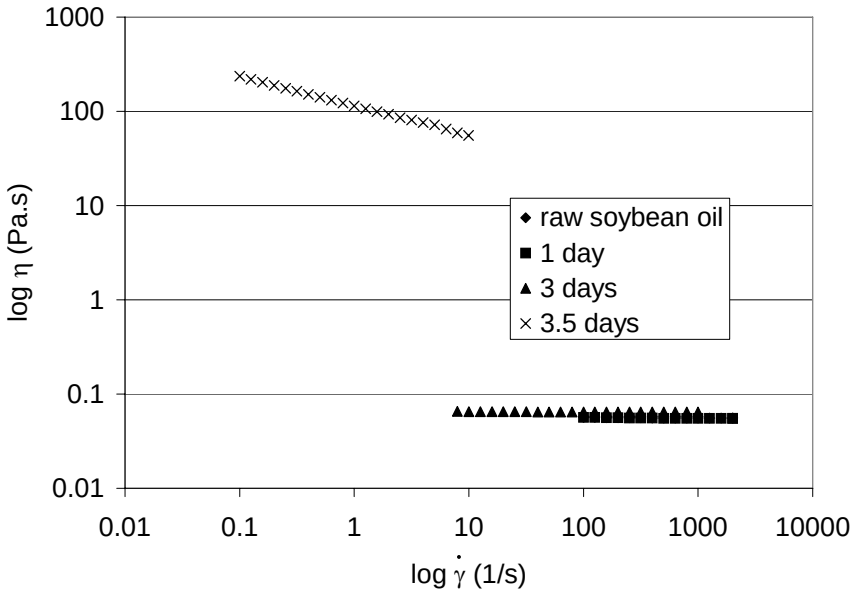

Figure 6.5. Increase in viscosity observed with time at 100 °C, 25 L/min. Raw soybean oil and 1 day are superimposable at the lowest viscosity.

Incorporation of the high hydroxyl number soy polyols into crosslinked polyurethane networks was discussed elsewhere.[246] The regimes of air oxidation established herein were used as a guide for the synthesis of either high hydroxyl number polyols or polymeric networks. The third regime of air oxidation for the synthesis of soybean oil-based coatings provides a unique opportunity to exploit the third regime of air oxidation for network formation.

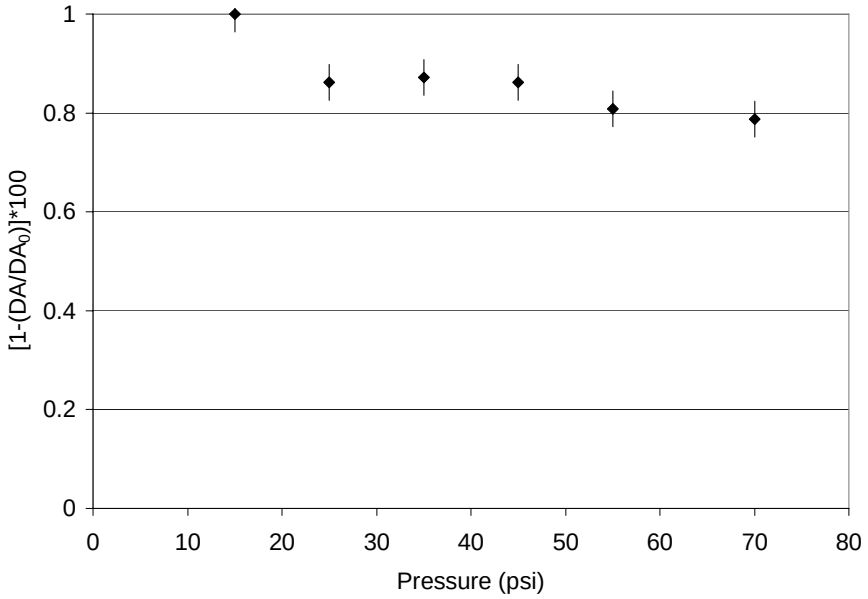

Figure 6.6: Effect of pressure on soybean oil oxidation at 110 ^{o}C for one day.

6.4.2 Crosslinked coatings

Coatings that utilize soybean oil derivatives and other renewable resources have garnered interest in recent years.[15] When renewable resources are used in coatings, they typically comprise only one component of the formulation.[234] However, from the definition of the three regimes of air oxidation, coatings that consisted of 100 % soybean oil were generated through exploiting the crosslinking that occurs during termination in the free radical reactions.

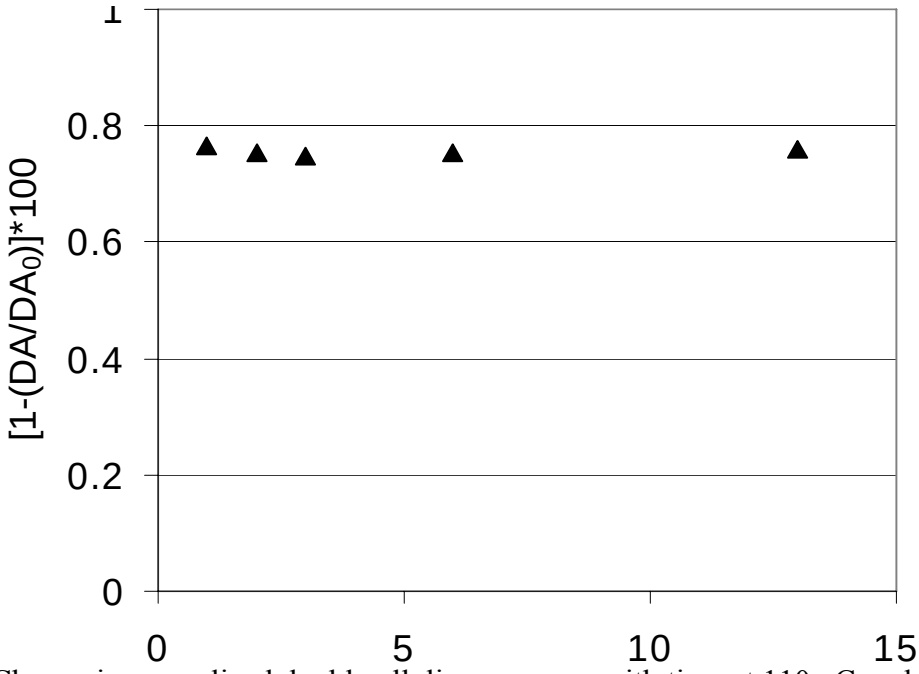

Figure 6.7: Change in normalized doubly allylic resonance with time at 110 oC under 75 psi charged air pressure

Cobalt catalysts are widely used in the oxidation of unsaturated compounds due to their activity with hydroperoxides.[247-249] In order to expedite the onset of the third regime of oxidation, cobalt(II) ethyl hexanoate (65 wt% in mineral oil) was used as a catalyst in a 5 w/v% mixture with raw soybean oil. Thin layers (~100 μm) of this homogeneous solution were uniformly coated on glass slides and placed in an oven at elevated temperature. The effect of reaction time, temperature, and irradiation on the soybean oil-based coatings was investigated. Tack tests and gel fraction measurements were utilized to gain insight into the degree of crosslinking and tackiness of the coating. In order to obtain tack-free films, a highly crosslinked coating was desired.

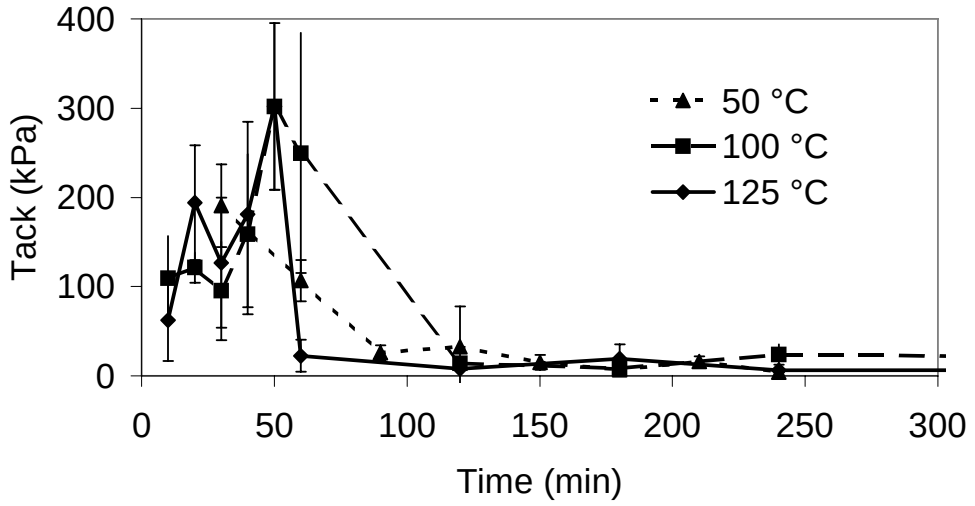

Figure 6.8. Decrease in tack of films over time at elevated temperatures.

A gradual increase in gel fraction was observed for the lower reaction temperatures (50 and 100 °C). As depicted in Figure 6.8, a longer reaction time was required for the formation of a tack-free coating at the lower reaction temperatures when compared to the coating formed at the highest reaction temperature (125 °C). All reaction temperatures resulted in tack-free coatings after two hours at elevated temperature. Figure 6.9 shows that a very high gel fraction, nearly 100%, from the coatings was achieved after several hours under the higher reaction temperatures (100 and 125 °C). The increase in tack observed during the first hour of reaction was attributed to the soybean oil behaving at first as a low viscosity liquid. As oxidation and crosslinking occurred, the soybean oil became more viscous. This phenomenon was observed in regime two for the air oxidation of soybean oil. The tack increased with an increase in the viscosity of the soy-based coating. As regime three was reached and the soybean triglycerides were chemically integrated into the network, a tack-free film was formed. Thermal analysis with differential scanning calorimetry of the films cured for 1

h at 50 °C and 125 °C showed similar behavior, where there was a significant reduction in the number and intensity of endotherms. Oxidation of the soybean oil resulted in a reduction in crystallizable triglycerides.[250] The TGA of a coating that was cured at 125 °C for 1 h indicated the onset of weight loss was at 100 °C.

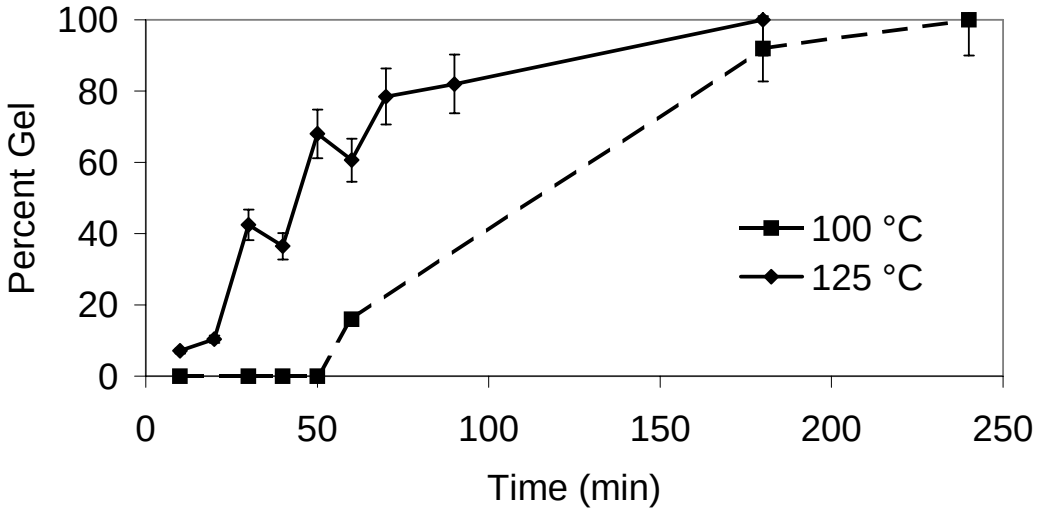

Figure 6.9. Percent gel of soybean oil coatings.

To decrease the reaction time for the formation of a tack-free coating, UV irradiation of the films was used. In the absence of heating, UV irradiation with a dose of 2.3 J/cm^2 of UVA did not result in a measureable gel fraction. When the soybean oil film was first heated and then irradiated with the same dose as before, the reaction time to achieve a high gel fraction decreased. The gel fraction was determined at ten-minute intervals for the irradiated samples. After 60 minutes at 100 °C followed by UV irradiation, a gel fraction of 80.2 % was achieved. Prior to one hour, a gel fraction was not observed for the heated and irradiated films. The gel fraction from the coating that was heated and irradiated is more than four times greater than for the coating that was

heated for 1 h at 100 °C alone (18% gel). It was also found that the tack of the irradiated and heated coating decreased with increased irradiation [Figure 6.10].

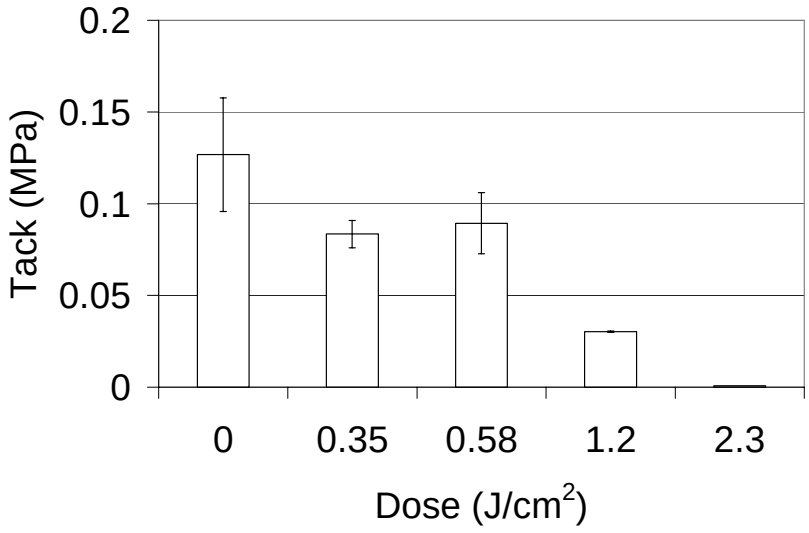

Figure 6.10. Decrease in tack observed with increasing UV irradiation for coatings cured at 100 °C for 60 min.

One can speculate on the influence of irradiation on the soy-based coatings. It was proposed that after some heating, conjugated hydroperoxides were formed and excited with irradiation, providing crosslinking sites for network formation [Figure 6.11]. This explanation accounts for the absence of a gel fraction for those samples that were only irradiated and not heated, because without the hydroperoxides, the soybean oil was only mildly affected with the irradiation.[251] This also accounts for the gel fraction observed after irradiation and heating.

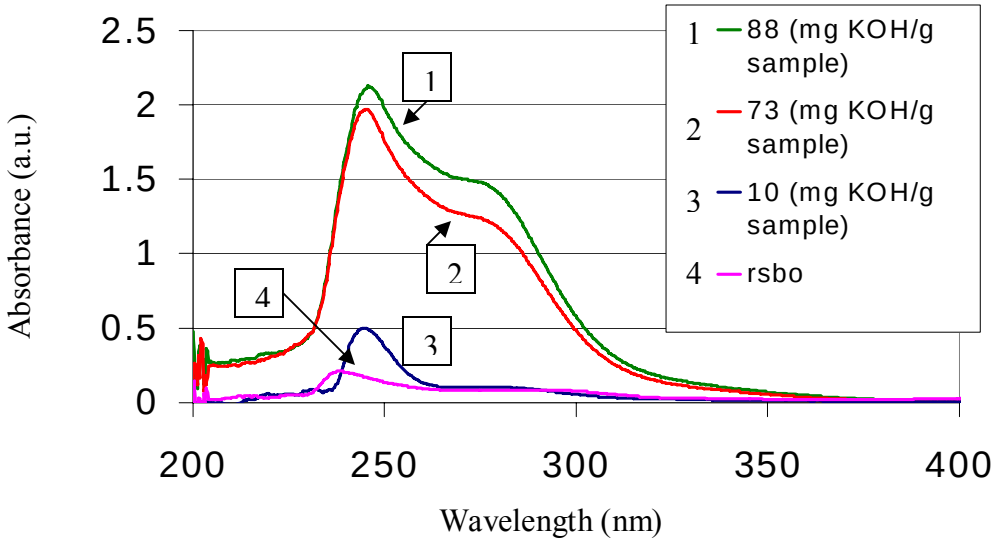

Figure 6.11. Increase in absorbance at 240 nm observed with an increase in hydroxyl number.

6.5 Conclusions

The air oxidation of soybean oil, a renewable resource, without the use of catalysts or added initiators was explored. A linear relationship between the hydroxyl number and the normalized integration of the doubly allylic resonance was found for soy polyols. This relationship was utilized to estimate the degree of oxidation that occurred in a soy polyol sample with the relatively simple technique of ^{1}H NMR spectroscopy rather than performing several titrations to determine the hydroxyl number. The application of ^{1}H NMR for an indication of the degree of oxidation provided a rapid, easy alternative technique to hydroxyl number determination. The three regimes of air oxidation were defined. The first regime consisted of insignificant oxidation of the triglycerides, where natural antioxidants were consumed and initiation occurred. Rapid

oxidation and reaction occurred during the second regime of oxidation, and high hydroxyl number (> 75 mg KOH/g) soy polyols were produced. During this second regime of oxidation, an increase in polydispersity from 1.01 for the raw soybean oil to 15.9 for soy polyol was observed. The increase in polydispersity was attributed to radical-radical coupling during the oxidation. In the third regime of air oxidation, crosslinking and termination of the free radical reaction ensued.

Observation of the third regime of air oxidation, where crosslinking occurs, inspired the synthesis of crosslinked, soybean oil coatings with the aid of a metal catalyst. The effect of reaction time, temperature, and UV irradiation on the formation of tack-free, soy-based coatings was determined. It was found that elevated temperatures decreased the time required for the synthesis of tack-free coatings. UV irradiation of coatings exposed to elevated temperatures decreased the cure time for the production of tack-free films.

6.6 Acknowledgements

The authors thank the Urethane Soy Systems Company for supplying raw soybean oil and the United Soybean Board for their generous financial support of this work.

6.7 References

1. Shogren, R. L.; Petrovic, Z.; Liu, Z.; Erhan, S. Z. *J. Polym. Environ.* **2004** 12, 173-178.

2. Petrovic, Z. S.; Zhang, W.; Javni, I. *Biomacromolecules* **2005** 6, 713-719.

3. Li, F.; Larock, R. C. *J. Appl. Polym. Sci.* **2000** 78, 1044-1056.

4. Mahapatro, A.; Kalra, B.; Kumar, A.; Gross, R. A. *Biomacromolecules* **2003** 4, 544-551.

5. Li, F.; Larock, R. C. *J. Appl. Polym. Sci.* **2001** 80, 658-670.

6. Bunker, S. P.; Wool, R. P. *J. Polym. Sci., Part A: Polym. Chem.* **2002** 40, 451.

7. Javni, I.; Zhang, W.; Petrovic, Z. S. *J. Appl. Polym. Sci.* **2003** 88, 2912.

8. Chen, J.; Soucek, M. D.; Simonsick, W. J.; Celikay, R. W. *Polymer* **2002** 43, 5379.

9. Uyama, H.; Kuwabara, M.; Tsujimoto, T.; Nakano, M.; Usuki, A.; Kobayashi, S. *Chem. Mater.* **2003** 15, 2492-2494.

10. Guo, A., Y. Cho, Z.S. Petrovic *J. Polym. Sci: Part A: Polym. Chem.* **2000** 38, 3900-3909.

11. Kandanarachchi, P.; Guo, A.; Petrovic, Z. *J. Mol. Catal. A: Chem.* **2002** 184, 65.

12. Petrovic, Z. S.; Guo, A.; Zhang, W. *J. Polym. Sci, Part A: Polym. Chem.* **2000** 38, 4062-4069.

13. Decker, C.; Viet, T. N. T.; Thi, H. P. *Polym. Int.* **2001** 50, 986.

14. Tsujimoto, T. U., H.; Kobayashi, S. *Macromolecules* **2004** 37, 1777-1782.

15. Zlatanic, A.; Petrovic, Z. S.; Dusek, K. *Biomacromolecules* **2002** 3, 1048-1056.

16. Khot, S. N.; Lascala, J. J.; Can, E.; Morye, S. S.; Williams, G. I.; Palmese, G. R.; Kusefoglu, S. H.; Wool, R. P. *J. Appl. Polym. Sci.* **2001**, 703-723.

17. Williams, G. I.; Wool, R. P. *Appl. Comp. Mater.* **2000** 7, 421.

18. Esen, H.; Kusefoglu, S. H. *J. Appl. Polym. Sci.* **2003** 89, 3882.

19. Larock, R. C.; Li, F. *J. of Appl. Polym. Sci.* **2002** 84, 1533-1543.

20. Tappel, A. L., In *Free Radicals in Biology*. Academic Press: New York, 1980; Vol. IV, p 1-47.

21. Manju, V.; Namasivayam, N. *Clinica Chimica Acta* **2005** 358, 60-67.

22. Das, S.; Otani, H.; Maulik, N.; Das, D. *Free Radical Research* **2005** 39, 449-455.

23. Kan, M. J.; Lee, E. K.; Lee, S. S. *Nutritional Sciences* **2005** 8, 10-15.

24. Neff, W. E.; Byrdwell, C. *J. Chromatogr., A* **1998** 818, 169-186.

25. Brimberg, U. I. *J. Am. Oil Chem. Soc.* **1993** 70, 249-254.

26. Abramovic, H.; Abram, V. *Food Technol. Biotechnol.* **2005** 43, 63-70.

27. Ramirez, M. R.; Cava, R. *Food Sci. Technol.* **2005** 38, 726-734.

28. Hung, S. S. O.; Slinger, S. J. *J. Am. Oil Chem. Soc.* **1981** 58, 785-788.

29. Romero, A.; Cuesta, C.; Sanchez-Muniz, F. J. *J. Am. Oil Chem. Soc.* **2003** 80, 437-442.

30. Kim, I.; Choe, E. *Food Sci. Biotechnol.* **2004** 13.

31. Sun, X.; Moreira, R. G. *J. Food Proc. Pres.* **1996** 20, 157-167.

32. Zhong, B.; Shaw, C.; Rahim, M.; Massingill, J. *J. Coatings Tech.* **2001** 73, 53-57.

33. Erich, S. J. F.; Laven, J.; Pel, L.; Huinink, H. P.; Kopinga, K. *Progress in Organic Coatings* **2005** 52, 210-216.

34. Ahmad, I.; Mufakkar, M.; Khan, F.; Shahid, S. *J. Nat. Sci. Math.* **2003** 43, 105-109.

35. Biermann, U.; Friedt, W.; Lang, S.; Luhs, W.; Machmuller, G.; Metzger, J. O.; Rusch gen. Klaas, M.; Schafer, H. J.; Schneider, M. P. *Angew. Chem., Int. Ed. Engl.* **2000** 39, 2206-2224.

36. Alam, M.; Sharmin, E.; Ashraf, S. M.; Ahmad, S. *Progress in Organic Coatings* **2004** 50, 224-230.

37. Rakotonirainy, A. M.; Padua, G. W. *J. Agric. Food Chem.* **2001** 49, 2860-2863.

38. Hutchinson, G. H. *Reports Prog. Appl. Chem.* **1969** 54, 600-604.

39. Reidy, L. J.; Meier-Augenstein, W.; Kalin, R. M. *Rapid Commun. Mass Spectrom.* **2005** 19, 1899-1905.

40. Hanlon, M. C.; Seybert, D. W. *Free Radical Biology & Medicine* **1997** 23, 712-719.

41. Isnardy, B.; Wagner, K.-H.; Elmadfa, I. *J. Agric. Food Chem.* **2003** 51, 7775-7780.

42. Jiang, Y. J.; Hammond, E. G. *J. Am. Oil Chem. Soc.* **2002** 79, 791-796.

43. Brimberg, U. I.; Kamal-Eldin, A. *Eur. J. Lipid Sci. Tech.* **2003** 105, 83-91.

44. Mikula, M.; Khayat, A. *J. Am. Oil Chem. Soc.* **1985** 62, 1694-1698.

45. Doi, M.; Edwards, S. F., In *The Theory of Polymer Dynamics*. Oxford University Press: New York, 1992; Vol. 73.

46. Pechar, T. W.; Sohn, S.; Wilkes, G. L.; Ghosh, S.; Frazier, C. E.; Fornof, A.; Long, T. E. *J. Appl. Poly. Sci.* **2005** submitted.

47. Sercheli, R.; Ferreira, A. L. B.; Baptistella, L. H. B.; Schuchardt, U. *J. Agric. Food Chem.* **1997** 45, 1361-1364.

48. Hancock, R. A.; Leeves, N. J.; Nicks, P. F. *Progress in Organic Coatings* **1989** 17, 337-347.

49. Jacobs, R. L. *J. Org. Chem.* **1977** 42, 571-573.

50. Che Man, Y. B.; Tan, C. P. *Phytochem. Anal.* **2002** 13, 142-151.

51. Coppin, E. A.; Pike, O. A. *J. Am. Oil Chem. Soc.* **2001** 78, 13-18.

Chapter 7: Overall Conclusions

Tailored branching was introduced to multiple chemistries, and the impact of branching on polymer intermolecular interactions was determined. Ionenes, which have quaternary ammonium salts along the backbone, were synthesized via a novel approach with varying distances between branch points. The branching in the ionic segments of the ionenes led to some disruption of microphase separation. The mechanical properties of the branched ionenes were reduced when compared to linear analogs.

Branching was then introduced to polyurethanes with polyether soft segments. Branching was characterized with a novel approach utilizing ^{13}C NMR spectroscopy. All of the units, dendritic, linear, and terminal, were observed in the quaternary carbon region of the ^{13}C NMR spectra. From these assignments, the classical degree of branching was determined. An alternative to the classical degree of branching, which is generally applicable to highly branched polymers, was proposed.

With the degree of branching and efficiency of branching well-described, the rheological behavior and ionic conductivity of highly branched polyurethanes was compared to linear analogs. For the first time, it was found that the highly branched polyurethanes had much lower melt and solution viscosities than the linear counterparts, which has implications for the processability of polyurethanes. The relaxation times of the highly branched polymers were significantly reduced. However, the observation of a relaxation time indicated the presence of entanglements. The solution viscosity was performed to deconvolute the interaction of intermolecular interactions, hydrogen

bonding, and entanglement effects. The solvent in the solution viscosity experiments disrupted hydrogen bonding, and evidence of entanglements was observed. Therefore, for the first time, the presence of entanglements in highly branched polymers was confirmed. The influence of branching was also probed for highly branched poly(ether urethane)s, which were doped with a metal salt, lithium perchlorate. The branched poly(ether urethane)s had much higher melt viscosities and relaxation times when doped with lithium perchlorate. This observation suggested a high degree of physical crosslinking between the polyether soft segment and lithium perchlorate. The significant degree of interaction led to ionic conductivities approximately four orders of magnitude higher than the linear counterpart of the same molecular weight and dopant level.

The possibility of using a renewable resource, soybean oil, as a monomer feedstock was probed. Soybean oil is comprised primarily of triglycerides. The synthesis of soy-based polyols based on air oxidation was followed with a statistical design of experiments. The impact of time, temperature, and air flow rate was determined for the first time in a systematic way. The synthesis of soy-based polyols was achieved through an inexpensive and simple approach. The relationship between disappearance of the resonance attributable to doubly allylic protons in the ^{1}H NMR spectrum of oxidized soybean oil and hydroxyl number, an indication of the degree of functionalization of the soy polyol, was elucidated for the first time. The doubly allylic resonance from the ^{1}H NMR spectrum of soy polyols was successfully used for following the oxidation of the soybean oil. For the first time, three regimes of oxidation were defined for oxidation of soybean oil. The knowledge from the three regimes of oxidation

was utilized in the synthesis of crosslinked soy-based coatings. The tack and percent gel of the coatings was followed. Exposure to UV light after some heating increased the crosslink density at shorter reaction times.

Chapter 8: Suggested Future Work

8.1 Synthesis and Gene Transfection Studies of PEG-Based Ionenes

Trukhanova et al. probed the effect of charge density on the gene transfection efficiency of aliphatic ionenes.[208] A greater aliphatic spacing between ionic groups led to a lower cell viability. Poly(ethylene glycol) is biocompatible and even prevents protein adhesion. A PEG-based ionene is a great candidate for a gene transfection agent. Ionenes are polycations, which is necessary for binding with DNA, and the soft segment, PEG, is biocompatible. There are several synthetic approaches for incorporation of PEG into ionenes. However, it is proposed for PEG-based ionenes to be synthesized through a Menschutkin reaction of a bis(dimethylamino)-poly(ethylene glycol) and a reactive dihalide. Cell viability and gene transfection studies will focus on adjusting the distance between ionic groups through changing the length of the PEG segment and understanding the influence of charge density without cell viability problems due to the soft segment.

8.2 Highly Branched PTMO-Based Ionenes with Viologen-Type Branching Agents

The synthesis of PTMO-based ionenes through a modified Menshutkin reaction was described in Chapter 3. However, another synthetic approach, which would require fewer steps, is suggested. The living cationic polymerization of PTMO would

be the same as described in Chapter 3. The living PTMO could be added dropwise to a terpyridine solution. Thus, a highly branched, PTMO-based ionene could be synthesized in just two steps. The viologen-type linkage provides greater thermal stability and could be an interesting approach to highly branched, PTMO-based ionenes. This could also be a useful approach for the synthesis of highly branched and linear PEG-based ionenes.

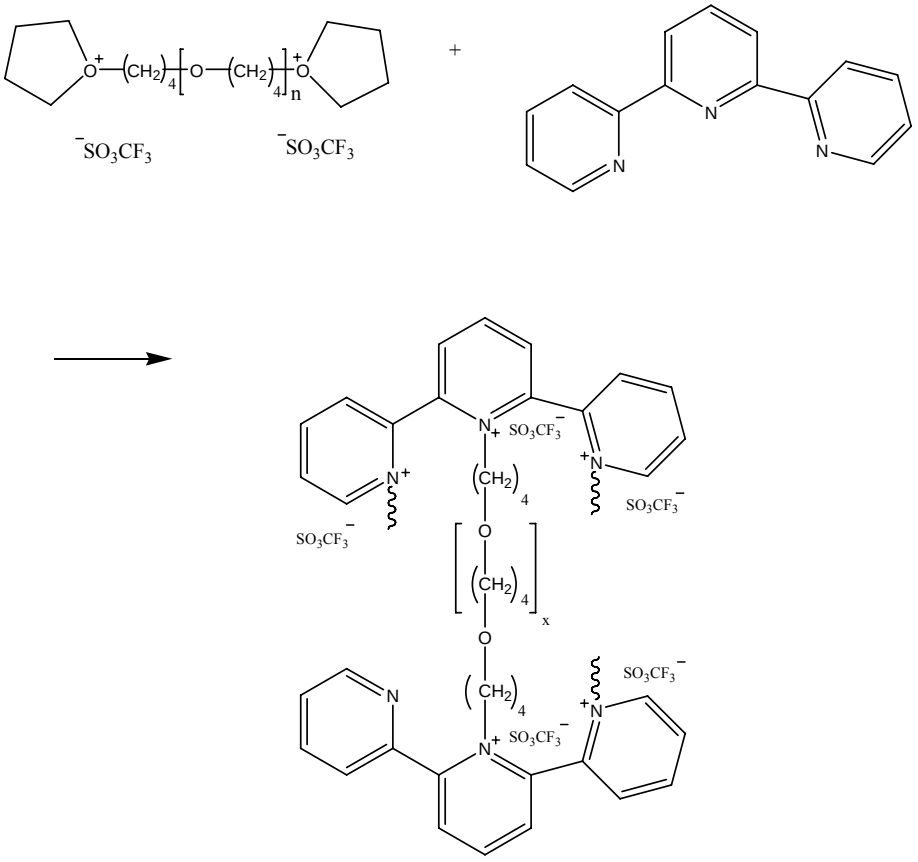

Scheme 8.1 Synthetic scheme for viologen-type, highly branched, PTMO-based ionenes

8.3 Ionic Conductivity of Highly Branched, PTMO-Based Ionenes

Polyethers have ionic conductivity when doped with a metal salt. Highly branched polymers were shown to have much higher ionic conductivity than linear

counterparts in Chapter 5. The PTMO-based ionenes have better mechanical properties than PTMO alone, and the polymer itself is also charged. The influence of varied amounts of salt and distance between branch points for the highly branched ionenes.

8.4 Probe the Influence of Hard Segment on Ionic Conductivity and Interaction with Lithium Salts

Sheth et al. determined that doping a model poly(urethane urea) with lithium chloride had a significant impact on the long range ordering of the hard segment.[16] Aneja et al. found that lithium bromide interacted preferentially with urea over the polyether soft segment or urethane.[252] While poly(urethane urea)s have experienced wide-spread interest for applications requiring ionic conductivity, the impact of the metal salt dopants on the hard segment were not explored. It would be interesting to determine with ^{7}Li NMR spectroscopy how the lithium salt interacts with the hard and soft segments. Systematic changes in the amount of hard segment incorporated and subsequent determination of the ionic conductivity could elucidate the role of the hard segment on the ionic conductivity of poly(urethane urea)s. Also, an investigation of the difference in ionic conductivity between poly(urethane)s and poly(urethane urea)s with the same polyether soft segment and dopant levels would be a useful contribution to understanding the role of the hard segment in ionic conductivity.

8.5 Determine the Influence of Branching on the Swelling Behavior of PEG-based Polyurethanes

Lithium batteries have traditionally utilized liquid electrolytes for the primary conductive component. Recently, significant effort was devoted to the development of ionically conductive gel membranes.[253] PEG-based polymers are considered an attractive alternative to the standard liquid electrolytes. However, significant improvement in the ionic conductivity over that of PEG doped with a metal salt is required for lithium ion battery applications. It was observed in this work that the ionic conductivity of the highly branched PEG-based polyurethane was greater than for the linear counterpart. The influence of swelling the highly branched PEG-based polyurethane with water and determining the ionic conductivity would be useful information for potential application in lithium ion batteries.

8.6 Determine Influence of Hydrogen Bonding on Melt Rheological Behavior

The rheological behavior of highly branched poly(ether urethane)s was investigated in Chapter 5 of this dissertation. However, the melt rheological behavior of the highly branched poly(ether urethane)s was complicated with the influence of microphase separation and hydrogen bonding. Highly branched polyesters were synthesized recently in our research group. It would be interesting to investigate a highly branched polymer that is not complicated with hydrogen bonding and elucidate if the

highly branched polymers follow a Rouse-type behavior like hyperbranched polymers or if the entanglements are sufficient to cause a departure from Rouse-type behavior.

Appendix A

Copyright Permissions

Dear Dr. Fornof,

Thank you for your email.

We hereby grant permission for the requested use expected that due credit is given to the original source.
Please note that the author's permission is also required.

With kind regards

Yours sincerely,

Bettina Loycke
****
Bettina Loycke
Copyright & Licensing Manager
Wiley-VCH Verlag GmbH & Co KG
Boschstr. 12
69469 Weinheim
Germany
Phone: 0049 6201 606 280
Fax: 0049 6201 606 332
Email: rights@wiley-vch.de

Dear Ms Fornof

The Royal Society of Chemistry hereby grants permission for the use of the material specified below in the work described and in all subsequent editions of the work for distribution throughout the world, in all media including electronic and microfilm. You may use the material in conjunction with computer-based electronic and information retrieval systems, grant permissions for photocopying, reproductions and reprints, translate the material and to publish the translation, and authorize document delivery and abstracting and indexing services. The Royal Society of Chemistry is a signatory to the STM Guidelines on Permissions (available on request).

Please note that if the material specified below or any part of it appears with credit or acknowledgement to a third party then you must also secure permission from that third party before reproducing that material.

Please ensure that the published article carries a credit to The Royal Society of Chemistry in the following format:

[Original citation] – Reproduced by permission of The Royal Society of Chemistry

Regards

Gill Cockhead
Contracts & Copyright Executive

Gill Cockhead, Contracts & Copyright Executive
Royal Society of Chemistry, Thomas Graham House
Science Park, Milton Road, Cambridge CB4 0WF, UK
Tel +44 (0) 1223 432134, Fax +44 (0) 1223 423623

http://www.rsc.org and http://www.chemsoc.org

Virginia Tech
Chemistry Department (0212)
Blacksburg, VA 24061-0212
Fax: 540-231-8517
Phone: 540-231-9503
Email: afornof@vt.edu
4/5/06
w-halperin@northwestern.edu
Dear Prof. Halperin:
I am completing a doctoral dissertation at Virginia Tech entitled "Synthesis and Characterization of Multiphase, Highly Branched Polymers." I would like your permission to reprint in my dissertation excerpts from the following:
Mai, Y.; Zhou, Y.; Yan, D.; Hou, J. *New J. Phys.* **2005** 7, 1-9.
The excerpts to be reproduced are: Figure 4
The requested permission extends to any future revisions and editions of my dissertation, including non-exclusive world rights in all languages, and to the prospective publication of my dissertation by UMI Company. These rights will in no way restrict republication of the material in any other form by you or by others authorized by you. Your signing of this letter will also confirm that you own [or your company owns] the copyright to the above-described material.
If these arrangements meet with your approval, please sign this letter where indicated below and return it to me in the enclosed return envelope. Thank you very much.
Sincerely,
Ann Fornof
PERMISSION GRANTED FOR THE
USE REQUESTED ABOVE:

_____
[Type name of addressee below signature line]
Date: _____

PERMISSION TO REPRODUCE AS REQUESTED
IS GIVEN PROVIDED THAT:

(a) the consent of the author(s) is obtained
(b) the source of the material including author/editor, title, date and publisher is acknowledged.

IOP Publishing Limited
Dirac House
Temple Back
BRISTOL 6/4/06 .....

BS1 6BE Date Rights & Permission

PERMISSION REQUEST FORM FOR FIGURES/TABLES

[Click in gray or yellow boxes and type information, hit enter key when needed.]

Date: 4/5/06

To: [Include publishers contact info.]
ACS Copyright Office

FAX: 202-776-8112

From: [Include your name, address, etc.]
Ann Rohrer
Chemistry Department
Virginia Tech
Blacksburg, VA 24061-0212

Your Phone No. 540-231-9503
Your Fax No. 540-231-8517

I am preparing a paper entitled: Synthesis and Characterization of Multiphase, Highly Branched Polymers

to appear in [Include ACS journal, magazine, or book title] dissertation

which is published by the ~~American Chemical Society, a not-for-profit membership society.~~

I would appreciate your permission to use the following material in all formats including but not limited to print, microform, electronic, and/or CD-ROM from the following reference:

From a journal or magazine:

Publication Title	Year	Vol.	No.	Page(s)Material to be used
Macromolecules	1997	30	23	7024-7033, Scheme 1, Figure 1
Macromolecules	2003	36	2	399-406, Figure 8
Macromolecules	2002	35	25	9605-9612, Figure 9
Macromolecules	2004	37	26	9814-9820, Figure 4
Chemistry of Materials	2005	17	5	1148-1156, Figure 4

From a book: include book title, series name and number, year, page(s), book editor=s name(s), chapter author's name(s), and material to be used, such as Figs. 2 & 3, full text, etc.

If you have a required credit lir

PERMISSION TO REPRINT IS GRANTED BY THE AMERICAN CHEMICAL SOCIETY

ACS CREDIT LINE REQUIRED. Please follow this sample: Reprinted with permission from (reference citation). Copyright (year) American Chemical Society.

For your convenience, you may ment.
Please return this form to me at

APPROVED BY: 4/6/06
ACS Copyright Office

☐ **If box is checked, author permission is also required. See original article for address.**

Agreed:

6/21/99-4/11/00

PERMISSION TO REPRODUCE AS REQUESTED
IS GIVEN PROVIDED THAT:

(a) the consent of the author(s) is obtained
(b) the source of the material including author/editor, title, date and publisher is acknowledged.

IOP Publishing Limited
Dirac House
Temple Back
BRISTOL 16/4/06

BS1 6BE Date Rights & Permission

Jill Membrey/IOPP
06/04/2006 09:17

----- Forwarded by Jill Membrey/IOPP on

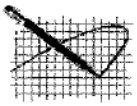

Tim Smith/IOPP
06/04/2006 08:57

Subject Fw: Re: copyright permission

Vita

Ann R. Fornof was born in Toledo, OH on May 31, 1979 to John and Judy Fornof. She attended Notre Dame Academy for high school and graduated in 1997. She entered Columbia University in the fall of 1997 and graduated in 2001 with a B.S. in Chemical Engineering. She attended Virginia Tech and entered the Macromolecular Science and Engineering program in 2001.